LUND UNIVERSITY

Humidification Processes in Gas Turbine Cycles

Thern, Marcus

2005

[Link to publication](#)

Humidification Processes in Gas Turbine Cycles

Marcus Thern

December 12th 2005
Doctoral thesis
Division of Thermal Power Engineering
Department of Energy Sciences
Faculty of Engineering
Lund University
Sweden

To my family

Abstract

The global climate change caused by emissions of greenhouse gases from combustion processes has been recognized as a continuously growing problem and much research focuses on improving the environmental performance of gas turbines. The potential of improving gas turbine component efficiencies has become smaller each decade and therefore, thermodynamic cycles have become more interesting for power producing units. One of these cycles is the evaporative gas turbine cycle, also known as the humid air turbine.

This thesis presents a theoretical model developed for the humidification tower in an evaporative gas turbine. The developed theoretical model has been validated with measurements from experiments conducted in a $600\,\mathrm{kW_e}$ pilot plant. This thesis presents the installation of a plate heat exchanger in the pilot plant. The experience from the pilot plant is used in a comparative study. This study evaluates the influence of the aftercooler on the performance of the evaporative gas turbine. A test facility for evaporation processes at elevated pressures and temperatures have been built. Evaporation of binary mixtures into a compressed air stream has been performed.

Experimental studies with the pilot plant have revealed that it is possible to use a plate heat exchanger as aftercooler in the evaporative gas turbine. The pressure drop on the air side in the aftercooler has been experimentally determined to 1.6% and the pinch-point to 0.1°C. The reconstruction of the pilot plant from a simple cycle to an evaporative cycle has resulted in an increase in thermal efficiency from 21% to 35%. A theoretical model has been developed for the humidification process that predicts the height of the humidification column with an error of 10–15%. Thermodynamic analysis of the bio-EvGT has been performed which have showed that the bio-EvGT cycle has an optimum efficiency of 34%. Further thermodynamics analysis has indicated that the bio-EvGT is a viable alternative to the biomass fueled steam turbine cycle.

Contents

Nomenclature

Variable	Explanation	Unit
a	Specific packing surface	m^2/m^3
A	Area	m^2
A_t	$a \cdot A$	m
c_t	Molar density	mol/m^3
c_f	Fuel cost	$/kg
c_p	Specific heat	kJ/(kgK)
C	Cost	$
d	Exact differential	
d_{eq}	Equivalent diameter	m
D	Diameter	m
D_{ab}	Diffusion coefficient	m^2/s
h	Specific enthalpy	kJ/kg
h	Mass transfer coefficient	$W/(m^2K)$
h_d	Mass transfer coefficient	m/s
h_{fg}	Heat of vaporization	kJ/(kgK)
HTU	Height of a transfer unit	m
k	mass transfer coefficient	m/s
J_1	Diffusive molar flux	mol/m^2
k^*	Mass transfer coefficient	m/s
L	Liquid flow rate	kg/s
Le	Lewis number	-
$\dot{m}$	Mass flow rate	kg/s
m''	Mass flow rate per unit area	$kg/(sm^2)$
N	Molar flux	mol/m^2 s
NTU	Number of transfer units	-
Nu	Nusselt number	-
pp	Pinch point	$°C$

Continued on next page

Variable	Explanation	Unit
P	System pressure	Pa
p	partial pressure	Pa
P	Power	W
P'	Specific work $(P/m_{c,i})$	J/(kg air)
q	Heat per unit area	W/m^2
Q	Heat	kJ/kg
R	Gas constant	kJ/(kgK)
Re	Reynolds number	-
s	Thickness	m
Sc	Schmidt number	-
Sh	Sherwood number	-
T	Temperature	°C
$T_e q$	Operating hours	h
T_c	Critical temperature	K
U	Operating and maintenance cost	\$/MWh
v	Velocity	m/s
V	Volume	m^3
V	Vapor flow rate	kg/s
w	Velocity	m/s
x	Mole fraction in liquid phase	-
X	Equipment size	-
y	Mole fraction in gas phase	-
z	Position in packing	m
Z	Height of packing	m
W	Specific work	W
Greek symbols		
α	Heat transfer coefficient	W/(mK)
γ	Activity coefficient	-
Δ	Finite difference	
δ_l	Film thickness	m
ε	Effectiveness	-
η	Efficiency	-
κ	Specific heat ratio	-
λ	Thermal conductivity	W/(mK)
π	Pressure ratio	-
ρ	Density	kg/m^3

Variable	Explanation	Unit
ν	Kinematic viscosity	m^2/s
ν	Specific volume	m^3/kg
ψ	Annuity factor	-
υ	Diffusion volumes	-
ω	Humidity	kg H_2O/kg dry air
ω	Humidity (mass transfer)	kg H_2O/kg mixture
Ξ	Ackermann factor	-
Φ	Heat transfer rate factor	-

Subscripts

a	Air; Above	
n	Energy	
fuel	Fuel	
g	Gas	
heat	Heat	
i	Inlet; Interface; item	
in	Inlet	
l	Liquid; Local	
m	Mechanical; Metal	
u	Liquid side control surface	
s	Gas side control surface	

Abbreviations

AHAT	Advanced humid air turbine	
COE	Cost of electricity	\$/MWh
COEn	Cost of energy	\$/MWh
EGT	Evaporative Gas Turbine	
EvGT	Evaporative Gas Turbine	
FCI	Fixed capital investment	\$
Fluegas	Flue gas system	
GT	Gas turbine	
GEN	Generator	
HAT	Humid Air Turbine	
HE	Heat exchanger network	
HP	High pressure	
HT	Humidification tower	
log	Logarithmic	

Continued on next page

Variable	Explanation	Unit
LP	Low pressure	
Mash	Ethanol production facility	
MAT	Moisture air turbine	
PEC	Purchased equipment cost	$
Pump	Pump	
STIG	Steam injected gas turbine	
TCI	Total capital investment	$
TET	Turbine exhaust temperature	°C
TIT	Turbine inlet temperature	°C

Chapter 1

Introduction

1.1 Background

Gas turbines have, during the last decades, become more common as a power generating engine due to its flexibility and its low specific investment costs. Development of gas turbines for power generation has gone hand in hand with the development of new gas turbines for use in aircraft engines. This has meant that today's state-of-the-art gas turbines have compressor and expander efficiencies of up to 92% at pressure ratios exceeding 30 and firing temperatures at 1650K. The potential of improving gas turbine component efficiencies has become smaller each decade and therefore, thermodynamic cycles have become more interesting for power producing units.

Combined-cycles are today an established technology in the electricity market and presently it is even used for base load operation. However, even if the combined cycles are economically profitable, new thermodynamic cycles are being introduced and investigated for future power generation. The research in this area is driven by economical factors, environmental and/or a need for cycles which allows for a more flexible operating scheme. Several advanced gas turbine cycles have been identified as future competitors to the combined cycles and among them are the steam-injected gas turbine cycle (STIG) and the evaporative gas turbine cycle, (EvGT).

In 1993, a group consisting of Swedish universities and industries commenced a research project which related to one of these advanced gas turbine cycles, the evaporative gas turbine (EvGT) project. The EvGT project places the emphasis on novel technologies of utilizing gas turbines for power generation and cogeneration. The EvGT project investigates the thermodynamic and dynamic modeling of the EvGT and also the economical issues.

The result of the EvGT research program was the construction of the first evaporative gas turbine pilot plant in the world.

The EvGT cycle uses a complex heat recovery system which utilizes low-level heat from both the compression process with an intercooler and after-cooler and from the hot exhaust gases with an economizer. The recovered low-level heat is then utilized in a humidification process with the compressor discharge air, so that the mass flow through the expander increases. A variant of the EvGT called the part-flow evaporative gas turbine was also studied by the EvGT project, which is a combination of the steam-injected cycle and the evaporative gas turbine cycle. In this cycle, 20–40% of the airflow is directed through the humidification circuit where it is being humidified and the remaining part of the air is passed directly to the combustor, where it is mixed with steam that has been generated in a heat recovery steam generator.

The global climate change caused by emissions of green house gases from combustion processes, has been recognized as a continuously growing problem and much research focuses on improving the environmental performance of gas turbines [25]. In order to meet this need, the EvGT research project has therefore identified several other configurations based on the EvGT cycle, i.e. the IGHAT, indirect fired evaporative gas turbines, part-flow evaporative gas turbine and the bio-EvGT.

The evaporative technique showed great potential for enhancing the performance of gas turbine and it was soon found that the evaporation technique could be used to evaporate both water and a fuel to the gas turbine. This evaporation is performed by the same heat recovery system as in the ordinary EvGT cycle therefore decreasing the complexity to the system. Consequently, this technique make it possible to introduce biofuel into gas turbines and other engines as a clean gaseous fuel, thereby reducing the CO_2 emissions.

The participants of the EvGT-project have been Lund University, Royal Institute of Technology, Vattenfall, Sydkraft (E.ON since September 2005), Volvo Aero Corporation, ALSTOM Power, ABB, Siemens, ELFORSK, Energi E2 and Swedish Energy Agency.

1.2 Objective

The overall aim of this thesis is to improve the knowledge of the humidification process in the evaporative gas turbine cycle (EvGT). This thesis will describe the use of the aftercooler in the EvGT and its importance to the

heat recovery system and the humidification process and will present experiments that show the benefits of introducing an aftercooler to the EvGT cycle.

Some specific issues that this thesis intends to draw attention to is:

- to study the humidification process in the EvGT cycle;

- to integrate an aftercooler in the EvGT pilot plant and analyze its performance;

- to develop a theoretical model of the humidification process;

- to validate the established theoretical models with measurements from the humidification tower;

- to design, build and evaluate an experimental test facility for the evaporation of fluids into an airstream at elevated pressures and temperatures; and

- to use the experimental results from the pilot plant to investigate theoretical models for the evaporation of ethanol and water into an airstream at elevated pressures and temperatures.

1.3 Restrictions

The study presented in this thesis has the following limitations:

- the thermodynamic evaluation of the evaporative gas turbine is limited to the static first-law heat balance calculations when evaluating the measured data;

- the analysis of the bio-EvGT cycle is limited to the first law of thermodynamics; and

- simplified equations for the evaporation of the binary liquid has been used for the economical calculations.

1.4 Methodology

In order to achieve the stated objective, a thorough literature study has been conducted for wet cycles and humidification towers. This study has not focused on the evaporative gas turbine cycle alone. Additionally, it has

also focused on recuperated water injected cycles (RWI), steam injected cycles (STIG) and evaporative cycles (EvGT) as can be seen in figure 1.1. In turn, the focus has been aimed at the evaporative gas turbine cycles and its development. Of particular interest in the literature study is the evaporative gas turbine cycle and the parts concerning the aftercooler, humidification tower and the biofuel. As a follow-up to the literature review, experimental
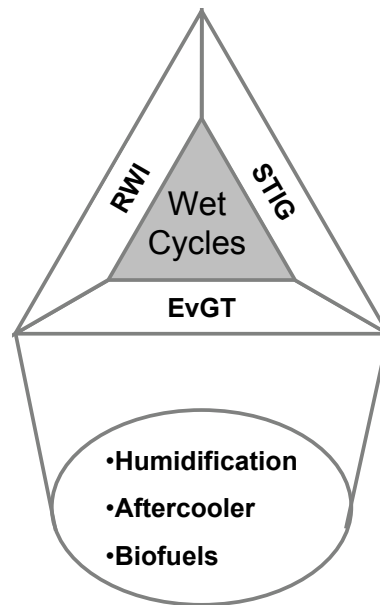
Figure 1.1: Literature study and focus of thesis

work was also undertaken. Together with Torbjörn Lindquist, a laboratory was constructed to evaluate the potential of the aftercooler in a power plant environment. The proper flow sheet was determined, including manoeuvrability and the safety of the plant was also considered. The test facility was then built according to the flow sheet which was followed by a testing period. During this time, vital knowledge of experimental work was learnt and later used to construct the new test facility where ethanol-water evaporation was studied.

This experimental work formed a foundation for the theoretical models used to evaluate the potential of the cycles. The models used for heat and mass balances of power plants were all performed in the equation solving software IPSEpro™. These calculations led to case studies which have been used to illuminate the potential of the different cycles and parts studied.

To model the differential equations required to solve the behavior of the humidification tower, a calculation software MATLAB® was used.

1.5   Thesis Outline

This thesis consists of seven chapters followed by two appendices and seven papers. The main goal this thesis is to illustrate and improve the knowledge of the humidification process in an EvGT cycle. The report is based on both experimental as well as theoretical results. The experiments were conducted in the EvGT pilot plant located at the Lund University. The EvGT pilot plant has been described in numerous articles and foremost in a licentiate thesis by Lindquist [135].

The report includes seven papers that are each summarized in chapter seven. To gain a comprehensive view of the EvGT, the thesis begins in chapter 2 with a literature review of wet cycles in general. Chapter 3 presents the general EvGT cycle and its components, followed by a description of the use of an aftercooler in an EvGT cycle based on both experimental and theoretical results from **paper II**. Further on, this chapter presents the gas turbine pilot plant located at Lund University. A description is provided presenting the installation of the aftercooler in the EvGT pilot plant which made it possible to investigate the behavior of the humidification process in the humidification tower.

Chapter 4 presents the theoretical and experimental work from **paper I** and **paper VI**, which was conducted on the humidification process of both two and three component evaporation. Chapter 4 describes the results obtained from experiments conducted with the humidification tower. Resulting from these experiments, a theoretical model has been developed that describes the humidification process in the EvGT. This chapter presents the experimental setup and the experimental planning for the pilot plant.

Chapter 5 presents experiments with the humidification of water and ethanol. This chapter presents the results from the evaluation of the experimental test facility including a thermodynamic estimation method which captures the behavior of the ethanol-water humidification process, presented in **paper VI**. Further on, a thermo-economic comparison performed in **paper V** and **paper VII** is made between the bio-EvGT and a simple steam turbine using biomass as fuel. Chapter 6 presents the concluding remarks of the thesis and chapter 7 presents a summary of papers written.

1.6 Acknowledgements

I would like to thank my professor and supervisor Tord Torisson for providing me with the opportunity to take part in this very interesting and unique project and for all his invaluable support and guidance throughout the project. I am very thankful that I had the opportunity to be a part of a great project where I was first was able to learn the craft of experimental work through Tord Torisson and Torbjörn Lindquist and then to apply that knowledge into work by constructing a new laboratory and perform the experiments.

I would like to thank my assistant supervisor and friend Doctor Torbjörn Lindquist who taught me everything I know about wet gas turbines and who also gave me constructive criticism and support throughout my Ph.D studies.

I would like to thank Björn Eriksson for all the good times we have had during the project. Thank you for teaching me that one should not believe everything that is written in a book. I would like to thank Ingjald Andreasson and Fredrik Johansson for making this work even more fun.

The EvGT project was possible with financial support from the Swedish Energy Agency, ELFORSK, Volvo Aero Corporation, ABB, ALSTOM Power, Siemens, Vattenfall, Sydkraft (E.ON since September 2005) and Energi E2. I would like to thank all members of EvGT project for all their valuable cooperation, comments and guidance.

I would also like to thank my friends and colleagues at the Department of Heat and Power Engineering. In particular, Göran Grönhammar who has given me advice on the practical aspects of this study. I have really enjoyed all your stories about Misterhult. Thanks to Björn Fredriksson-Möller for all the fun conversations during our PhD. studies. I would like to thank Miriam and Mikael for proofreading the material and for introducing me to the typesetting tool LaTeX. Thanks to Jens Klingmann and thanks also to everyone at the Department of Energy Sciences for making the everyday work at the department more interesting and fun. I would also like to thank my father Sven and my mother Gunn who always believed in me and for always being there. I would also like to thank all my brothers, Patrick, Rickard and Andreas and their respective families for giving me all the support during my work at the department. Emelie, thank you for waking me every morning, you are just adorable. Last but not least, I would like to thank my wonderful, wonderful wife who made this work possible. Without your support this thesis would not have been written.

Chapter 2

Literature Review

Wet cycles is a category of gas turbine power plants that use water to enhance the power plant performance. Mixtures of water and air in thermodynamic cycles have been used for many years [172] and gas turbines have been operated with water during the last decade. The purpose for the use of water has varied throughout the years from cooling the compressor and combustor, to reducing emissions from the gas turbine.

In 1903, Ægidius Elling ran the first gas turbine that produced a net power output where water was used to cool the compression process [117]. The injected water evaporated in the compressor, whereby it reduced the temperature of the compressor discharge, therefore preventing the high temperatures to deteriorate the compressor blades. When Armengoud and C. Lemâle started their gas turbine power plant, water was used to cool the combustion chamber [80]. The gas turbine had a 25 stage centrifugal compressor with two intercoolers. During this process, steam was used to cool the combustor which was then injected into the airflow again, creating the first steam-injected gas turbine.

Water was also found to have a great impact on emissions. By injecting water or steam, it was found that the emissions of nitrogen oxides or NO_x was reduced.

In 1971, Dibelius et al. presented an article discussing the impact of NO_x reduction by steam injection [77]. It was concluded that when steam was injected into the compressor discharge was 2% of the total air flow. The nitrogen oxides were reduced by 50% in comparison to no steam-injection for a given load in a gas fired machine. When the steam flow was increased to 4%, the nitrogen oxides dropped to 25% of the value with no steam.

The way in which water has been applied to the gas turbine has varied from time to time and today, three different ways of utilizing water can be identified:

- Injecting water into the airstream;

- Injecting steam into the airstream; and

- Injecting humid air into the airstream.

These three methods of using water in gas turbine has not been commercialized to date. To identify the different technology levels that these technologies represents, they are divided into different technology stages. In the literature review, it will be stated wether the cycle exists in paper, laboratory, field or as a commercial unit. As a paper unit only theoretical studies have been performed and no actual experience is connected to the cycle. The laboratory stage consists of both theoretical and experimental work performed on the gas turbine. The cycle has been tested in a small scale facility and the operability of the cycle has been verified. In field experience with the gas turbine, actual engines have been placed in the electrical grid and tested under actual operating conditions. If the technology is commercial, the engine maybe sold by an industrial partner.

The following chapters will focus on the different cycles, however, it should be remembered that the development of the cycles have been closely related to each other throughout history.

2.1   Water-injected Cycles

In water-injected cycles, water is injected in liquid phase at different locations in the gas turbine. The aim to use water in the gas turbine has varied from just cooling the compression process to increasing the power output and the thermal efficiency.

In 1938, Lysholm patented the first gas turbine systems which incorporated water to lower the exhaust gas temperature thereby increasing the efficiency [144, 145]. Lysholm used water droplets as a means in which to cool the compressed air exiting the compressor. In Lysholm's engine, the compressed air was mixed with the humidification water in a pressure vessel. This resulted in a temperature reduction of the air and also an increase in mass flow through the expander. It was realized that the air had to be heated up before entering the combustor and if not, fuel had to be used to increase the temperature of the fluid. The latter would mean that the thermal

efficiency of the cycle would decrease. Lysholm also foresaw the possibility of heating the water used to humidify the compressed air and pointed out that the additional heat from the exhaust gases could be used to generate steam. Steam would then be injected into the compressed air to increase the mass flow through the expander. This is similar to the steam-injected gas turbine cycle (STIG). Lysholm's invention differs from the EvGT pilot plant built in Lund due to the amount of injected water whereby it does not circulate more water in the water circuit than it can evaporate.

In 1959, Foote [84] patented a process similar to the one Lysholm patented 26 years before him. Foote used a process scheme from Lysholm whereby a heat exchanger preheats the feed water before the evaporator. The only difference is that Foote raised the temperature of the compressed air before it entered the evaporator. Foote assumed that the air preheating increased the final temperature of the air-water mixture which allowed it to contain more water than would be possible otherwise.

In 1969, Lorgere and Carrasse performed studies on water injection into a gas turbine [141]. The turbine had a fixed pressure ratio of 6.9 and a fixed turbine inlet temperature of 845°C. In this gas turbine cycle, water was injected after the compressor and exhaust gases heated the compressor discharge air before it entered the combustion chamber. These studies showed that injection of water increased both specific work and thermal efficiency of the gas turbine. The thermal efficiency increased from 24.5% to 40.5% while the power output increased by 39.3%.

In 1970, Găsparović et al. started to perform thermodynamic calculations of a wet cycle based on Lysholm's patent with water injection prior to the recuperator [96]. Găsparović et al. concluded that there is an increase in efficiency and specific power from the wet cycle. The increase in efficiency corresponds to an increase in turbine inlet temperature of 100°C. Găsparović et al. carried out further studies on heat recovery with water in the flue gases from a gas turbine [96–98]. The two gas turbines studied were both one and two shaft engines. The authors investigated two different proposals of how to inject the water into the air. The first alternative is to only inject the water at full power and then continue adding water until the air can no longer absorb more water. The other configuration is to inject water at all loads therefore saturating the air at all times. The authors favored the first alternative due to the higher efficiency at a given load. Găsparović and Stapersma concluded that it would be difficult to distribute the water evenly as it would impede the capability of saturating the air. As a solution Găsparović et al. injected less water than was required to saturate the air. Găsparović et al. also concluded that there is no risk of surge in the

compressor due to the addition of water into the compressed air. Finally, Găsparović et al. also discussed the part load performance for both a single-shaft engine and a two-shaft engine. A proposition was made that the water injection should be used to control the gas turbine and a discussion of the behavior of the turbomachinery was also provided.

In 1988, Frutchi and Plancherel presented a study where the authors compared the performance of the combined cycles, the steam-injected cycles and the evaporative cycles [86]. The evaporative cycles considered in this article were water-injected cycles. The authors do not perform any calculations themselves, however they compare values with the literature. They believe that it is feasible to obtain thermal efficiencies of 43% to 45% for the evaporative and the steam-injected gas turbines. However, it was found that the combined cycle achieved efficiencies of 47%, making a conclusion that it is better to build combined cycles. In their study they also stated that the part-load behavior of a combined cycle is superior to the wet cycles for use in a cogeneration mode.

In 1991, Annerwall et al. compared the evaporative cycles with the STIG cycles and the combined cycles. The gas turbine modeled in this study was based on the commercial gas turbine ABB GT10. There were 13 different configurations considered in this study. Annerwall et al. modeled the evaporative gas turbine with four different heat exchanger configurations. All of the water that was injected into the compressor discharge air evaporated, and no additional water circulated in the system. The evaporation process was carried out in one or two steps. When the evaporation occurs in two steps, the recuperator is split in two and a humidification tower positioned prior to the recuperator. The minimum temperature difference of the heat exchangers was assumed to be 15°C for gas/liquid exchangers and 30°C for gas/gas exchangers. Seven different configurations were modeled for the STIG cycle. Annerwall et al. concluded that the evaporative cycles showed the greatest potential for the future with respect to the thermal efficiency [7].

In 1993, Rogers and Archer studied gas turbine cycles with water injection, including different possibilities of injecting water [191]. Rogers and Archer proposed two different locations for the water injection of the compressor inlet, namely between the compressor stages and in a water-assisted regeneration. Rogers and Archer studied the different cycles based on a reference gas turbine cycle with the same pressure ratio, turbine inlet temperature and pressure losses. This meant that no parameter variation was performed. The authors concluded that the cycle with water injection into the compressor and water regeneration outperformed the other cycles, achieving a thermal efficiency of 52.2%. They also estimated that the gas turbine

required 44% less cooling air according to models of film cooling by Rosen-how. Rogers and Archer also discussed atomizers which produce the fine mist in the injection mode where water is injected into the compressor. The authors claim that the droplets for the evaporation process must be in the order of tens of a micron. The authors also discussed that the evaporative generation should be accomplished by injecting water into the regenerator, which creates a thin film of water on the surface of the regenerator.

In 1995, Bolland et al. presented a theoretical study which compared the simple cycle (SC), steam-injected gas turbine (STIG), dual-recuperated intercooled/aftercooled steam-injected cycle (DRIASI) and the combined cycle (CC) [30]. The comparisons were based on state-of-the-art gas turbine technology and cycle parameters in four classes; large industrial (123–158 MW), medium industrial (38–60 MW), aero-derivatives (21–41 MW) and small industrial (4–6 MW). The DRIASI cycle combined steam injection, recuperation and water injection into one gas turbine exhaust heat recovery. Water injection is introduced into the compressor and/or after the compressor which reduces the stack temperature, and thus reduced the temperature of the cycle heat rejection, therefore increasing the thermal efficiency. Bolland concluded that the DRIASI cycle is found to provide comparable or superior efficiencies to the combined cycle which is superior to the STIG cycle. In the medium size range, the combined cycle showed best performance but is challenged by the DRIASI cycle. The combined cycle is still the best cycle for large scale power plants.

In 1996, Camporeale and Fortunato continued the work by Găsparović et al. [39–42]. The aim of this work was to investigate plants obtained by upgrading a simple cycle aero-derivative gas turbine engine with additional devices and a limited number of modifications of the base engine. The authors studied two thermodynamic cycles; the recuperative water-injected gas turbine (RWI) and the steam-injected gas turbine (STIG). They restricted the amount of injected water to 10% of the compressor airflow in order to minimize the required modifications of the high-pressure turbine. The aero-engine General Electric LM2500 was chosen as the gas turbine for the project, which had a pressure ratio of 18.7, a turbine inlet temperature of 1523K, a thermal efficiency of 35.5% and a power output of 21.87 MW. To thermodynamically model the expansion and cooling of the gas turbine hot parts, an estimation method based on El-Masri's thermodynamic cooling model was employed [40]. Generalized maps for the expander and the compressor was used to estimate the off-design performance of the gas turbine. If more than one stage was needed for the expansion, the author assumed that the second stage had the same loading coefficient as the first stage. The primary results

of the thermal efficiency of the RWI were 47.1% compared to the simple cycle performance of 32.7%. The power increased from 19.6 MW to 23.8 MW. As a comparison the STIG engine had a thermal efficiency of 41.6% and a power output of 31.7 MW [39]. More detailed calculations indicated that the optimum efficiency for a RWI cycle using the same turbine inlet temperature and pressure ratio as the base engine was 41% with a water injection rate of 10% water-to-air ratio [40]. They also presented calculations of the upgraded version of the gas turbine and studied the increase in pressure ratio and turbine inlet temperature. Considering the surge margin and the maximum blade temperature, the plant obtained a thermal efficiency and power output of 44.2% and 28.9 MW respectively [40]. In their study, they concluded that the expander vanes had to be modified in order to accommodate the larger mass flow. When the injected mass flow of water is less than 10% of the inlet air mass flow, only the stator vanes need to be altered. A complete new design of both rotor and stator blade is required if more water is injected.

In 2000, Camporeale and Fortunato presented a modeling study which determined the behavior of the evaporative industrial gas turbines power plants at part-load and for varying ambient temperatures [41]. In this work, water was injected until the compressor discharge air was saturated with water. Controlling the free power turbine was performed by altering the position of the nozzle guide vanes. The off-design analysis of the RWI cycle gas turbine was carried out in order to determine the efficiency and the power output at part-load and the ratings at high ambient temperatures. The theoretical model was validated against the industrial gas turbine ABB Cyclone, with a net efficiency of 32.8% and a power output of 12.49 MW. The agreement was good between the experimental and simulation results. The aftercooler was designed so that saturation always occurred. Design characteristics of the LP and HP expander was calculated using a theoretical model developed by the authors. Three different control strategies were chosen for the study; variation of the water flow to the aftercooler to maintain the same turbine exhaust temperature, variation of the water flow to maintain complete saturation of the air after the aftercooler, and combining water rate and variation of nozzle guide vanes positioned to maintain the following criteria.

- variation of NGV to maintain constant TET; and

- variation of water rate to reach saturation at the exit to the aftercooler.

The exhaust gas temperature was kept constant to avoid too high temperatures in the recuperator. The authors concluded that at a 50% load, only 3%

of the thermal efficiency were lost. On hot days with ambient temperatures of 40°C, the power output decreased from 17 to 14 MW while the efficiency decreased from 44.5% to 42%.

In 1998, Horlock presented the evaporative gas turbine cycle, EGT [107]. In this study, Horlock continued on the work carried out by Găsparović et al. and attempted to find the optimum pressure ratio for this cycle. In the first part of the study, Horlock described the theory of the EGT cycle from the same reasoning as Hawthorne and Davies [101, 102]. In the second part of the study, Horlock presented calculations of real cycles. The conclusion of this paper indicated that the closed cycle analysis is not valid for real cycles and cannot foresee the optimum pressure ratio for which the highest thermal efficiency is reached. The real analysis showed that the optimum pressure ratio which was rather low at around 8–10, was comparable to Bolland and Stadhaas results [30]. This would, according to Horlock, imply that industrial core engines are more suitable for the EGT cycles than the aero-derivative engines. Horlock also investigated the construction of the heat exchanger required to evaporated the water into the compressed air and a theoretical model was developed which predicts the behavior of the heat exchanger in an EGT [107].

In 2001, Bassily [20] presented theoretical studies for four different recuperative cycles; the recuperated cycle with evaporative inlet cooling and aftercooling (RDECEA), the recuperative cycle with evaporative aftercooling (REA), the recuperative cycle with evaporative inlet cooling (RDEC) and the recuperative cycle (R). Cooling the inlet air with evaporative coolers gives the RDEC an advantage of 0.7% compared to the (R) cycle. They both have a maximum efficiency at a pressure ratio of 5.8. The REA and RDECEA shows similar performance and achieves the maximum efficiency of 55% at a pressure ratio of 8.7. The specific power increased with the amount of water-injected into the system. All cycles showed an increased efficiency and the optimum compressor discharge pressure also increased with TIT. The RDEC and the RDECEA are the cycles which are most sensitive to the relative humidity, due to the fact that less cooling effect is achieved at higher relative humidity. The authors concluded that by adding an evaporative inlet cooling to the recuperative cycle, the thermal efficiency achieved a 2.85% increase. Applying evaporative aftercooling to the recuperative cycle increases the thermal efficiency by 6.4%. The author continued his work on water-injected cycles.

In 2001 Bassily presented theoretical studies of five different recuperative cycles [21]; the indirect intercooled reheat regenerative cycle with indirect evaporative cooling of the inlet air and evaporative aftercooling (DECIEA),

the intercooled reheat regenerative cycle with direct evaporative cooling of
the inlet air and evaporative aftercooling (IECIIEA), the intercooled reheat
regenerative cycle with evaporative aftercooling (IEA), the direct intercooled
reheat regenerative cycle with indirect evaporative cooling of the inlet air
(IECII) and the intercooled reheat regenerative cycle with direct evaporative
cooling of the inlet air (DECI). The best cycles are the (DECIEA) and the
(IECIIEA) which attains a thermal efficiency of 58% at a pressure ratio of
approximately 22. This specific power increases with increasing water in-
jection. As the turbine inlet temperature increased the thermal efficiency
reached 64%. The cycles with no inlet air cooling are less sensitive to the
relative humidity. Bassily concluded that by adding an indirect evapora-
tive cooler to the inlet air when the humidity is high, results in an increase
in thermal efficiency by 2.5%, which is 0.9% higher than direct inlet cool-
ing. Adding evaporative aftercooling would therefore increase the thermal
efficiency by 4.5%. Adding an indirect evaporative cooler to the inlet air
because of high ambient temperatures would increase the thermal efficiency
by 3% and adding an evaporative aftercooler would increase the thermal
efficiency by 5%.

Bassily also studied the performance improvements that could be ob-
tained by using an absorption inlet cooling combined with evaporative af-
tercooling [22]. The absorbtion unit used was a lithium-bromide cooling
system. The author concluded that an absorbtion cooling system would in-
crease the thermal efficiency by 6.6% compared to evaporative inlet cooling,
which increase the thermal efficiency by 3.9%. The author also concluded
that when using evaporative aftercooling with absorbtion cooling of the in-
let air, this leads to an improvement in thermal efficiency by 3.5% and an
increase in specific power by over 50%.

In 2002, Szargut presented a study on cogeneration of network heat in
the water-injected gas turbines [206, 207]. This study comprised the REVAP®
or EGT that De Ruyck et al. had presented. Szargut presented the cy-
cle without an aftercooler. The operational parameters are the compressor
compression ratio, coefficient of air excess, amount of injected water and the
temperature of the preheated air. It was concluded that the water-injected
cycle is good for cogeneration.

In 2002, Szczygiel presented a thermodynamic study of different HAT
(EGT) cycles [208] The studied cycles are:

- single point injection of water;

- multi-point injection of water;

- water-injected with an open blade which is cooled by the air taken from the mid-stage of the compressor;

- water-injected with applied final air cooler (aftercooler); and

- water-injected with final air cooler applied to the blade cooling air.

The author performed the calculations at three different temperatures; 1200°C, 1300°C and 1400°C. Szczygiel concluded that the use of an aftercooler decreased the thermal efficiency of the water-injected cycle by increasing the exergy losses.

In 2002, Aronis presented a study where low level heat is integrated in the combined cycle by means of evaporation [10, 11]. The condensate from the flue gases is pumped back into the system and injected into a humidification chamber prior to the combustion chamber. The main idea is to only compress as much air that is needed for the combustion. The surplus of air is then replaced with water. The study was carried out for three different turbine inlet temperatures while the pressure ratio and the amount of injected water was varied. Aronis concluded that it is possible to integrate low quality heat sources into a conventional combined power plant with increased thermal efficiency as a result. The highest efficiency of over 60% is achieved for low turbine inlet temperatures and recuperation of the moist air.

2.1.1 The REVAP® Cycle

A special cycle of the water-injected cycle is the REVAP®. The development of the REVAP® cycle began in 1991 with the feasibility study of a biomass fueled evaporative gas turbine for the University of Brussels [74]. This gas turbine engine operates at a pressure ratio of 7.0 and a turbine inlet temperature of 860°C. The compressed air enters a humidification tower where humidification water is injected into the compressed air. To enhance the performance direct injection of water is performed in the humidification chamber after the compressor. The humidified air is passed to the recuperator where it is heated to 860°C. The humidified air then enters the expander where the air expands to 483°C. The exhaust gases from the expander is then combusted with biogas until it reaches 900°C. An external firing temperature of 1000°C has also been tested. The results from this feasibility study showed that the externally fired EvGT attains an efficiency of 35.7% compared to the natural gas fired EvGT with an efficiency of 24.3%. The

authors concluded that it is possible to attain high efficiencies power output from the bio-EvGT cycle compared to the dry cycle.

In 1994, De Ruyck et al. presented further developments of the bio-EvGT project [75]. A UT 600 gas turbine with a pressure ratio of 8.5 and an turbine inlet temperature of 1000°C replaced the original gas turbine. The authors presented off-design calculations for the gas turbine and they also estimated the amount of injected water which leads to surging.

In 1996, Bram and De Ruyck presented a study which compared; a dry gas turbine with intercooler, an evaporative gas turbine without intercooler, an evaporative gas turbine with intercooler however the water is rejected, an evaporative gas turbine with intercooler and water injection and an evaporative gas turbine with intercooler and heat recovery [32]. This study led to a new cycle configuration called the REVAP®. The authors calls this cycle the REVAP® which stands for regenerative evaporation cycle [73]. The REVAP® cycle does not have a humidification tower. The water which is added to the compressor discharge air, is instead evaporated into the compressor discharge air in the tubes of the economizer, aftercooler and intercooler, as the two-phase flow passes through the heat exchangers. Therefore the heat exchangers have dry air on one side and a two-phase flow of water and air/steam on the other. The humidified air is then recuperated prior to combustion. De Ruyck claims that this cycle has the same performance as the EvGT and CHAT cycle. The authors further explained that the net resulting thermal efficiency is 54% and the two-phase flow is required to be further investigated. The net resulting thermal efficiency is 54%. Bram et al. concluded that optimal evaporative gas turbines yield performances similar to those of combined cycles.

2.1.2 Wet Compression

One water-injected cycle which is in operation today and commercially available, is the wet compression cycle [67,202]. The principle of wet compression is to inject a mist of water droplets into the airstream prior to the compressor. The mist cools the temperature of the air by saturating the air. In wet compression, more water is injected into the compressor than the air can contain. This means that water droplets will enter the compressor. The water droplets which have not yet evaporated, will do so within the first couple of stages in the compressor. This type of water-injection have been used for fighter aircrafts onboard aircraft carriers. The additional boost gained by injecting water is used to aid aircraft during take-off [152]. Washing of gas

turbine compressors also utilize water injection. The washing principle is to inject water which hit the blades and washes them [110].

The concept of wet compression has been used in different facilities with different gas turbines. The wet compression systems have shown an increase in power output with 15–20%, increasing the thermal efficiency by 1.5–3% [202]. Spray nozzles have been installed in front of the compressor and tests with the General Electric Frame 7E have shown that there is no problem with stall during operation [202].

General Electric also have a commercial engine with wet compression, the LM6000 SPRINT which utilizes spray injection prior to the compressor inlet and between the LP and HP compressor [67]. This results in an increase in power of 8% at ISO conditions. General Electric has also tested the impact of water injection on blade life. The tests showed corrosion on the first 3 blades which occurred after four months and after eight months, the corrosion rates have significantly decreased. No corrosion could be found on stages four through to 14. The blade life of the three first stages is today 16,000 hours however GE aims for 25,000 hours.

The concept of wet compression in axial compressors was first patented in 1948 by Kane when he patented the first evaporative cooled compressor [124]. In his patent, Kane injected water into the compressor at different locations with multiple spray nozzles. Kane considered both the injection into the compressor inlet and the injection of water throughout the compressor. The purpose of Kane's patent is a reduction of the compression temperature, resulting in a power boost.

In 1952, Hensley presented an article that described the theoretical performance with inlet water injection of an axial-flow compressor [103]. Hensley performed calculations of compressors with the pressure ratios of 4, 8 and 16. Continuous saturation of an air stream is assumed throughout the compression process. The theoretical model showed that the specific power of the engine increased with water injection.

In 1963, Hill presented theoretical investigation of the thermodynamic effects of coolant injection upon axial compressor performance [105]. This method solved the performance of a wet compressor based on dry operation. Hill reported that tests have shown that the size of the droplet is not essential to the performance of the axial compressor. The mixing and evaporation seemed to depend much more on geometry and speed of the compressor than on initial drop size and distribution. Hill also reported that injecting more than 2–3% water-to-air mass ratio would result in non-complete evaporation within the compressor. Hill also reported that experience with wet compression has shown that the average residence time of

the air within the compressor is so short that neither continuous saturation nor isothermal compression are even approximately realized. Hill tested his thermodynamic model against experimental data from two General Electric's turboshaft engines of different size and pressure ratio. The model predicted the performance of a wet compressor with the same degree of accuracy as off-design prediction procedures.

In 1996, Arsen'ev and Berkovich presented calculations of water injection into the compressor [12]. The calculations were conducted for a 150–200 MW gas turbine. The calculations were performed on every stage in the compressor starting from the guide-vane row. The variables calculated were the velocities and trajectories of the droplets, the amount of moisture separated on the blades and the compressor casing and the amount of water evaporated. Additionally, a computational technique was developed by Arsen'ev et al. to calculate the compressor characteristics which takes into account the moisture in the flow path. Arsen'ev et al. then calculated the characteristics of different compressors. These calculations showed major differences in droplet motion and evaporation between the compressors. Arsen'ev et al. specifically pointed out differences in the value of the hydrodynamic losses and the effect of water injection on the compressor characteristics. These losses are caused by different dimensions of the compressor flow path, the location of the point of water injection, the compression ratio, and the amount of water-injected. The evaporative cooling effect decreases the volumetric flow rates in the compressor stages, particularly in the last stages. As a result, the working point on the characteristics of each stage moves toward lower discharge coefficients and higher compression coefficients. For the compressor as a whole, its isodromes moved toward higher compression ratios and higher flow rates. The decrease in power consumed due to evaporative cooling of the air in the process of compression, exceeds the additional hydrodynamic losses due to the moisture. Arsen'ev et al. concluded that the net effect of wet compression is positive and an increase in compressor efficiency is expected with up to approximately 4% in relative value. The most intensive increase in efficiency and in compression ratio takes place when a small amount of water is injected (up to about 0.5% of the air flow rate). The above values are calculated using a compressor where the discharge coefficient is not designed for wet compression. If the compressor was designed for wet compression and the discharge coefficient is modified for this working mode, the values would be higher.

Arsen'ev and Berkovich also describe how the water injection influenced the efficiency of the total gas turbine. With a water injection of 0.5–2%, the power output of the installation increased by 7.5–14% and the increase in

efficiency levels off at 3.5% in relative values. If the discharge coefficients of the stages becomes optimal with water injection, the corresponding increase in power will be 8.5–17% and in efficiency 4–6.5% in relative value. Arsen'ev and Berkovich concluded that the mechanical losses are small and it is sufficient to design the compressor after optimal discharge coefficients. Arsen'ev and Berkovich calculated the influence of water injection on a combined cycle and it was found that there was no or very little effect on the bottoming cycle. Arsen'ev and Berkovich also showed with calculations that the erosion rate is minimal. One reason for this is the circumferential speed which is much lower in a compressor than in the steam turbine.

In 2001, Horlock presented a theoretical model for the prediction of the compressor performance with water injection [106]. Horlock concluded from his calculations that the later evaporating stages in the compressor moves away from their design point and may go into stall.

In 2002, Mathioudakis presented an analytical study of the effects of water injection after the compressor [149, 196]. The author compared the analytical results with experiments conducted on a Siemens V64.3 engine. Water was injected after the compressor to reduce the emissions. The author concluded that the theoretical model developed satisfactorily and determined the performance of a gas turbine during water injection. In 2005 Mathioudakis studied the inter-stage injection of water into the compressor [195].

In 2003, Härtel and Pfeiffer studied the effect of wet compression [108]. The authors used two different models; one thermodynamic model which assumes thermodynamic equilibrium and one heat and mass transfer model. Härtel and Pfeiffer verified the results from the models with experiments conducted by Utamura. The author did not take into account liquid film build-up on the compressor blading. Härtel and Pfeiffer concluded that wet compression is more beneficial for compressors with low polytropic efficiency. This finding contradicts other studies in the literature. The authors concluded that the droplet size is important for the effect of wet compression. A water spray of 1% of the compressor inlet air reduced the compression work with 7%. The smaller the droplet, the larger will the increase in performance. The authors also concluded that precaution should be taken when analyzing the results from theoretical models, as more extensive testing is required before any conclusions can be made.

In 2004, Li and Zheng presented a stability analysis of wet compression in compressors [134].

In 2004, Meacock and White presented a theoretical model to predict the behavior of a multi-spool engine during water injection [152]. The water

injection leads to higher pressure ratios and increased mass flows through the gas turbine. The result is that the earlier stages of the compressor shifts towards choke and the rear stages approaches towards stall. The low-pressure compressor is working at a very poor aerodynamic performance. The authors concluded that water injection leads to a substantial power boost and a slight increase in thermal efficiency.

In 2005, Hale et al. presented a one dimensional theoretical model for predicting the performance of a gas turbine engine when steam is injected into the compressor [99]. The theoretical model for the steam injection takes into account that the property state changes as it passes through the compressor.

2.2   Steam-injected Cycles

The second way to use water-air mixtures is the steam-injected gas turbine, STIG. In the STIG, the hot exhaust gases from the gas turbine heats water to produce steam in a heat recovery steam generator. The steam is then led back to the gas turbine expander. There have been many different ways of injecting steam. In the beginning steam was injected directly into the combustor liners. Presently, steam is injected into or around the fuel nozzles to reduce the NO_x levels [186–189]. Today, the STIG cycle is today commercially available around the world.

The first steam-injected gas turbine was patented by Miller in 1951 [156]. This cycle used the flue gases to boil water in an unfired boiler. Miller injected the steam into the regenerator to increase the mass flow through the expander. Miller believed that it was possible to obtain an increase in efficiency with 3%. In the patent, Miller also described a supplementary-fired STIG combined cycle. Kydd and Day continued and patented the concept of steam injection into fixed component gas turbines in 1972 [127].

In 1978, Boyce et al. presented a report that described the theoretical background for the development of an externally fired steam-injected gas turbine [31]. Boyce addressed the problem of corrosion due to high sulfur content in the fuel. This sulfur together with high humidity in the exhaust, can cause corrosion when the dew point is passed. Boyce et al. concluded that an injection of 5% steam will compensate for the pressure losses in the system.

In 1979, Fraize and Kinney presented a study performed by The US Department of Energy [85]. The authors studied three different thermodynamic cycles; the open cycle gas turbine with a condensing steam bottoming

cycle, the open cycle gas turbine with steam injection and the open cycle gas turbine with steam injection non-condensing steam bottoming cycle. The pinch-point in the heat recovery steam generator was set to 30°C and the minimum exhaust gas temperature was set to 135°C. The turbine inlet temperature was set at 1444°C. Fraize and Kinney performed parameter variations by varying the pressure ratio in fixed steps of 8, 12, 16 and 20. Without steam injection, the thermal efficiency was 30.2% and 38.0% respectively. The study did not address water recovery from the flue gases and therefore this water consumption is a large capital cost for the power plant. The authors concluded that the STIG cycle is competitive as a peak shaving unit.

In 1981, Brown presented a theoretical study whereby the steam-injected gas turbine is compared with a combined cycle [37]. The pressure ratios were varied between 8 and 30. The authors put criterions on the exhaust plumes and the humidity of the exhaust gases. The authors concluded that there is little cost benefits of the STIG cycle compared to the simple gas turbine.

In 1987, Burnham et al. presented a description of the on-engine and off-engine equipment [38]. The results were that the NO_X emissions significantly reduced below 25 ppm. With steam injection, output power of the LM5000 gas turbine increased from 29.9 MW to 41.9 MW and thermal efficiency increased from 36.0% to 41.8%.

In 1986, Cerri and Arsuffi presented a study of the STIG cycle which incorporates a desalting plant [46]. The authors concluded that steam injection raised both the thermal efficiency and the specific power output, highlighting that it is possible to include a desalting plant based on distillation processes. The STIG cycle has an optimum efficiency at lower pressure ratios than simple cycle gas turbines. Cerri and Arsuffi continued to study the STIG cycle with desalination plants. In their study in 1988, sea water was used as water to the STIG cycle [48]. They varied the pressure ratio from 3–30 and the turbine inlet temperature from 1000°C–1400°C with steam-injection rates of 0.3. The authors concluded that specific power output can be increased by 50–80% and thermal efficiency can increase by up to 40–50% compared to a simple gas turbine cycle.

In 1987, Cerri and Arsuffi presented a study of steam-injected gas generators with and without reheat [47]. The study investigated the thermodynamic performance of the gas turbine and also the modifications required in order to handle the increased mass flow rates. The authors concluded that high efficiencies could be achieved by using reheat in STIG cycles and therefore to accommodate the increased mass flow, the gas expander has to be modified.

In 1988, EPRI conducted a study where the combined cycle power plant was compared to the steam-injected gas turbines. This study was presented in the EPRI journal [56]. The result was that for the large, 350–400 MW category, the combined cycles had considerably lower fixed costs and lower capital costs than the STIG plant. The main cost factor was the high cost of the LM5000 steam-injected unit whereby it cost about twice as much on a kW basis, as the heavy-duty units used in the combined-cycle plant.

In 1988, Baken and Haspel investigated the operating principle and regime of the STIG concept [16]. Based on energy balances, a method was presented for optimizing the design and operation of STIG units in cogeneration for the Netherlands. The authors concluded that when supplementary firing was used in comparison to a simple cycle unit, the power and heat generating efficiency of a STIG unit decreased due to the injection of steam. The authors did not use a flue gas condensing unit and the exhaust gas energy was therefore not utilized. The authors concluded that the STIG cycle was not a suitable option for cogeneration, however energy costs can still be saved. The main conclusion is that the steam-injected gas turbine cogeneration units in the Netherlands are required to be operated as peak-shaving plants.

In 1987, Larson and Williams presented an overview of the steam-injected gas turbine [128]. The presentation included both a historical aspect and also a thermodynamic and economic analysis. The presentation explained the mechanisms behind the efficiency and specific power increase. The gas turbine studied is a Allison 501–KB, which has a power output of 3.4 MW and a thermal efficiency of 24%. The injection of steam increases the pressure ratio of the engine with 22% and increases the power output to 4.6 MW and the efficiency to 34%. The injection of steam in the combustor made it necessary to add more fuel to heat up the additional bulk flow. This extra heating lowered the gas turbine efficiency to 31%. The specific heat of steam is 25% higher than for air alone. This made it possible to extract more work and again the power output and the efficiency increased to 5.4 MW and 35% respectively. The thermodynamic evaluation indicated that the optimum steam-to-air injection ratio is 0.17. Calculations by General Electric showed that the potential of a intercooled LM 5000 steam-injected gas turbine is a power output of 110 MW and a thermal efficiency of 47–48%. The authors concluded that the steam-injected gas turbine is an important technology for the transition to the Post-Petroleum Era.

In 1988, Larson and Williams performed a study concerning the use of biomass in steam-injected gas turbines [129]. The study focused on a STIG cycle with a biomass gasifier that supplies fuel to the gas turbine. Lar-

son and Williams also performed an economic evaluation of the potential of introducing the concept to a sugar factory in Jamaica. The authors used two different gas turbine models to evaluate the biomass STIG, the Allison 501–K and the ASEA–STAL GT–35C. Temperature limits in the gasifier and the heat exchange equipment limits the turbine inlet temperature of the STIG, which in turn reduced the produced power and the thermal efficiency of the STIG. The thermal efficiency dropped by 10% units compared to a regular STIG. The authors concluded that the IFSTIG would therefore produce electricity 25–30% more efficiently than a conventional steam turbine facility. The gasifier STIG, GSTIG, would be more efficient than the indirectly fired STIG cycle, due to the increased turbine inlet temperature of the GSTIG. The performance of a biomass GSTIG is 10% lower than for a conventional coal GSTIG due to lower efficiencies in the biomass gasification process. The authors concluded that the use of a GSTIG at sugar factories provides technical and economical benefits compared to commercially established condensing extraction steam turbine systems. The authors also concluded that a pilot plant needs to be built in order to prove the technical feasibility potential of the system. The R&D costs of the project would be modest due to prior knowledge of coal gasification and a focus should be on minimizing the feedstock processing.

In 1989, Kolp and Moeller presented the results from an evaluation of the installation of a LM 5000 steam-injected gas turbine [126]. The result was that the specific power increased from 33 MW to 42 MW and the electrical efficiency increased from 36% to 42%. The data taken during this period indicated that plant availability was 95.6% with steam injection versus 96.0% with water injection for NO_X reduction. Reliability was 99.5% with steam injection and 98.5% with water injection. In addition, hot section distress was significantly reduced with steam injection. The conclusion indicated that massive steam injection has no deleterious effect on either gas turbine availability or reliability and in fact improves hot section component life. The capital costs of the engine is 30% of the comparable cost of a combined cycle.

In 1990, Negri di Montenegro calculated the performance of a STIG cycle with an in-house code. The result was that it gave the same result as other programs [159].

In 1990, Ito et al. presented a theoretical model that described the introduction of a steam-injected gas turbine into a cogeneration plant [112]. The authors presented a case study whereby they used the previously developed theoretical model. It was concluded that the installation of a STIG cycle greatly improved the flexibility between the heat and power production,

which in turn reduced the capital costs. The authors presented an operational strategy which utilized the superior flexibility and it was concluded that the STIG cycle is an economically viable alternative to the simple cycle with heat recovery system.

In 1991, Lundberg presented a study concerning the latent heat utilization in steam-injected gas turbines [142]. Lundberg used the exhaust gas energy to supply heat for the district heating system. Three different systems were introduced with two electric heat pumps, one with different coefficient of performance and one with an absorption heat pump. The author concluded that the absorption system provides the maximum overall efficiency but the poorest thermal efficiency.

In 1994, Ito et al. performed a numerical study on a plant for district heating and cooling i.e. cogeneration plant [113]. The authors described how the steam-injected gas turbines can improve the economic and energy-saving characteristics of a power plant. The authors also determined the capital cost of steam-injected gas turbines. The authors concluded that the installation of a STIG cycle greatly improves the flexibility between the heat and power production, which in turn reduces the capital cost.

In 2000, De Paepe et al. presented a study of steam-injected gas turbines [71] highlightning different configurations of the steam-injected gas turbines; the reheat engine, the intercooled engine, steam cooling and regeneration of the exhaust gases to the feedwater. The authors paid particular attention to gas turbine cooling models and used the thermodynamic cooling model previously developed by El-Masri. The author verified the gas turbine cooling models to four different gas turbines and trimmed the model by fixing the turbine outlet temperature. A table presented the data obtained from the calculations. The authors also validated the developed models on two steam-injected gas turbines. The blade temperature was set to 850°C and the required amount of cooling flow for the four gas turbines was between 9% and 13% of the compressor air flow. The authors presented calculations with parameter variations of the turbine inlet temperatures at 1100°C, 1250°C and 1400°C for different pressure ratios. A pinch-point of 40°C was set between the turbine exhaust and the produced steam. The author concluded that the optimum efficiency of a steam-injected gas turbine was 49%. Using steam as coolant, a maximum efficiency of 52% was achieved. Adding intercooling, reheat or recuperation increases the efficiency however the complexity of the cycle increased to much which meant that it was not a viable option.

In 2000, De Paepe et al. presented a study of water recovery in steam-injected gas turbines [72]. The study investigated three different types of

water recovery systems; water cooled condenser and water to air cooler, air cooled condenser, direct contact condenser and water to air cooler. Models were developed to accurately determine the condensation process. The condensers were divided into segments and the heat and mass balance was solved for each segment. The result from one segment was used as input to the next segment. It is assumed that the temperature increase of the coolant water is 75% of the temperature increase that would occur if cooling water and exhaust gases leave the segment at the same temperature. The calculation methods were validated on test rigs. The relative error between calculations and measurements is 3% maximum for the exit temperature and 10% for the condensate mass flow rate in case of the finned tube type condenser. For the direct contact condenser, these figures are respectively 4% and 1%. The authors concluded that the finned water-cooled condenser with water to air cooler is preferable due to its small size. Economics showed that the air cooled condenser is the best choice of the three condensation facilities.

In 2001, Fischer et al. presented a study of different cooling techniques for STIG cycles [82]. The authors make a distinction between three cooling strategies for a part-STIG cycle with reheat; partial STIG with fixed indirect cooling where the steam-injected cools the cooling flow, partial STIG with adjusted indirect cooling where additional steam or water cools the cooling flow and partial STIG with direct adjusted cooling where steam is injected into the cooling flow. It is determined that the different ways of cooling the turbine blades differ only slightly. The limiting factor for steam injection was the compressor surge margin. In spite of this, a 30% increase in power can be realized with the partial STIG.

In 2002, de Biasi described the Ukrainian Aquarius project [66]. The basis of the Aquarius system is a steam-injected gas turbine. A flue gas condenser condenses the water from the flue gases. The water is collected and chemically treated before it is returned to the main water tank. This project delivered three different gas turbine system; the Aquarius 16 which delivers 16 MW, the Aquarius 25 at 25 MW and the Aquarius 40 at 41 MW. This system has over 11,000 firing hours and it is reported that a simple cycle gas turbine can increase its power output by 50–80% with an increase in efficiency between 25–35%. The water quality was measured at different locations in the gas turbine. Measurement showed that the acidity level increased from an initial pH-factor of 7.0 to 6.5–6.0. Based on operating experience with the Aquarius plants, it is not expected that there would be a problem with water contamination or a need for special treatment procedures.

In 2001, Lupandin et al. presented the experimental result of a steam-injected gas turbine system equipped with a water recovery system [143]. The Aquarius project has accumulated over 12,000 operating hours. To test the water recovery, the authors built a test facility with a small gas turbine equipped with no steam injection but with water recovery. To simulate high water content in the exhaust gases, 30% of the exhaust gas flow passed through a heat exchanger network. The heat exchanger network produced steam that was mixed with the remaining exhaust gases. The result was high humidity gas flow. The authors found that 100% recovery of the water could be obtained. The authors also tested the build-up of impurities and the influence of ambient temperature on the water recovery efficiency by building a new test rig. A combustor produced the hot exhaust gases. The authors did not find any indication of corrosion due to the effect of impurities presence in the condensed water. The authors concluded that full water recovery is obtained when the condensing water is less than 30°C. The optimum injection rate for maximum NO_X reduction was 150% of the fuel flow. At rated power output the NO_X levels never rose to values above 24 ppm@15% O_2. CO emissions in the exhaust gas were measured in the range from 80 to 24 ppm@15% O_2 for the Aquarius power plant operation from idle to rated power through all test steam injection rates.

In 2002, Blanco et al. presented and discuss the results of a comparative economic analysis between the costs of installing and operating a water recover system and the costs of buying and treating water on a regular basis during the lifetime of a steam-injected gas turbine [29]. In this system, a LM 2500 operates with steam injection and two different water recovery systems, a packed tower and a finned tube condenser. It is shown that the water recovery system improves the economics of the power plant. The energy consumption of this type of system is also less than 1% of the power output and it is not a restriction for installing a water recovery system. It is concluded that installing a water recovery system is far better then purchasing treated water.

In 2002, Blanco et al. studied a water recovery system for steam-injected gas turbines [28]. A computer model was developed which allowed for rapid and accurate determination of optimum sizes, power requirements and initial capital costs of the heat exchangers in a water recovery system. Two different water recovery systems were tested; a packed tower/air cooled heat exchanger water recovery system and a finned-tube condenser/air cooled heat exchanger water recovery system. The power requirement for the water recovery systems were 2.2% and 1.9% of the power output from the gas

turbine. The initial cost of the water recovery system was 9.6% and 10.7% higher than for a normal steam-injected gas turbine.

In 2002, Akmandor et al. used genetic algorithms to optimize a steam-injected gas turbine plant [2]. This optimization was also carried out on a combined cycle and the two results were compared. It could be concluded that no steam injection was needed in the case of the combined cycle in order to obtain both maximum power output and maximum thermal efficiency. However, for the simple gas turbine, full steam injection was needed to obtain maximum power output. To obtain maximum thermal efficiency a steam injection of 79% was required.

2.2.1 The CHENG Cycle

A different type of STIG cycle is the CHENG cycle. The CHENG cycle is a steam-injected cycle where the amount of steam injected to the cycle is optimized based on best thermal efficiency. Dah Yu Cheng patented this cycle in 1978 and it is commercially available [50, 52].

In 1983, Messerlie presented test results of a steam-injected gas turbine [154]. The author tested an Allison 501–KB with two steam manifolds around the outer casing. The authors concluded that the CHENG cycle has the potential of increasing the thermal efficiency with 40% and the power by 60%. No adverse effects could be found by injecting steam into the gas turbine. Additionally, the emissions were not measured but calculations showed that the injection of steam lowers the emissions of NO_x.

In 1984, Digumarthi et al. presented the results of an experimental evaluation of the CHENG cycle [78]. The authors equipped a Garrett 831 gas turbine engine with steam injection equipment. The Garrett 831 have two radial flow compressor stages and three axial turbine stages. The authors modified the combustion chamber to allow for controlled steam injection. The steam injection was accomplished through eight steam nozzles directed towards the compressor discharge to obtain an enhanced mix of steam and air. The authors found that the CHENG cycle was insensitive to the ambient conditions and therefore delivered high efficiencies and power irrespective of the ambient conditions. The steam injection raised the turbine efficiency from 17.5% in simple cycle mode to 23.0% in CHENG mode. The authors concluded that both the capital investment and cost per unit energy are reduced compared to a normal Brayton cycle.

In 1991, Strasser presented the CHENG cycle in cogeneration mode [205]. The authors presented some results from experiments but mostly they presented the layout of the cycle and the advantages of the CHENG cycle.

In 2002, Cheng and Nelson described experimental results on the hot parts of a CHENG gas turbine cycle [51]. The experiments are conducted during injection of high temperature steam, approximately 18%. Steam was injected at different locations in the gas turbine and it was shown that the performance did not change depending on where the steam was injected. The measurements of the blade temperatures did not indicate any dramatic temperature changes due to the steam injection. It was concluded that the pressure ratio of the gas turbine under steam injection, should be raised due to the additional steam mass flow, and should only be limited by the compressor surge margin and not by the metal temperature increase.

In 2002, Nelson and Cheng presented calculations of a mid size CHENG cycle, +30MW [170]. The calculations showed that the ambient temperature did not impair the CHENG cycle efficiency as much the simple cycle. Nelson and Cheng also described in brief the starting technique where nitrogen pressurizes the cold drum which speeds up the rate temperature increase of the. A CLN™ technology for decreasing the emissions is also included in the analysis. The authors claim that this technology efficiently reduces both CO and NO_x.

2.3 HAT Cycles

Until 1981 the injection of water into gas turbines have been performed by directly injecting water into the airstream. In 1981, Sayama and Naka-mura [198] patented the first humid air turbine, HAT, where the circulating humidification water flow is larger than the water vapor that evaporates in the humidification tower. In their patent, Sayama and Nakamura used two humidification chambers to humidify the compressed air.

In 1982, Rao patented a similar process as that of Sayama and Naka-mura [182,183]. In the humid air turbine, water is circulated around a heat exchanger network. The water is heated by utilizing internal heat from the compression work and the hot exhaust gases. The heat which is transferred to the water, then enters a humidification tower where the compressed air encounters the hot water. Due to temperature and composition gradients within the tower, a process of heat and mass transfer begins inside the tower. Water therefore evaporates from the water surface and into the airstream and the humidification process makes it possible to have more mass flow through the work producing gas expander than the flow that passes through the gas compressor which makes it possible to produce more power from the HAT cycle than from the simple cycle. This additional power and the heat

exchanger network makes it possible to achieve high thermal efficiencies. A small laboratory of the humid air turbine currently exists at the Faculty of Engineering at Lund University and in the near future a laboratory will be functional at Hitachi in Japan.

In 1983, Mori et al. presented calculations of a water injected gas turbine based on Nakamura's patent [160]. The result was a thermal efficiency of 52.8% at a turbine inlet temperature of 1100°C.

In 1990, Rao and Joiner presented a technical and economic evaluation of the humid air turbine cycle with integrated gasification, IGHAT [184]. Two gas turbine manufacturer, ABB and General Electric, participated in the study. Rao et al. concluded that the part load behavior of the HAT cycle is superior to the combined cycle. This partly due to the twin-shaft arrangement of the HAT cycle and also due to the regenerative nature of the cycle.

Rao et al. also presented the integrated gasification humid air turbine (IGHAT) as a competitor to the Integrated Gasification Combined Cycle [57, 63,184]. The authors described that the IGHAT will have 15%–21% lower cost of electricity than the corresponding IGCC for a General Electric MS7001F. The advantage of the IGHAT is that it effectively uses the low level heat from the gasifiers which would otherwise be lost.

In 1991, Rao et al. presented the HAT as a closed cycle for use in nuclear power plants [185]. The optimum thermal efficiency of the cycle is 39% at a pressure ratio of 4.8 where it produced approximately 227 kW/kg/s.

In 1992, Day and Rao presented a concept where a HAT cycle was adapted to a Pratt and Whitney engine FT4400 [64]. The off-design performance of the HAT cycle was compared to that of a combined-cycle. The result was that the heat rate advantage increased from 5% at a full load to 20% at a 50% load. It is also shown that the HAT cycle has superior performance compared to a simple cycle at different ambient conditions. A flue gas condenser is also considered in this study.

In 1993, Rao presented an evaluation of different advanced gas turbine systems [180]. The aim of the study was to compare different advanced gas turbine cycles with the same base assumptions and the cost and part load behavior established.

Morton described the HAT in a report which describes the humid air turbine (HAT) [161]. In this article Morton shows the humidification process within the humidification tower. According to Morton a boiling curve for water that is not horizontal on a T-s diagram has been constructed due to the humidification tower. The authors conclude that the HAT cycle can achieve a thermal efficiency of 53.7% at a specific power output of 288 kW/(lb/s),

compared to a combined cycle in the same size range which has a thermal efficiency of 49.5%.

In 1993, Rao et al. presented a feasibility and assessment study of the humid air turbine FT 4000 [181]. The objective was to optimize the integration of the HAT circuit to the FT 4000 gas turbine and to also investigate the commercial viability of the HAT cycle. The fuel used in the cycle is syngas with natural gas as backup fuel. The study shows that IGHAT has 30% less NO_x emissions.

In 1993, Stecco et al. presented a study of the Humid Air Turbine (HAT) [203, 204]. Stecco et al. studied three different configurations of the HAT cycle; the ordinary HAT cycle patented by Rao (cycle I), a HAT cycle that uses a cooling system to cool the water flow from the evaporator which enters the compression system (cycle II) and a HAT cycle that uses cooling system to cool the total water flow (cycle III). The authors studied the influence of the pressure ratio between the compressors and allowed it to vary between 0.5 and 2, which corresponds to a pressure ratio of between 4.5 and 18. Stecco et al. also studies different humidification ratios at the humidification tower exhaust. The author concludes that the optimum cycle for optimum efficiency is cycle II which has a thermal efficiency of 58% at a turbine inlet temperature of 1273K, relative humidity of 40% and an optimum pressure distribution between the compressors of 0.5 (β_2/β_1). The absolute optimum configuration achieved a thermal efficiency of 54%–56% at a specific power output of 340–420 kW/kg.

In 1995, Chiesa et al. compared different mixed gas-steam cycles [53, 148]. The study included the following cycles; intercooled, steam-injected gas turbines, recuperative water-injected cycle (RWI) with an evaporative or a surface intercooler and the humid air turbine (HAT or EvGT). These are mainly based on aero-derivatives and they have been optimized based on the pressure ratio of the low-pressure compressor.

Chiesa et al. details the influence of different parameters, which have been chosen to match a specific engine. The authors specially discuss the influence of an intercooler on the cooling flows and the thermal efficiency. If intercooling was used, higher TIT can be used since colder air is supplied to the turbine blades. The authors conclude that intercooling, coupled with the higher pressure ratios and the higher turbine inlet temperatures made possible by the lower compressor temperature, can substantially enhance the efficiency and the power output of both simple and combined cycles based on current aero-derivative engines. On the contrary, intercooling did not lead to any efficiency improvement of heavy-duty-based combined cycles, although it still resulted in higher power outputs.

For the RWI, the spray intercooler resulted in less thermal efficiency than for the RWI with surface intercooler. This was due to the surface intercooler which cools the air temperature to a much lower temperature, therefore decreasing the compressor work. The specific power is however greater with the evaporative intercooler due to the increased humidity in the airstream. The efficiency of the EvGT cycle is between 2–3%-points higher than for the RWI cycle and the specific power is slightly higher in favor of the EvGT cycle. Chiesa concluded that the EvGT has the best efficiency of all investigated cycles, both for heavy-duty and aero-derivative engines. The efficiency of the EvGT is 1.5%-points higher than the CC with a 3 pressure reheat bottoming cycle and a condenser pressure of 0.05 bar.

In 1996, Rosén and Olsson presented a humidification process for diesel engines, HAM engines, which reduced the NO_X emissions [194]. The concepts includes humidification of the air before the engine. The authors performed tests with a Volvo THD–100 diesel engine equipped with a humidification circuit. The authors claim that the humidification process reduces NO_X emissions and particulate emissions and improve the thermal efficiency. The test results showed that with a water addition level of 10% the thermal efficiency rose by about 0.4% to 3%. The NO_X emissions reduced by 55–75% and the CO emissions increased by 0–25%. The authors also detail the possibilities of injecting a mixture of ethanol and water into the airstream. This would make it possible to increase the thermal efficiency of such cycles as the latent heat of vaporization is removed prior to the cylinder.

In 1997, Gallo et al. investigated the blade cooling in HAT cycles [89]. Gallo pointed out four different locations where the cooling flow could be extracted; the high pressure compressor exit, the aftercooler exit, the evaporator exit and the recuperator exit. Gallo et al. performs parametric studies in order to determine the effect of the cooling flow injection point. A conclusion is made that it does not matter where the cooling flows are extracted from as the resulting efficiency is nearly the same. However, the cooling flow should not be taken from the recuperator exit due to high temperatures. Gallo also concludes that extracting the bleed flows following the evaporator gives the highest efficiency and the lowest water consumption. Gallo does not investigate the effect of taking out cooling flows at lower pressure ratios for turbine stages at lower temperatures.

In 1999, Gallo investigated the potential and difference between the simple cycle, recuperative cycle, intercooled and recuperated cycle, the STIG cycle, the HAT cycle and the combined cycle [88]. Gallo used blade-cooling models to describe the expansion of the turbine. If the cycle incorporates an intercooler, Gallo optimized the intermediate pressure for best efficiency.

Minimum temperature difference between cold and warm streams was set to 25°C. Gallo concludes that the HAT cycle consistently has the best efficiency. Gallo also concludes that the intercooled/reheated cycle is a competitor to the STIG cycle, since it has approximately the same thermal efficiency to the STIG cycle which produces more power. Gallo also details the water quality for the different cycles. Gallo suspects that the HAT cycle will be required to use the same degree of water purity as the STIG cycle. Gallo adds that water entrainment in the flow is not an issue for the HAT cycle as the water will evaporate in the recuperator, therefore never reaching the combustor and turbine. Gallo also acknowledges the necessity for water recovery in order to make the system more economically feasible.

In 1999, Di Maria and Mastroianni presented a theoretical study of a second law analysis of the HAT cycle and its components. They also performed an exergetic analysis of the effect of different bleed points for blade cooling on cycle performance and on cooled expansion [76]. The authors considered a HAT cycle with intercooler, aftercooler and economizer. The cycle also used a flue gas condenser to recover the heat from the flue gases. The water that condensed was brought back into the cycle. A part of the water from the humidification tower was cooled in an external cooler and mixed with the make-up water and then circulated through the intercooler and the aftercooler. To model the gas turbine expansion thermodynamically, the authors used the cooling model developed by El-Masri. The authors concluded that the humidification process, which took place in the humidification tower, is an efficient process. Additionally, the largest exergy destruction were found in the combustion chamber.

In 1999, von Heiroth et al. developed models which facilitated the evaluation of a HAT pilot plant to be built at The Faculty of Engineering at Lund University [219]. The paper included detailed models of the components in a HAT cycle. The flue gas condenser and the economizer were not modeled and the models are implemented in the software IPSEpro™. The humidification tower is modeled according to the Mickley approach and the theoretical model calculated the height of the tower as detailed by Richardson and Coulson [58].

In 1999, Lindquist presented the first experiments on an evaporative gas turbine [135, 139, 140]. This thesis presented the EvGT pilot plant from the simple cycle mode through the recuperated mode and finally the evaporative mode. The gas turbine used was a VT 600 equipped with a bleed-off valve to bleed off the extra mass flow caused by the evaporation process. The experiments were successful and it was shown that it is possible to operate an EvGT with fast start-up times and high efficiency.

In 2000, Kim et al. presented a study of the influence of the ambient conditions on the performance of the humid air turbine [125]. In this study, the authors assumed a pinch-point at the top and a pinch-point at the bottom of the tower. This meant that the working line can intersect the saturation curve resulting in the conservation equations within the tower to be violated. The authors concluded from this study that an increase in temperature slightly increases the specific work of the cycle. This happens as more water evaporates in the cycle. The authors concluded that the HAT cycle have better part load behavior than the combined cycle.

In 2000, Jordal and Torisson presented a comparison between different cooling techniques for a gas turbine [122]. The authors studied the difference between dry air, humid air and steam as a cooling agent for gas turbine vanes. The authors used a model developed by El-Masri to determine the cooling flows. Jordal and Torisson investigated four different cycles; the simple cycle, the combined cycle, the steam-injected gas turbine and the humid air turbine. The authors conclude that the combined cycle is the cycle that would benefit the most from a redesign to include a closed loop steam cooling system which would gain approximately 1.5% points. The simple cycle and the humid air turbine without intercooler would also benefit from the redesign. It is not sure whether the HAT with intercooler and the STIG would benefit from a redesign.

In 2000, Carcasci et al. presented a study of a semi-closed HAT cycle which aimed at capturing the CO_2 emissions [43]. In the SC–HAT, the economizer was substituted by the heat load required for the regeneration of the amine scrubbing solution, which allowed to reach an exit temperature of the gas stream in the range of 80°C. This meant that on the whole, it is possible to add less water to the gas turbine stream (typically, an upper limit of about 20% was found), as preheating water before injection is only provided by the two intercoolers and the two aftercoolers. The author concluded that due to the recirculation of the flue gases the compressor will work at elevated temperatures. This can be avoided by using absorption cooling of the flue gases before the compressor. Assuming an 80% removal of the CO_2 emissions, the SC–HAT releases 76.9 kg of CO_2 per MWh produced compared to an open high efficiency cycle which achieves values of 300–500 kg of CO_2 per MWh.

In 2000, Ishida and Ji presented a different configuration of the HAT cycle [111].

In 2000, Rosén presented an extensive calculation of different process schemes of the EvGT [192]. The EvGT was based on the proposal from Nakamura wherby more water in the circuit than is evaporated. Rosén concluded

in his thesis that the EvGT cycle has at least the same efficiency potential as the combined cycle. Rosén's licentiate thesis in 1993, was the beginning of the Swedish EvGT project which aimed to build a pilot plant based on the evaporative technique. Rosén also included the chance of introducing the evaporative technique into Diesel Engines. The technique was called the humid air motor, HAM, which is patented by Rosén and Olsson [193, 194].

In 2000, Ågren presented a doctoral thesis on humid gas turbines containing a detailed description of the humidification process in EvGT cycles [95]. Ågren discussed the two-column split up of the humidification process. This resulted in a lower exit temperature for the humidification water, which meant that more low-level heat could be extracted from the exhaust gases.

In 2001, Lindquist et al. presented a study concerning humid cycles for marine propulsion systems [137]. The humid air motor or HAM is introduced for the first time. The HAM is an turbo charged engine whereby the air is humidified after the compressor. The humidification process lowers the emissions from the engine. In this article the concept of Trigeneration^{TM} is introduced. The basic principle is that the expansion is aborted before the atmospheric pressure. The air passes through a heat exchanger where the air is condensed and temperature is reduced. The air is then allowed to expand again. Due to the expansion, very cold exhaust gases are obtained.

In 2001, Mesbahi et al. presented a way in which to predict and normalize the experimental test results to standard ambient conditions for evaporative gas turbine cycles [153]. Mesbahi et al. used artificial neural network, ANN, to construct performance maps for the EvGT gas turbine. A feed forward network with 5 inputs, 20 hidden neurons and 52 outputs were used. The authors concluded that by having only 12 data sets for training, the ANN mathematical model of the EvGT could sufficiently and accurately predict performance parameters with non-linear interpolations and extrapolations.

In 2001, Bartlett et al. performed experimental evaluations of the water and air chemistry of the EvGT pilot plant to look at how the air filters and the flue gas condensers influence on the air quality of the EvGT cycle [17]. Because the water cycle is closed, the main source of contaminants in the cycle is the salt particles in the ambient air. It was concluded that the filter bank drastically decreased the number of particles entering the cycle through the compressor intake. About 91% of the particles can be reduced by the filters and the humidification tower acts as a scrubber in the EvGT cycle, which removes particles from the airstream. It was also concluded that the water retains its high quality even when treated, recycled condensate is used instead of fresh deionized water. This means that the EvGT cycle can be made self-sufficient of evaporation water.

In 2001, Bartlett et al. presented a theoretical model to determine the alkali contaminant flows in evaporative gas turbines [18]. It was concluded that the EvGT receives air that is slightly superior to the simple cycle.

In 2001 Dalili et al. presented a literature review detailing the thermodynamic properties for air-water mixtures [61]. The result was that the improved model by Hyland and Wexler predicted that the air can absorb more water than can be predicted with the simpler model. Although the model developed by Hyland and Wexler is not based on measurements above 75°C and Hyland and Wexler themselves questions the applicability above 100°C, Dalili et al. felt that this is still the best model available for predicting the equilibrium for air-vapor mixtures.

Lindquist presented a doctoral thesis on evaporative gas turbines in 2002 [136] detailing concepts based on experiments from the pilot plant. This thesis also presents a concept study to evaluate the plant size and cost for the EvGT.

In 2002, Lazzaretto and Segato performed an analysis of the heat exchanger network in the humid air turbine [130–132]. The authors divided the optimization procedure in two steps, first they optimized the basic components and second they optimized the heat exchanger network. The authors performed the first optimization by separating the heat exchanger network from the gas turbine with a black box. Lazzaretto and Segato subjected the black box to boundary conditions. These boundary conditions allowed the authors to study the gas turbine without the network. The authors then analyzed the heat exchanger network with pinch analysis thus producing composite curves. The authors simulated the saturator with a model in AS-PEN. The optimum value of the compression ratio between the high pressure compressor and the low-pressure compressor was close to the optimum value of an intercooled gas turbine. The optimum pressure ratio of the HAT cycle was 20 bar. The authors concluded that aftercooling has an effect on the efficiency only if the water can be used in the humidification process. The compressor pressure ratio does not affect the plant efficiency by much. The maximum efficiency of 54.59% is obtained for a pressure ratio of 20.

In 2002, Jin et al. presented a study of the externally fired humid air turbine, EFHAT [116]. In their calculations the authors uses coal as fuel but other fuels such as biomass are also feasible. The authors presents results from a TIT of 1123K with an efficiency of 48.33%. The EFHAT uses the latent heat of the flue gases by condensing the water from the exhaust gases.

In 2002, Jonsson and Yan presents an exergy study of the part-flow evaporative gas turbine [119, 120]. In the first part of the study Jonsson and Yan describe the background to the part-flow evaporative gas turbine. The

authors also describe the methods used in the paper to calculate the thermodynamic properties. The authors detailed two different gas turbines; the GTX–100 and the Trent engine. Jonsson and Yan investigate the exergy destruction as a function of percentage of part-flow. Further analysis shows that the highest exergetic efficiency is found for a full-flow evaporative gas turbine based on the GTX–100 gas turbine. For the Trent engine, a part-flow percentage of 20% gives the highest efficiency.

In 2002, Bartlett presented a doctoral thesis on humidified gas turbine cycles [19]. The main parts of the thesis are the water recovery from the exhaust gases. Bartlett also studied the concept of part-flow humidification whereby only a fraction of the compressor discharge air is passed through the humidification circuit. The remaining air is passed directly to the combustion chamber. The idea is to produce steam and humidified air which obtains a higher degree of humidification in the exhaust gases. Bartlett concludes that the investment cost of the part-flow EvGT is lower than for the full-flow EvGT. The part-flow STIG has the same thermal efficiency than the full-flow EvGT.

In 2002, Rydstrand et al. presented an analysis concerning humidified gas turbine in district heating [197]. The author considers three different cycles; the conventional steam-injected gas turbine with district heating, a humidified steam-injected gas turbine and the saturated steam-injected gas turbine. The author used a GTX–100 gas turbine to compare the three different cycles, each of which are analyzed with and without a pre-humidifier. The author used a temperature difference, the pinch-point, in the superheater of 30°C, 20°C in the economizers, 10°C in the boiler and 5°C in the humidification tower. A 10% part-flow of air is passed through a humidification circuit in the humidified steam-injected gas turbine. To make up for pressure losses, a booster fan was installed. The maximum attainable overall efficiency is 106%, which was close to the theoretical maximum of 111% (the ratio between the higher and lower heating vales, HHV/LHV). The economic feasibility study is performed without concern for taxes and fees. The authors conclude that humidified gas turbines have similar electric efficiencies and higher total efficiencies than combined cycles. They also conclude that operating the humidified cycle with an optional air pre-humidifier increased the overall efficiency to over 100% and adds flexibility to the cycle. Due to the low specific investment and the effective utilization of the fuel, humidified cycles become more economically feasible at electricity prices 5–8 €/MWh lower than combined cycles.

In 2002, Traverso and Massardo performed calculations on mixed gas-steam cycles [212]. The studied cycles are the steam-injected gas turbine

(STIG), the water-injected gas turbine (RWI) and the humid air turbine (HAT).

In 2003, Dalili presented a doctoral thesis on humidification in evaporative power cycles. In this thesis Dalili introduced a new way to humidify air in gas turbines by using a tubular humidifier. The tubular humidifier applies the gas turbine exhaust gases directly onto the tubes wherby the energy is directly used in the humidification process [62].

In 2003, Jonsson and Yan presented an economic and thermodynamic comparison of four different gas turbine cycles; one full flow evaporative gas turbine, two part-flow evaporative gas turbine cycles and one steam-injected turbine [121]. Jonsson and Yan study these gas turbine cycles on three different gas turbine engines; the GTX–100, the Trent and the Cyclone. The author also introduced an ejector, which was supposed to counteract the pressure drop in the humidification circuit between the compressor and the combustion chamber. To determine the costs of the system the authors applied the approximation method developed by Guthrie. The authors conclude that the cost of electricity is approximately the same for the different cycles studied. The specific investment cost is lower for the part-flow evaporative gas turbine cycle with an optima at high pressure ratios.

In 2003, Parente et al. presented an analysis of a microturbine equipped with a humidification process [173, 174]. Parente performed an thermodynamic optimization of the microturbine. From the optimized values, equipment sizes are determined. The authors conclude that the thermal efficiency increases by 5% points compared to the ordinary microturbine, while the specific work output increases by 50%.

In 2003, Ågren and Westermark presented a design study of a part-flow evaporative gas turbine [92, 93]. The study concentrated on both aero-derivative and industrial core engines. A thermal efficiency of 52.9% is attained with an aero-derivative gas turbine at a bypass flow of 20%. The author claimed that a decrease in the heat exchanger area of 50% is achieved at the same time the thermal efficiency increases by 1.4% points. For the industrial core a thermal efficiency of 52.6% was achieved for the full-flow evaporative gas turbine. This optima was however, quite flack which meant that a bypass of 40% can be used without much loss in efficiency. The authors conclude that for an industrial core engine the bypass ratio should be in the vicinity of 20–40%.

In 2004, Fredriksson-Möller et al. presented a study of a humid air turbine (HAT) with post-combustion CO_2-capture [158]. Möller et al. performed thermodynamic and thermo-economic optimization with genetic algorithm's (GA). The three cycles were; the reference HAT cycle, the reference HAT cy-

cle with post-combustion CO_2 removal with energy taken from the exhaust gases and the reference HAT cycle and the reference HAT cycle with post-combustion CO_2 removal with energy taken from a separate biomass boiler.

In 2005, Jonsson and Yan presented a complete literature review of wet gas turbine cycles [147].

2.3.1   CHAT Cycle

A project which was aimed at developing the humid air turbine technology, was initiated by the Electric Power Research Institute, EPRI. The project was named the Cascaded Humidified Advanced Turbine, CHAT, power plant. Several EPRI reports have been published regarding the CHAT technology [162–165].

In 1994 Nakhamkin et al. tested different configurations of a combustor for humid air in order to determine the influence of water injection on flame stability, combustion efficiency, emissions, and combustor liner wall temperatures [166]. The maximum amount of water that still gives high combustor efficiencies is of primary interest in the study. The authors used a TF15 combustor from the AGT1500 gas turbine, which drives the army battle tank M1A1. The authors created the high humidity by injecting steam 61 meters prior to the combustion chamber. The tests were performed between 385°C and 510°C at 14.82 bars pressure. The authors concluded that the maximum amount of injected water into the air while still maintaining good performance was 28% H_2O/Air at an inlet temperature to the combustion chamber at 510°C. The authors made a recommendation that more testing should be done in order to determine the stability limits at high temperatures and pressures.

In 1995 Nakhamkin et al. presented the Cascaded Humidified Advanced Turbine (CHAT) [169]. The authors predicted that the CHAT will synchronize with the grid in approximately 8 minutes and will be up and running at full power within 30 minutes. The authors also predicted that the part load performance of the CHAT is superior to both the combined cycle and the simple cycle. The estimated specific capital cost for a CHAT plant is 15–20% less than for a combined cycle.

In 1995, Nakhamkin and Gulen presented an analysis of the dynamic behavior of a Cascaded Humidified Advanced Turbine, CHAT [168]. This study aimed at describing the CHAT response to a cold start-up and sudden load changes. Nakhamkin and Gulen used performance maps to describe the performance of the compressor. Heat and mass balances and the ordinary conservation equations describes the time influence of the CHAT system.

During start-up blow-off valves prevented the compressor from going into surge. The authors concluded that the start-up time for a CHAT to reach full power is 30 minutes.

In 2000, de Biasi reported on a suggestion for a 12–MW demo plant based on the HAT technique [65]. In this article, Dr. Michael Nakahamkin is interviewed about the possibilities of a CHAT demo plant. It is believed that a 12–MW CHAT plant is ready for field demonstration of the sophisticated cycle integrating intercooling, reheat, recuperation and humidification features. The demo plant should emphasize on optimization and validation of part-load operation, controls, transients, emissions and other aspects specific to novel design features. Calculations showed that the off-design performance of the CHAT is superior to combined and simple cycle power plants. The CHAT can operate at 95% of its full-load efficiency at 50% output. The high part-load performance was maintained by four adjustable parameters:

- HP fuel flow;

- LP fuel flow;

- humidification level; and

- second-shaft speed.

In 2000, Nakhamkin et al. presented the technology of injecting humidified air into the gas turbine [167]. This technique allowed greater flexibility of the operating characteristics. The humid air injection also give the engine better part-load behavior.

In 2001, de Biasi reported on the DOE evaluation of the CHAT for next generation gas turbines [68].

In 2002, de Biasi described a system which injects dry or humid air prior to the gas turbine combustor [69]. The system had been tested by Calpine on a PG7241FA gas turbine peaking installation. As a precaution, only 3.5% was used which General Electric (GE) specifies as a moisture limit for Fr7FA.

2.4 The MAT Project

In 1998 Utamura et al. presented theoretical and experimental results of the Moisture Air Turbine, MAT cycle [216]. Moisture Air Turbine, MAT, is described in the literature as a cycle that uses wet compression to increase the output and hopefully the electrical efficiency of the gas turbine. In the MAT cycle, very fine water droplets are injected in front of the compressor.

Before the air enters the compressor, it has been evaporatively cooled by a process called fogging. This allows the temperature to decreased as much as possible. During the cooling, an over-spray is added to achieve wet compression, which means that more water is added to the process than the air can contain. Since the droplets have not been completely evaporated in the air, some droplets will accompany the saturated air into the compressor. These droplets will evaporate later during the compression. In an ideal case it can be assumed that the evaporation process remains saturated and the total entropy of the two component two-phase mixture is unchanged.

There are two different mechanisms, which raised the output of the machine associated with wet compression. These are:

1. Cooling of the inlet air to the compressor which increases the air mass flow-rate into the compressor increase; and

2. Cooling of the internal gas due to evaporation of liquids which decreases the compressor work.

One of the first design issue to consider is blade erosion due to water droplets collision with the blade. To be able to account for this, Utamura et. al 1999 solved the two-dimensional potential flow field along the gas path with computational fluid dynamics [217]. Knowing the velocity of the water droplet at the inlet and exit of the inlet guide vanes, the velocity vector was calculated for the entire flow using Newton's equation of motion for a specific droplet size. This showed that droplets with a mean Sauter diameter of less than 20 μm should follow the flow path without hitting the blades.

Another problem with water injection was to grasp the condition for the water droplet entering the compressor to complete its evaporation within the compressor. With a quasi-steady heat and mass transfer model, calculations were performed stage by stage using a F9E compressor by Utamura et al. 1999 [217]. This compressor has 17 stages. The calculation was performed on droplets with a diameter of 10 μm, 20 μm and 30 μm. The calculation showed that droplets smaller than 20 μm will evaporate within the compressor, while droplets bigger than 30 μm will most likely not complete its evaporation within the compressor. Utamura et al. predicts that droplets with a diameter of 10 μm will evaporate at stage number 8. This means that after the 8th stage there will be no more droplets in the flow. The 20 μm droplet is predicted to evaporate completely at stage no 13. Utamura also calculated the risk of erosion due to water injection. By using a method developed for steam turbines [214] the erosion rate was estimated to be in the size of one-hundredth of that observed at the last stage of steam turbine.

The results of the calculations made Utamura et al. 1999 choose a Sauter mean diameter of 10 μm.

2.4.1   Experimental Results

The test was carried out on an F9E gas turbine rated at 115 MW at 15°C with a turbine inlet temperature of 1155°C at a pressure ratio of 12.4 which ran on kerosene. The feedwater came from a water tank containing de-mineralized water. The maximum amount of water delivered to the gas turbine was 150 l/min, which corresponds to an injection capacity of maximum 0.65% air to mass ratio. Utamura et al. compared this flow to a quarter of the fuel flow.

The tests were performed in two different ways; first the turbine inlet temperature was kept constant and second the power output was also constant. During the test, the IGV was set to 84°.

Altogether Utamura et. al performed 33 tests with ambient temperatures ranging from 14.9°C to 33.5°C and the relative humidity ranging from 30 to 95%.

When the turbine inlet temperature was kept constant and by injecting 0.65% to air mass ratio, this resulted in an increase in power output from 94 MW to 103 MW. The temperatures at compressor inlet and exit and at turbine exit, decreased by 8°C, 20°C and 6°C respectively. Extrapolations of this data, made by Utamura et al., suggests that an injection of 1% water to air mass ratio should yield an increase in power output by 10% and an increase in thermal efficiency by 3% in relative value. Note that this data is not based on ISO conditions and the gain in power is also due to the cooling effect of the water droplets. When the power output was kept constant, the fuel-flow decreased with the amount of spray injected into the compressor.

Another experience with the water-injection was a reduction in the NO_x concentration due to the temperature reduction in combustion temperature. The study did not include information on how much the decrease in NO_x was on this machine.

From these tests, it was shown that a spray amount of 0.4% results in an increase in power by 4% at ISO conditions. The demonstration of the MAT machine has continued since 1997. Since the machine has been operated as a simple cycle prior to 1997, comparison can be made between compressor degradation on the simple cycle and the MAT cycle. During overhauls it has been confirmed that the MAT cycle suppresses the degradation of the compressor adiabatic efficiency.

When the compressor was opened during the overhauls, the visual inspection verified that there was no evidence of erosion or corrosion due to collision of water droplet against the rotor blade.

The absence of erosion was confirmed by long-term operation experience with a type K–1290 centrifugal compressors with water injection and with the axial compressor of a type GTT–3 industrial gas turbine installation at Azot PO in the city of Nevinomyssk. These experiments also showed that there was no corrosion of the metal or deposits in the compressor flow path. The water injection functions as a compressor cleaner [217].

The moisture air turbine has been in operation since 1997 but only as a laboratory.

2.5   The AHAT Project

The Japanese company Hitachi has commenced building a humid air turbine for commercial use. The first step in this project was the construction of a pilot plant. The pilot plant is a 3.5 MW single shaft engine with a rotational speed of 17,000 rpm. The engine used a 2 stage centrifugal compressor that delivered a pressure ratio of 8. The turbine inlet temperature was 1100°C. The project was called the advanced humid air turbine, AHAT.

In 2003, Higuchi et al. presented studies of different types of blade cooling for the Advanced Humid Air Turbine (AHAT) [104]. The AHAT system use wet compression to cool the compressor air which reduce the compression work. The air is passed through a humidification tower which humidifies the compressor discharge. A recuperator then heats up the cold humidified air until the air reaches the turbine inlet temperature. The air then enters the combustion chamber where it is combusted. The turbine exhaust gases pass a recuperator and an economizer before it is heated again and passed out the chimney. The authors considered three different ways of cooling the turbine; cooling the turbine with compressor air, cooling the turbine rotor blades with compressor air and cooling the turbine stator blades with humidified air and cooling all turbine parts with humidified air. Modeling of the gas turbine expander occurred stage-by-stage and the model takes losses into account with the AMDC–KO loss model. To model the compressor work during droplet injection, the author uses a model developed by Utamura. Utamura used a CFD code to predict the evaporation profile within the compressor. The authors concluded from the calculations that the humidified air results in highest thermal efficiency of the AHAT system. The system that used humidified air as cooling fluid shows an improvement in thermal efficiency by

1.7% points. The author also presented theoretical results from a remodeling of a simple gas turbine cycle to a AHAT system. The authors concluded that the thermal efficiency increases from 37.7% to 54.7%. The author also conclude that the thermal efficiency of the AHAT system is 1.3% points higher than for a combined cycle with the same core engine.

In 2004, Dodo et al. presented a theoretical and experimental study of a micro turbine operating on a humid air turbine cycle [79]. The aim was to present a 150 kW microturbine with an electrical efficiency of 35%. The authors explained the development of a low NO_x combustor, bearings, operation of water supply for HAT and features of the prototype machine. The authors also presented some experimental data from the HAT cycle. The microturbine concept used a water atomizing inlet air cooling, a system wherby small droplets of water are sprayed into the compressor. This system acts as an intercooler which reduce the compressor work. A radial gas expander was developed during the project and vibrational and strength test were performed. A 95.6% combustion efficiency was obtained. Power output was 150.3 kW at an efficiency of 32%.

In 2004, Hatamiya et al. described the AHAT system and performed extensive experimental testing and some system modeling [100]. Hatamiya discussed the outline of a more simplified version of the AHAT system. This system is similar to the cycle patented by Lysholm and discussed by Găsparović and Stapersma [96–98]. Instead of using a humidification tower, Hatamiya injected water after the compressor with spray nozzles. Part of the water evaporates in the humidification chamber and the air that exits the humidification chamber is a two-phase flow. The air contained some droplets which evaporates in the recuperator. To validate the spray injection system, Hatamiya et al. built a six meter long tube with a diameter of 0.250 meter. 12 nozzles ensured the water evaporation in the tube. In this platform, Hatamiya et al. conducted testing to see how much water evaporates within a given length. The tests was performed with 0.8 MPa and 570K to simulate a real small size gas turbine engine. The result was found that the test section evaporates 7 weight percent water to air stream within 0.5 sec that 7 weight percent water to air stream which could be evaporated. Hatamiya et al. also tested a water recovery system. This system consisted of nozzles spraying cold water on the exhaust gases. During the contact between the exhaust gases and the water, water condenses out from the exhaust gases. Tests showed that this water recovery system attains full water recovery. The full water recovery occurs at a ratio between the cooling water and the exhaust gas of around 2. Hatamiya et al. also performs

cycle calculations and finds that the AHAT system has 5% higher thermal efficiency than a comparable combined cycle.

2.6   The TOPHAT System

In 2000, Liere and Laagland presented the TOPHAT® concept [218]. This system used the exhaust gases to heat up water. Newly developed nozzles sprays the water as a mist into the compressor. The high temperatures ensures that the droplets will have a small diameter of approximately 2.2 microns. The injected water decreases the temperature of the water after the compressor. Experiments show that injecting 2% water into the compressor of a General Electric Frame 6 engine will reduce the compressor outlet temperature with 57K. This makes it possible to utilize the colder compressor air to cool the turbine blade temperatures. Calculations have shown that for the case of 2% water injection, the blade life will increase from 32,000 hours to 44,000 hours. Experiments with a 400 kWe gas turbine at the university of Delft showed that the compressor outlet temperature decreases by 25K for every percent water-injected into the compressor. The authors also showed that 1.5% water-injected results in 10% power augmentation, a 2% relative increase in efficiency and a 25% reduction in NO_x emissions. The authors claimed that the turbine can be constructed for the highest efficiency (57.4%) with a specific power of 430 kWe/kg or for the highest power output (700 kWe/kg) and an efficiency of 55%. This system is still only in a laboratory, however it is available to the industry.

Chapter 3

The EvGT Process

The literature study in chapter 2 illustrates that the wet cycles are an interesting research area. The water injected cycles have already been used commercially for the General Electric LM6000 SPRINT, which uses wet compression to boost thermal efficiency and power output. The STIG and CHENG cycles are also present in the gas turbine market today. In both the water-injected and steam-injected gas turbines, significant amount of research is conducted by both the industry and the academia. The literature study highlights that there is not as much work carried out in the field of humid air turbines. Misconceptions still exist concerning the use of an aftercooler heat exchanger in the humid air turbine [208]. There is also not a lot of experience in the use of plate-heat exchangers as an air-water heat exchanger in power plant environments. In the literature review it is also clear that the operation of the humidification tower and the principle of the working line are theories that have not been experimentally proven. Throughout the history of the evaporative gas turbine cycles, researchers have made different assumptions regarding the performance of the equipment in the humid air turbine, which has led to many different conclusions. A more unified approach is needed to be able to predict the performance of the humid air turbine. Therefore, it is of importance to future studies of evaporative gas turbines that the performance of such equipment is determined by experiments. In 1993 the evaporative gas turbine (EvGT) project started as a response to the need of experimental data on evaporative gas turbine cycles. This project has been developed in co-operation between universities, gas turbine manufacturers, utility power companies and research organizations in Sweden. The goal of this project is to develop a sound understanding of evaporative gas turbines, which has led to the construction of the first

official pilot plant for humid air turbines at The Faculty of Engineering at Lund University in Sweden. This pilot plant is called the evaporative gas turbine pilot plant, the EvGT pilot plant.

Lindquist and Rosén have made large contributions in the experimental field of the humid air turbine and they have successfully shown that it is possible to operate a gas turbine in a humid air turbine mode [135–140, 192–194]. Although Lindquist and Rosén have made large contributions in both the experimental and theoretical field, more experimental data is required to further clarify the operating performance of the humid air turbine. As a preceding of their work, more experimental work has been performed and it is presented in this chapter. The experimental work lays a foundation for the understanding of the working principle of the humid air turbine and the humidification process [135–140, 192–194]. The work presented in this chapter is an expansion of the experimental and theoretical work in **paper I, II and VI**.

3.1   The EvGT Cycle

The study of thermodynamic cycles evolved from Carnot's work presented in 1824 where he presented a theory of the ideal thermodynamic cycle. In his work, he presents the Carnot heat engine which lay the foundation for the theory of thermodynamics which evolved through great scientists including James Prescott Joule, Rudolph Clausius, Lord Kelvin and William Rankine to name a few [44]. Carnot's heat engine and all other heat engines can be thought of as working between two heat reservoirs. Figure 3.1 shows a visualization of a heat engine that is working between a hot and a cold reservoir. Through the theory of thermodynamics, it can easily be shown that the Carnot engine is the most efficient engine that operates between two thermal reservoirs [45]. Studying the efficiency of engines through thermodynamics, it can easily be seen that the efficiency of the Carnot process is detailed in equation 3.1.

$$\eta_{Cycle} = \frac{Q_H - Q_L}{Q_H} \xrightarrow{\left[\frac{Q_H}{Q_L} = \frac{T_H}{T_L}\right]} \eta_{Carnot} = 1 - \frac{T_L}{T_H} \qquad (3.1)$$

As can be seen from equation 3.1 the maximum attainable efficiency of a thermodynamic cycle is dependant on the temperature difference of the thermal sources. It is however very difficult to construct a real engine that works according to the principles of a Carnot engine. Cycles that are possible to
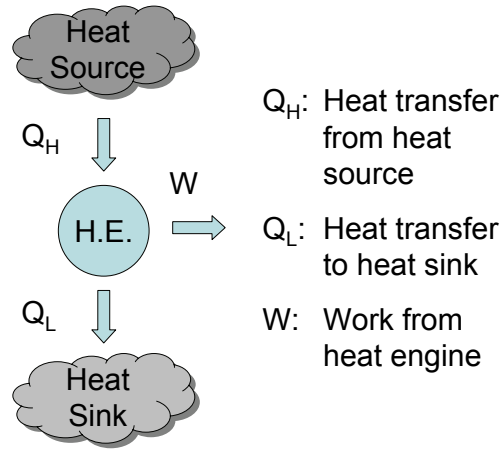
Figure 3.1: Theoretical heat engine

build have been studied over several years and the cycle which resembles the gas turbine engine, is the Brayton cycle. The Brayton cycle is an internally reversible engine which has the thermal efficiency described by equation 3.1. One major disadvantage of the Brayton cycle is the high thermal energy of the exhaust gases, which is not utilized in any way within the gas turbine cycle. These hot exhaust gases therefore lead to poor efficiencies compared to equivalent technology.

A way of utilizing the energy in the exhaust gases is to transfer that energy back into the gas turbine process through heat recovery from the flue gases. This heat recovery can be performed with an internal water circuit that extracts this energy by increasing the temperature of a water mass flow. The warm water from the heat recovery system is passed through a humidification process where the warm water is evaporated into the airstream through a heat and mass transfer process. This evaporation process creates a larger mass flow through the expander compared to the mass flow that passes through the compressor. The evaporated mass flow is then expanded in the expander together with the exhaust gases of the turbine.

This additional mass flow of water through the expander has been compressed as a liquid but is being expanded as a gas through the gas turbine expander.

$$W_{compression} = \int_{1}^{2} \nu dP \qquad (3.2)$$
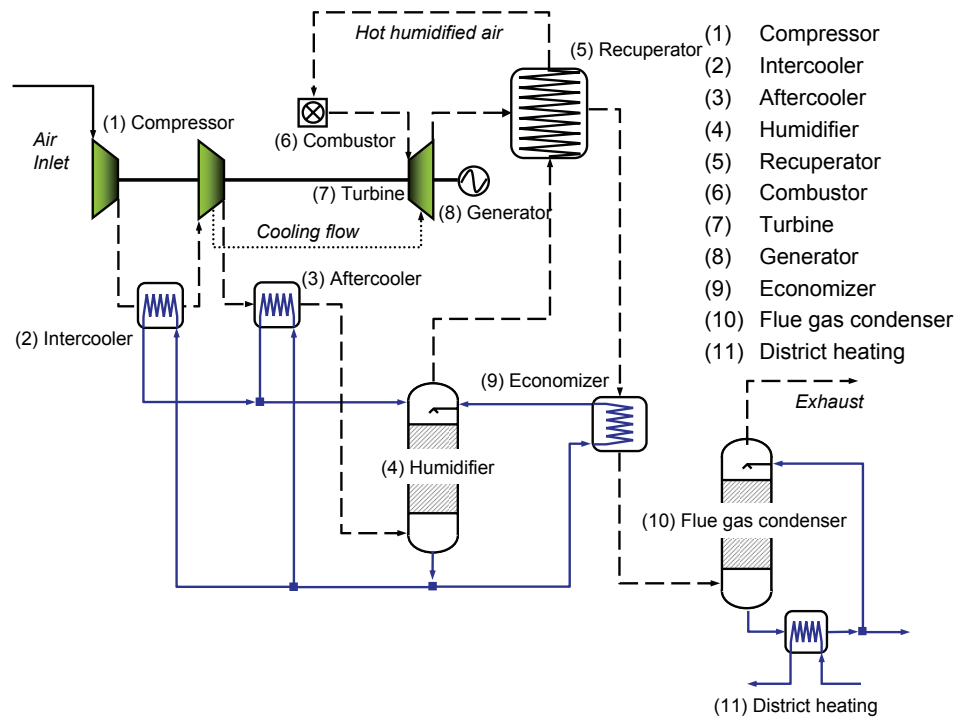
Figure 3.2: Flowchart of an intercooled and aftercooled EvGT.

To explain the beneficial effects of the evaporation process, equation 3.2 shows the ideal work required for a compression process where the parameter, ν, is the specific volume and, dP, is the pressure difference which the compression process must overcome. Since the specific volume of a gas is much greater than for a liquid, equation 3.2 shows that the energy required to compress the gas is greater than the energy needed to compress a liquid. The additional mass flow has therfore been compressed in a more efficient way than if the same additional mass flow would have been compressed as a gas which leads to increased thermal efficiency. Figure 3.2 shows the flowchart of an evaporative gas turbine cycle which uses the principle of evaporating water into the airstream in a heat recovery process described in the last paragraph.

In figure 3.2, the air is led into the gas turbine compressor (1) where the air pressure is increased to the system pressure. The compression process is divided into two steps with an intercooler heat exchanger (2) placed between the two sections. The intercooler decreases the temperature of the air which

lowers the compression work. After the compressor the air then passes an aftercooler (3) which decreases the temperature of the air once again before it enters the humidification tower (4).

The air then passes the humidification tower where it encounters warm water which has been heated in the heat recovery process in the intercooler (2), aftercooler (3) and economizer (9). Heat and mass transfer occurs causing the water to cool down and evaporate while the mass flow of air increases due to evaporation.

The air leaves the humidification tower saturated with air and at a low temperature. The air then passes the recuperator (5) that preheats the air with the help of the exhaust gases from the gas turbine expander (7). The air is then burned in the combustor together with natural gas in order to reach the combustor outlet temperature. After the expansion in the expander (7), exhaust gases passes the recuperator (5) where it is cooled down by the humidified air. The flue gases then passes the economizer (9) where it heats a part of the humidification liquid. The EvGT cycle in figure 3.2 has been equipped with a flue gas condenser (10) which extracts the remaining energy from the flue gases by condensing some of the water in the flue gases. This condensation makes it possible for the EvGT cycle to be self-sufficient of water. The heat extracted in the flue gas condenser (10) is delivered to a district heating network through the heat exchanger (11).

3.2   Discussion on the Aftercooler

It can be concluded from the previous section and from equation 3.1 that the thermal efficiency of a heat engine depends on the temperature difference between the thermal reservoirs where the heat engine is operating. In gas turbines, which have very high exhaust gas temperatures, it is important and beneficial to decrease the temperature of the exhaust gases in a heat recovery system in order to increase the efficiency.

Figure 3.2 shows the heat recovery system of the EvGT cycle. In this flowchart it is easy to see the benefits of using an intercooler (2), which lowers the compression work in the gas turbine and increases the thermal efficiency. It is also fairly easy to see the advantages of using the economizer (9) as it recovers low-level heat from the exhaust gases and uses this energy for the humidification process. The use of an aftercooler is not that easy to see and there have been misconceptions about its use [208]. To study the influence of an aftercooler, a simple version of the EvGT, which only incorporates an

economizer (9), will be used. This simple EvGT recovers low-level heat from the exhaust gas by circulating water through an economizer.

The heat recovery in an EvGT cycle depends on the difference between the water temperature at the inlet and outlet of the economizer. High water temperature is important to the humidification process since it improves the rate of evaporation of water [138]. The highest water temperature in the EvGT always occurs at the outlets of the heat exchangers in the heat recovery system. Temperatures above the saturation temperature at the operating pressure are unfeasible due to the fact that boiling would occur within the pipes and the heat exchanger. The mass flow of the circulating water is therefore optimized so that the highest water temperature is limited to 10°C below the boiling point at the heat exchanger exit at the specific operating pressure to ensure that boiling does not occur [136]. The economizer therfore heats up the water to a temperature that is as high as possible. With this temperature at a fixed value, the heat recovery depends on the inlet water temperature to the economizer.

Figure 3.2 show that the inlet water temperature to the economizer (9) is the same water that exits the humidification tower (4) which means that they have the same temperature.

Reducing the temperature of the water exiting the humidification tower means that the temperature of the water entering the economizer decreases. This decrease in temperature leads to the improvement of the heat recovery in the EvGT cycle.

The temperature of the water that leaves the humidification tower depends somewhat on the temperature of the incoming air. For a simple EvGT without the aftercooler, the compressor discharge air is at temperatures above the boiling point of water at the given operating pressure. When the hot compressor discharge air meets the circulating humidification water, the air quenches almost immediately during an intense heat and mass transfer process. Due to the hot air, the temperature of the water leaving the humidification tower (4) is high. This high water outlet temperature impedes the potential to recover low-level heat from the exhaust gases and it is therefore important to lower this temperature.

The lowest possible temperature of the water that exits the humidification tower (4) is the adiabatic saturation temperature of the entering air. Cooling the compressor discharge air before it enters the humidification tower, lowers the adiabatic saturation temperature of the air. This means that if the humidification system can lower the temperature of the incoming air, it would improve the heat recovery.

HT without AC

Heat utilisation (%):   56.6

Humidity (kg H2O/kgair):   0.2009

HT with AC

Heat utilisation (%):   64.4

Humidity (kg H2O/kgair):   0.2244
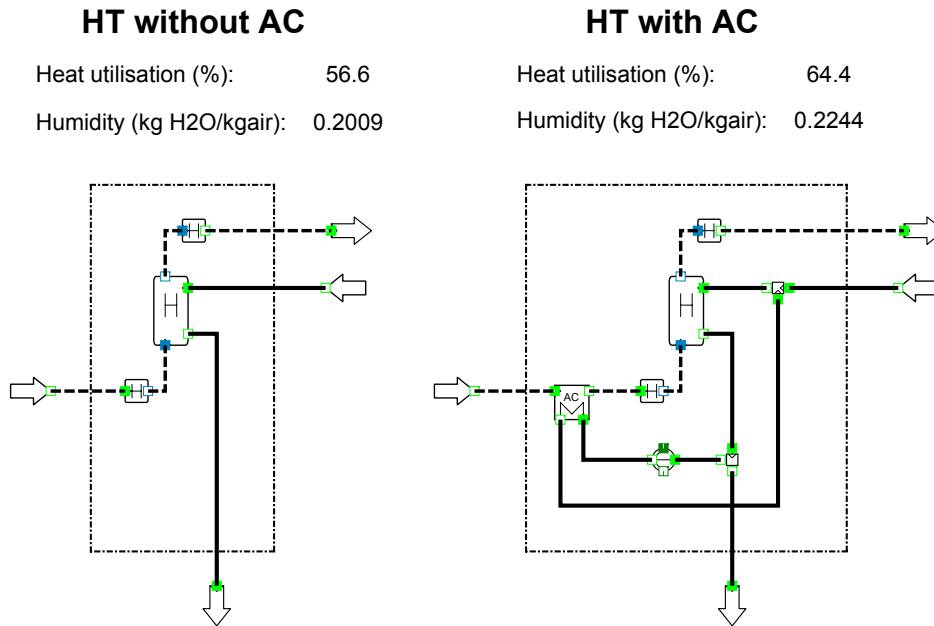
Figure 3.3: Heat balance with and without an aftercooler

A heat exchanger installed prior to the humidification tower and the aftercooler, accomplishes this temperature reduction by using a part of the humidification water to cool the compressor discharge air. This temperature reduction leads to considerable reduction in the water temperature after the humidification tower and thus improves the heat recovery.

Figure 3.3 shows the importance of recovering low-level energy from the exhaust gases. It describes two different humidification systems with control volumes around them. The humidification systems are operating at the same condition as each other, which means that the inlet conditions are the same for both control volumes. The difference between the two humidification processes is that the one on the right is using an internal water circuit to cool the incoming air. An energy balance applied to the control volume in figure 3.3 shows that the heat utilization is much better for the system that incorporates the aftercooler. The heat utilization is defined by equation 3.3.

$$Heat\ utilization = \left(\frac{\dot{m}_{w,in} \cdot h_{w,in} - \dot{m}_{w,out} \cdot h_{w,out}}{\dot{m}_{w,in} \cdot h_{w,in}} \right) \cdot 100 \qquad (3.3)$$

The heat utilization is a measurement of how much energy the system extracts from the economizer.

As can be seen from the calculation in figure 3.3, a higher heat utilization leads to a higher rate of humidification. Since both the heat from the air and water going into the system is constant, the only way to balance the energy supplied to the system is to increase the humidity of the outgoing humidified air. This can be seen in equation 3.6 since the only parameter that is altered in the equation is the outlet water temperature. According to the simplified equation 3.6, the enthalpy of the gas will now increase and it will increase in both temperature and more evaporated mass. The foregoing discussion indicates that by circulating water in an internal water circuit alter the energy balance around the humidification tower. This internal water circuit makes it possible to increase the humidity of the compressed air and improve the difference between the work delivered by the expander and the work required by the compressor.

3.2.1   Operating Line

The previous paragraph provided a discussion on the aftercooler and its advantages to the heat recovery system. The energy recovered from the exhaust gases has to be utilized in the humidification tower. To predict the performance of the humidification tower in the EvGT cycle, advanced heat and mass transfer equations are to be used. However, it is possible to derive an expression from the more advanced theory which also makes it possible to visualize the humidification process in a simple way.

Paper I describes the complete working principle of the humidification tower. This analysis studies the thermodynamics, heat and mass transfer inside small control volumes of the humidification tower. In **Paper I**, it is shown that the increase of enthalpy through the humidification tower can be written according to equation 3.4 [138]:

$$\frac{dh_g}{dz} = \frac{\rho \cdot h_d}{m_g} \cdot \left(h_i - h_g\right) \cdot \underbrace{\left(Le^{-s} + \frac{\omega_i - \omega_g}{1 - \omega_i}\right)}_{\approx 1} \tag{3.4}$$

In equation 3.4, ω_i and ω_g is the air humidity, h_d is the mass transfer coefficient, m_g is the mass flow of air, Le is the Lewis number, h_g is the enthalpy of the air and ρ is the density of the mixture. Equation 3.4 is a combination of the conservation of energy equation for a control volume and the conservation of mass equation. It is equally simple to show that a similar equation

can be derived for the increase of enthalpy of the liquid through the tower. This is performed in **Paper I**.

Equation 3.4 shows that the last term in the parenthesis is a factor of the humidity in the gas. The humidity in the gas is normally a low number and the difference between the humidity at the interface and at the bulk flow is very small. The denominator contains a number very close to one. This fraction can readily be approximated to one. The parenthesis also contains the Lewis number and for air-water mixtures at normal conditions this number is equal to one. It can therefore be concluded that the parenthesis can be approximated as one. A similar manoeuver can be made for the liquid side. These simplifications are fairly reasonable for cooling towers operating at low temperatures and pressures but for pressurized towers they are somewhat crude. To obtain a more useful expression, the equation for the increase of enthalpy air through the tower is divided with the equation for the increase of enthalpy of the liquid through the tower which yields equation 3.5 [157].

$$\frac{dh_g}{dh_l} = \frac{\dot{m}_l}{\dot{m}_g} \tag{3.5}$$

Equation 3.5 can be integrated along the humidification process if it is assumed that the different mass flows are independent of the humidification process. This assumption is not valid for humidification towers due to the large difference in mass flows through the humidification tower, however it is still an acceptable approximation in the development of a visual approach. The integration makes it possible to determine the enthalpy of the outgoing gas as equation 3.6.

$$h_g = h_{g,in} + \frac{\dot{m}_l}{\dot{m}_g}\big(h_l - h_{l,out}\big) \tag{3.6}$$

This equation is called the operating line of the humidification tower and relates the enthalpy of the gas to the enthalpy of the liquid in every part of the tower. This equation is often drawn together with the saturation curve of the air. In such a figure, equation 3.6 becomes a straight line. Using the simplifications that lead to equation 3.6 shows that the slope of the operating line is given by the relationship between the liquid and vapor mass flow ($\dot{m}_l/\dot{m}_g$).

The basic principle is that the operating line cannot intersect the saturation curve. The energy equation may show a solution where the operating line intersects the saturation line but the mass transfer process required to do it would be impossible. As a contrast, a flue gas condenser would cool
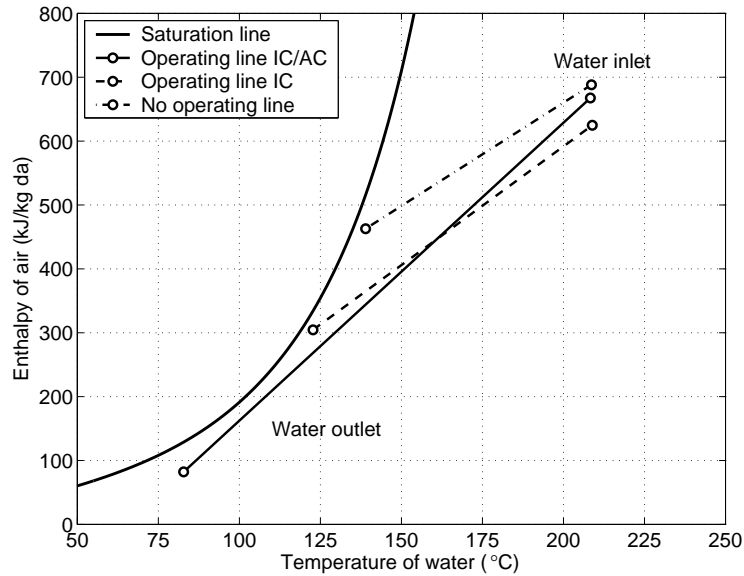
Figure 3.4: Operating lines for different EvGT systems.

down the gas by simultaneously condensing water and the operating line would therefore be located to the left of the saturation curve. Figure 3.4 shows three different operating lines from three different EvGT cycles. The operating lines are typical for a gas turbine with an operating pressure of 20 bar. The upper operating line is associated with the EvGT without both an aftercooler and an intercooler, (No operating line). The lower operating line represents the EvGT with an aftercooler and an intercooler, (Operating line IC/AC) and the operating line in between the others is for an EvGT with an intercooler but no aftercooler, (Operating line IC).

In figure 3.4 the simple EvGT represents a low ratio $\dot{m}_l/\dot{m}_g$ which determines that the slope of the operating line is great. In this cycle, the air temperature that enters the humidification tower is very high. Similarly, this makes the temperature of the water leaving the tower high as well. As the ratio of $\dot{m}_l/\dot{m}_g$ increases as in the case of (Operating line IC), the temperature of the water is lowered. The reason for this temperature reduction is that the intercooler lowers the final compression temperature which in turn makes it possible to attain a lower water temperature. The best temperature reduction is when the aftercooler is installed. Figure 3.4 shows an

AC: Aftercooler
BO: Bleed off
CT: Condensate treatment
ECO: Economizer
FGC: Flue gas condenser
HB: Hydraulic brake
HT: Humidification tower
MT: Mixing tank
NG: Natural gas
REC: Recuperator
PRV: Pressure relief vessel
WR: Water reservoir
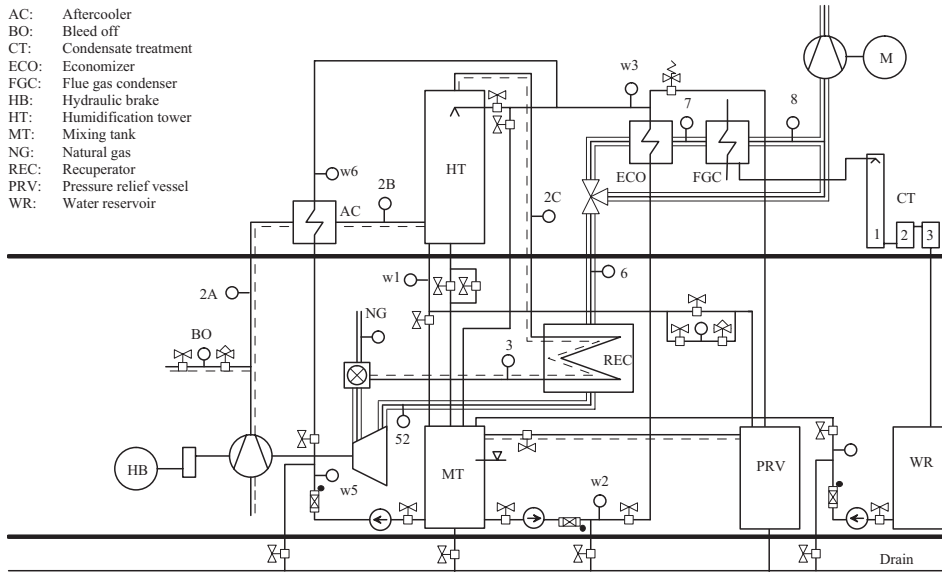
Figure 3.5: Flowsheet of the Evaporative Gas Turbine, EvGT

increased ratio of $\dot{m}_l/\dot{m}_g$ but also a significantly lowered outlet temperature of the water.

3.3 The Pilot Plant

This section describes in brief the EvGT pilot plant which has been used for the experimental investigations in **paper I, II** and in **paper VI** depicted in figure 3.5. The pilot plant consists of a gas turbine, recuperator, humidification tower, aftercooler and an economizer and is located on two floors in the laboratory at Lund Institute of Technology in Sweden. The gas turbine, the hydraulic brake and the recuperator are located on the first floor. The remaining components i.e. the heat exchanger network, is located on the second floor. The pilot plant has also been presented by Lindquist, who provides a more thorough description of the EvGT pilot plant in his licentiate thesis [135].

3.3.1   The Gas Turbine

The gas turbine is a VT 600, which is a simple cycle, single shaft engine developed by Volvo. The engine has a single-stage centrifugal compressor with a two-stage axial expander. Air is sucked into the engine at a mass flow of 3.4 kg/s. The air passes through a filter bank which cleans the air from any particles that can be entrained in the airflow. The centrifugal compressor delivers a pressure of eight bar and a temperature of the compressor discharge air of around 330°C. The air is then combusted with natural gas in the combustor until the air attains a combustor outlet temperature, COT, of around 1000°C. The rated output of the engine is 600 kW with an electrical efficiency of 22%.

The pilot plant is not equipped with a generator but instead has a hydraulic brake that absorbs the energy produced by the gas turbine engine. The speed range of the brake is from zero to 5500 rpm with a permissible torque of 5750 Nm. Water is supplied to the hydraulic brake at a pressure of 2.5 bar.

3.3.2   The Heat Exchanger Network

During the humidification process, the temperature of the compressor discharge air decreases to approximately 117°C. A recuperator is installed prior to the combustion chamber by using the hot exhaust gases to preheat the compressor discharge air up to a temperature of around 510°C. The preheating allows the engine to operate with less fuel and still reach the same TIT. The recuperator is a primary surface counter-current heat exchanger with a surface compactness of 1657 m²/m³.

After the recuperator the exhaust gases have a temperature of around 225°C and still contains some energy. This additional energy is recovered by the economizer shown in figure 3.5. The economizer is a compact heat exchanger with a large heat transfer area. The humidification water is supplied from the mixing tank at a temperature of around 78°C and the economizer extracts the energy from the exhaust gases and delivers it to the humidification water. The humidification water is heated to 10°C below the boiling point. This can of course be adjusted by adjusting the mass flow through the humidification pumps.

The Pre-cooler

In the heat exchanger network an additional heat exchanger has been installed, the pre-cooler that cools the temperature of the water flowing to the

aftercooler. This heat exchanger is a copper-brazed plate heat exchanger. The heat exchanger uses a separate water circuit, which is disconnected from the EvGT pilot plant. The pre-cooler makes it possible to investigate the operating line in the humidification tower. Since the pre-cooler lowers the temperature of the water to the aftercooler it makes it possible to extract more heat from the compressor discharge air. This makes the water that leaves the humidification tower reduce the temperature.

3.3.3 The Measurement System

A measurement system is used to measure and record the data from the test run with the pilot plant. The measurement system has no other function than collecting and presenting the data. To achieve this four boxes have been placed around the laboratory. The transmitters convert the measured value of the instrument to a 4–20 mA signal. This signal is transferred to the connection boards in the main switch cabinet. The connection boards are in turn connected to an analog or digital box. The analog box contains eight measuring cards which in turn contains 16 analog input signals. The digital box contains three measuring cards and one interface card. Each card contain 16 digital input signals. All signals from the digital and analogue box are transferred to a computer card delivered by Microstar. The computer reads every channel 1,000 times per second and stores 100 of those values.

The measurements have been conducted with three measurements devices at each point. With three measurements it can be seen if one of the measurement devices are malfunctioning. The tests have been run for ten minutes after a 15 minute stabilization period.

3.3.4 Humidification Tower

The main purpose of the humidification tower is to humidify the compressor discharge air. This is realized by creating a large contact surface between the water and the air which makes the humidification process effective. The air enters at the bottom of the tower and then passes through a structured packing where it encounters the humidification water coming from the top of tower. The humidification water and the air are not at equilibrium with each other. Since they are not at equilibrium, a concentration difference exists between the water and air phase. This concentration difference acts as a driving force for heat and mass transfer across the phase boundary, which occurs on the surface of the structured packing. After the structured packing, the tower exits the humidification tower saturated with water.
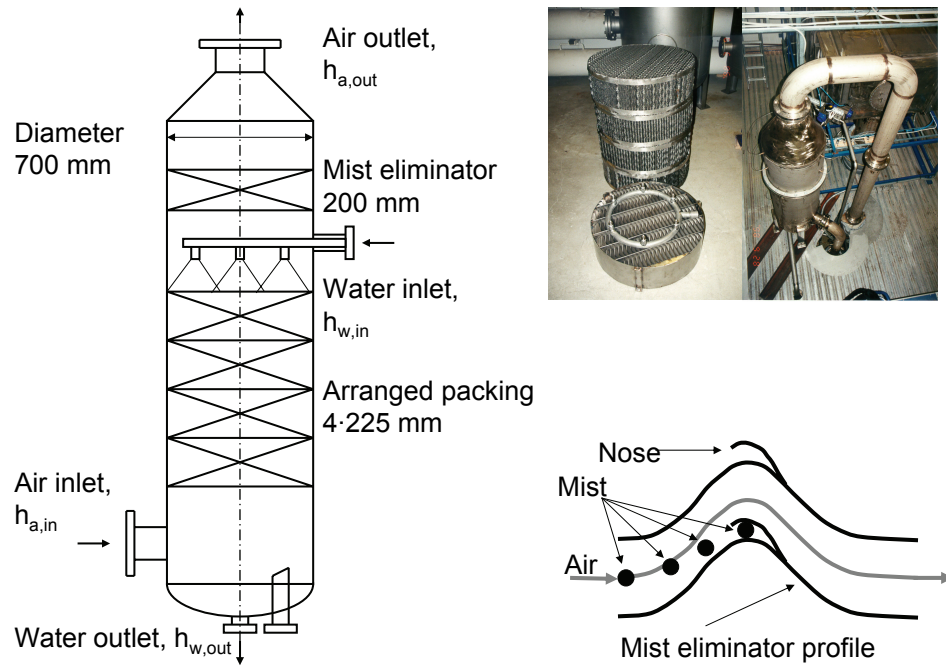
Figure 3.6: Arranged packing, water nozzles, mist eliminator and humidification tower

Figure 3.6 shows the humidification tower in the EvGT pilot plant. The tower is similar to absorption towers used in chemical industries and is a cylindrical pressure vessel which is designed to handle an operating pressure of around eight bar. The humidification tower consists of structured packing, a water distributor, a mist eliminator and inlet and outlet water and air-flanges. The overall height of the humidification tower is around 3 m and the inner diameter is 0.7 m.

Figure 3.6 also shows the structured packing. The packing is made of stainless steel plates that are formed in a way to produce small, narrow triangular channels. The triangular channel gives a high transfer area per volume of tower and the specific surface area of the packing in the laboratory is 240 m^2/m^3. The structured packing has low pressure-drop which affects the gas turbine process as little as possible. The structured packing is 900 mm high and consists of four equally sized units, which can be separately removed from the tower in order to vary the height of the packing. In the gas turbine process, air enters the humidification tower at the bottom of the

column, passes through the packing and exits the column in the top. Six nozzles located at the top of the tower, ensure that the water distributes evenly over the packing. Good water distribution is important to achieve good wetting performance in the tower which in turn defines the transfer area achieved with the process equipment. The size of the droplets from the nozzles is as large as possible in order to minimize the risk of natural water droplet entrainment into the air. If the circulating humidification water is not de-ionized, the entrained droplets are undesired. A mist eliminator at the top of the humidification tower ensures that the air exiting the tower is not contaminated. Figure 3.6 shows the working principle of the mist eliminator. The operation of the mist eliminator is the difference between the density of water and air. The mist eliminator therefore separates the droplets from the air by inertia.

The measurement system around the humidification tower consists of several measuring points. The temperature is measured by three different thermocouples at all inlets and outlets. Pressure sensors are also installed prior and after the humidification tower so that the pressure drop over the humidification tower can be measured.

In the EvGT pilot plant the humidification tower is divided into two parts. A mixing tank is located just below the humidification tower. This mixing tank is not necessary in a real power plant, however it is installed as a safety precaution. With the mixing tank installed it is easier to separate the water circuit and the air circuit. The amount of water evaporated in the humidification tower, is achieved by keeping the water level in the mixing tank constant. Since water is evaporated from the water circuit, a pump must maintain the constant water level by pumping water into the mixing tank. The amount of water injected into the cycle is therefore measured by measuring the amount of water that passes through the pump.

3.3.5 Aftercooler

The purpose of the aftercooler (AC) is to facilitate the extraction of low-level heat from the exhaust gases. The AC cools the air that enters the humidification tower. This reduces the temperature of the outgoing water from the humidification tower. This reduction of the water temperature increases the heat recovery in the EvGT cycle. With a lower temperature of the circulating water, the economizer can extract more low-level heat from the exhaust gases. The humidification water that circulates the EvGT is divided into different flows. One flow cools the compressor discharge air in the aftercooler while the other flow cools the exhaust gas in the economizer.

Figure 3.7: Installation of the plate heat exchanger aftercooler

Figure 3.7 shows the aftercooler in the EvGT pilot plant. The AC in the pilot plant is a brazed-plate heat-exchanger type. The heating surface consists of thin corrugated metal plates stacked on top of each other. The number of plates is 170 and the total dry weight is around 300 kg. The AC is around 1 m high, 0.4 m wide and 0.7 m in length.

3.4   Experimental Evaluation

When evaluating the measurements obtained from performance tests of gas turbines, the data has to be normalized in order to be able to compare the results from different atmospheric inlet conditions. The International Organization for Standardization (ISO) has developed a standard to be used for comparison of measurements performed during different ambient conditions. In the ISO standard, all measurements should be re-calculated to a standard day that is defined as 15°C, 1.01325 bar and a relative humidity of 60%.

In wet gas turbine cycles, the increased mass flow due to water injection creates a mismatch between the flows through the compressor and the expander. The rate of evaporation is related to several factors, among other

things the ratio between the liquid and the vapor mass flow in the humidification tower. The gas turbine in the pilot plant is of a standard type where the mass flows through the compressor and expander which are both equal. To compensate for the extra mass flow through the expander, the pilot plant uses a bleed-off valve to bleed off excess air after the compressor (figure 3.5). The ISO standard was not developed to compensate for the excess humidification or the bleed-off airflow. This makes it impossible to use the current ISO standard in the evaluation of the measurements from the pilot plant. Since there is no accurate method to correct the collected data, the performance test is required to be carried out on an almost standard day. To be able to predict the true work output and efficiency that would have been obtained if the compressor had been rebuilt, process calculations have to be made. The software used to evaluate the pilot plant is IPSEpro™, developed by SimTech, Simulation Technology. The models of the components have been validated by several experiments [135–140]. The atmospheric conditions during one performance test were 9°C, 1.000 bar and 70% relative humidity in the air.

3.4.1   Experimental Testing

The experiments in **paper II**, were carried out during several days and data was collected during all experiments. The installation of the aftercooler did not pose any problem to the starting procedure of the pilot plant. The starting sequence of the EvGT pilot plant can be found in Lindquist's thesis [135]. The hydraulic brake on the gas turbine is set on the pre-determined load. The tests were performed at 40, 50, 60 and 70% load. The measurements does not start for a period of 15 minutes after the pilot plant has started. This is done to ensure that the values obtained from the measurements are stationary and stable values. The measurement points of temperatures, pressures and mass-flows can be seen in figure 3.5.

3.4.2   Efficiency and Global Parameters

Figure 3.8 shows the experimental values of the thermal efficiency of four different thermodynamic cycles; simple cycle (1), recuperative cycle (2), EvGT cycle without aftercooler (3) and the EvGT cycle with the aftercooler (4). The extrapolation of the data to full power is also shown. The tests were all carried out at different days and thus with different ambient conditions. The values can therefore not be compared straight away. The experiments were however conducted at similar conditions which merits some attention.
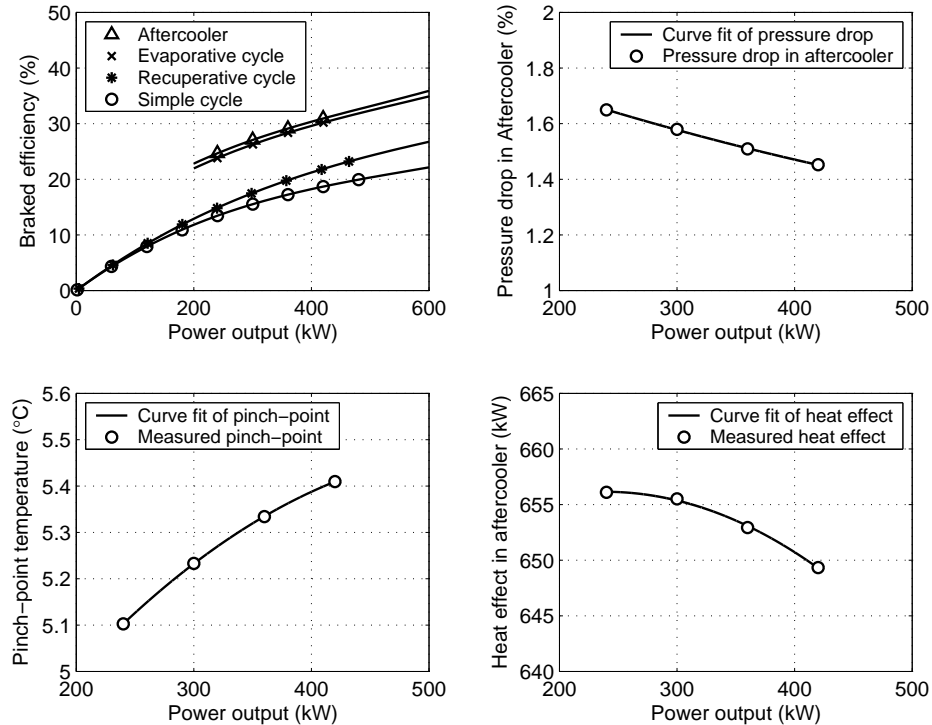
Figure 3.8: Experimental result of the development of the EvGT pilot plant

It is also educational to se all the cycles represented in the same diagram. The test of the cycles 1–3 were carried out by Torbjörn Lindquist and are represented in his thesis [135].

Figure 3.8 shows that the thermal efficiency of the aftercooler cycle has increased the performance of the cycle. At full power, the estimated thermal efficiency is 35.9% compared to 34.9% for cycle number 3. The increased thermal efficiency can be explained by the increase of humidification within the cycle. This increased humidification is due to the installed aftercooler.

Humidification Tower

In the humidification tower, the pinch-point plays an important role in the heat recovery system. The pinch-point is the smallest difference between the water temperature from the heat recovery system and the saturation temperature of the compressed air. With a low pinch-point in the humidi-

fication tower, the water exiting the humidification tower can be low. With a low pinch-point, the outlet water temperature from the tower will also be low. A low pinch-point increases the capability to recover more low-level heat from the aftercooler and economizer.

The pinch-point is also a measure of the difficulty of performing the evaporation of water. An increased pinch-point indicates that the evaporation in the tower has become more difficult. Earlier experiments with the evaporative gas turbine without an aftercooler and 900 mm of packing showed that the pinch-point varied between 3°C and 3.5°C [135]. This leads to a water outlet temperature from the humidification tower of 105°C [135]. Figure 3.5 shows experiments with the aftercooler using the same packing height in the tower as before. The result shows that the pinch-point increases and attains a value of 5.1°C to 5.4°C. The explanation of this observation is that the aftercooler lowers the saturation temperature of the incoming air. This reduction in saturation temperature means that a greater enthalpy exchange has to occur in the tower to achieve a similar evaporation. To respond to the greater enthalpy exchange using the same packing height, the pinch-point will increase in the tower. High inlet water temperature to the humidification tower is favorable to the evaporation process [138]. The EvGT should therefore operate at the highest water inlet temperatures to the humidification tower as possible at the design pressure. The temperature of the water entering the humidification tower on the test day is at 143°C, which is 27°C lower than the saturation temperature at the operating pressure. With the aftercooler installed and the inlet water temperature at 143°C, the water temperature after the humidification tower reduces to 79°C.

The Aftercooler

The biggest concern when installing a heat exchanger in a power plant environment is the pressure drop associated with the installation of the heat exchanger. Introducing pressure drops drastically impedes the thermal efficiency of the power plant. The pressure drop in different heat exchanger configurations for gas turbine cycles greatly influences the calculation results of the thermal efficiency and the economical result of the calculations. Throughout the literature several different values have been assumed for the pressure drop in the intercooler and the aftercooler [19–22, 92–95, 118–121, 203, 204]. The pressure drop was thus a vital parameter to investigate during the test period. Figure 3.9 shows that the pressure drop is approximately 1.55%. The inlet temperature of the air en-
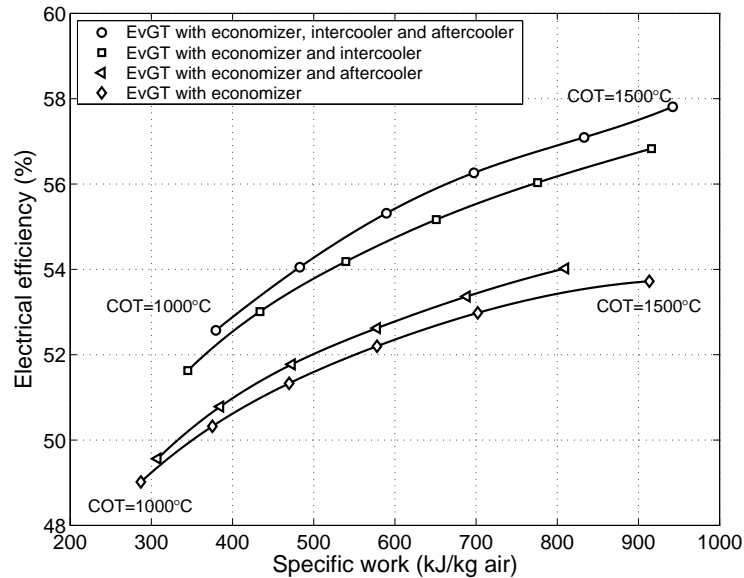
Figure 3.9: Thermodynamic optimization results

tering the aftercooler was on the test day 370.8°C at a pressure of 8.24 bar$_a$. The temperature of the air after the aftercooler was reduced to 72.9°C

Another important factor to investigate is the pinch-point in the aftercooler. This temperature difference is also important for the thermal efficiency. From the experiments it can be concluded that the pinch-point on the cold side is around 0.1°C. This is a very low number and may occur because the plate heat exchanger is oversized for its present duty. However, it is constructive to see that a very low pinch-point can be achieved in the power plant.

3.5 Thermodynamic Evaluation

In order to verify that there are benefits to using an aftercooler, process calculations are made in **paper II**. In the process calculations, it is assumed that the gas turbine is modified to handle the extra mass flow through the expander. The gas turbine used in the calculation is a mid size gas turbine when working in the simple cycle mode. The experimental data obtained from the pilot plant is used as input parameters to the calculations. This means that the pressure drop and pinch-point in the aftercooler are directly

transferred to the calculations. It is assumed that the plate heat exchanger can be manufactured in a size required for the application and pressure ratio of the gas turbine in the calculations. To calculate the required blade cooling to cool the blades in the expander, a theoretical model developed at the department has been used [123].

Figure 3.9 shows the result from the thermodynamic evaluation of the EvGT cycles. The complexity of the heat exchanger network is added. The EvGT cycles calculated are an EvGT with an economizer as the only water heat exchanger, EvGT ECO, the EvGT with an aftercooler and an economizer, EvGT ECO AC, the EvGT with an economizer and an intercooler, the EvGT ECO IC and the EvGT with an economizer, intercooler and aftercooler. The values plotted in figure 3.9 are the optimum values for each specific value of turbine inlet temperature. The optimization parameter has been the compressor discharge pressure and the intermediate compressor pressure. Higher turbine inlet temperature leads to higher electrical efficiency. As can be seen from figure 3.9, electrical efficiency is increasing as the thermodynamic cycle becomes more complex. The increase in electrical efficiency from a cycle that is not using an aftercooler to a cycle that is using an aftercooler is around 0.3–0.5% units. This increase is due to the increased enthalpy exchange within the humidification tower and the reduced temperature leaving the tower. The real increase in electrical efficiency is when an intercooler is employed in the cycle. This is because the compression work is reduced and therefore more work can be extracted from the gas turbine. As a result, the increase in electrical efficiency is then 3.0 to 3.8% units.

Chapter 4

The Humidification Process

This chapter presents the theory behind the humidification tower in an evaporative gas turbine cycle. This chapter begins with a literature review, which details the simultaneous heat and mass transfer theory for cooling towers and humidification towers. Section 4.2 presents the heat and mass balances of the humidification process. The first part of the section deals with the control volume analysis of an incremental part of the tower. The second part develops the expressions required for solving the equations from the control volume analysis. The theoretical model solves the heat and mass balances from the bottom of the tower and integrates the values upwards through the tower. Section 4.4 presents results from experiments in the pilot plant in Lund. The theory presented here is an extension of the theory from **paper I** and **paper VI**.

4.1 Literature Review

In 1925, Merkel presented one of the first methods for predicting the performance of humidification towers. The method aimed at describing the behavior of atmospheric cooling towers. Instead of using the concentration difference as a driving force for mass transfer, Merkel introduced the enthalpy difference as the driving force. In his theoretical model, Merkel uses several assumptions in order to simplify the mathematics behind the method. In 1949, Mickley presents an extended version of Merkel's model. Mickley visualize the physical behavior of the humidification process. The models presented by Merkel and Mickley are both developed to describe the behavior of the cooling tower. There are many similarities in the mathematics, which govern the humidification towers and the cooling towers. Due

to these similarities, Merkel's and Mickley's methods solve the process of humidification including cooling towers [157]. Experiments conducted with atmospheric humidification and cooling towers show that the models can predict the performance within a few percent accuracy [157]. These models agree very well with experiments conducted for atmospheric humidification towers with approximately the same accuracy. The method of extrapolating this method to high-pressure humidification towers is common. Experiments in the pilot plant show that Merkel's method is insufficient to determine the height of the humidification tower. At temperatures exceeding 60°C, the error associated with Merkel's and Mickley's method becomes large [200]. Since EvGT cycles humidify air at temperatures that far exceed this temperature, the Merkel method cannot accurately predict the performance of such cycles.

In 1988, Benton et al. began analyzing the cooling process in evaporative cooling towers [26]. In his paper Benton studies the cooling process from the basic equation. The idea of the project is to go from more graphical methods, as those of Mickley and Merkel, to more sophisticated computer models. Benton thus analyzes the evaporative cooling from a control volume analysis. The theoretical model developed solves the transport equations throughout the tower. Benton et al. compare their model to both natural draft towers and mechanical draft towers.

In 1994, Enick focused the attention from cooling towers to humidification towers in humid air turbines [146]. Enick's theoretical model estimates the height of the humidification tower with some simplifications to the physics. One of these is that Enick considers the interface temperature between the liquid and air interface has the same temperature as the bulk liquid. This means that Enick assumes that the heat transfer in the liquid occurs instantaneously so that the resistance to heat transfer is large. This theoretical humidification model has been evaluated both on evaporative cooling towers and has found to agree well with experimental data. With a theoretical model similar to the one developed by Enick, Gallo et al. study the humidification process with a model similar to Enick [90]. The model aims at determining the height of a humidification tower with dumped packing in a HAT cycle. In their model Gallo et al.acknowledge that the heat transfer from the liquid side occurs over a temperature difference. Gallo et al. calculate this heat transfer in his model, including the interface temperature. The model has been validated against atmospheric evaporative cooling towers. This validation shows that the height of the cooling tower is estimated within 1% of error.

In 1997, Ågren presented his licentiate thesis were he describes a model based on the transfer unit methodology [94]. In his model a constant value of the height of a transfer unit, given by the manufacturer of the packing, is used for the height calculations.

In 2003, Dalili presented his doctoral thesis on humidification in evaporative power cycles [62]. Dalili goes one step further than Ågren and determines the value of the height of a transfer unit. Dalili correlates the value given by the manufacturer to operating conditions which correspond to evaporative gas turbine cycles with good results. Dalili also presents a humidification theory for tubular humidifiers.

In 2003, Aramayo-Prudencio and Young presents a paper in a two part discussion including the thermodynamics and heat and mass transfer of the humid air cycle. In the first part of their paper, they present the general thermodynamic theory of the humidification process. This model is intended to be used with parameter optimizations of humid air turbines. The theory of Aramayo-Prudencio and Young do not rely on the *straight line approximation* as many other methods do. In the *straight line approximation*, the operating line within the humidification tower is considered to be a straight line. The performance of the humidification tower can then be related to the saturation line with a small temperature difference called the pinch-point [123]. This pinch-point is a measurement of how well the humidification process is conducted by the equipment. The model uses an invariant which is exactly constant throughout the saturator whereby no approximation is required.

In the second part of the paper, Aramayo-Prudencio and Young presents the theory of the heat and mass balances within the humidification tower. This method is similar to the model developed by Lindquist et al. [138] in **paper I**. The difference between the two models is the reasoning concerning the liquid side heat transfer coefficient, α_l. Aramayo-Prudencio and Young argue that the flow of liquids and gases inside the tower is very complex. According to the authors this means that the model developed by Lindquist et al. [138] has some weakness which appears when Lindquist et al. approximates the liquid side heat transfer coefficient as the ratio of the heat conductivity to the film thickness. Aramayo-Prudencio and Young uses an approximation of the Nusselt number based on past knowledge of heat transfer theory. Aramayo-Prudencio and Young then approximate the coefficients of the Nusselt number based on prior knowledge of heat transfer and to fit current experimental data. They still acknowledge that it is hard to see how a more reliable theory than the one presented by Lindquist et al. [138] could be constructed that would give better results to the humidifi-

cation process. Aramayo-Prudencio and Young also use a second parameter to tune the mass transfer of water in the humidification column. They conclude that a model for the humidification process has been more rigorously developed then before. It is concluded that more experimental data is required to obtain the heat and mass transfer correlations that are needed for humidification towers. The authors also consider the potential of super saturation of the air at the top of the humidification column. According to the authors, it is not likely that super saturation occurs because water entrainment and particles in the air would make it impossible for the air to become supersaturated.

In 2003, Parente et al. present a model that predicts the performance of the humidification tower [171]. In their model Parente take data taken from Lindquist's licentiate thesis and uses it to evaluate their model. In the paper, the authors use a model for the mass transfer coefficient developed for the packing material of Raschig Rings. The authors use a model for Raschig rings and evaluates it against measurements of the performance of a structured packing. To accommodate the difference between the measurements and the theoretical model they use a correction factor which is trimmed to match the experimental data. With this correction the authors feel that the theoretical model works satisfactorily. This model is then used to do carry out an economic evaluation of a saturator. The authors also conclude that the cost of the humidification tower is a small cost compared to the other equipment in the humid air cycle.

In 2004 Cevasco et al. presents an off-design and transient analysis of the humidification tower for humid air turbines [49]. The analysis of the humidification tower in transient analysis and off-design performance is in good agreement with experimental data.

In 2004, Liu et al. presents the theory of dynamic modeling of spray evaporators. Liu et al. uses a one-dimensional control volume method to determine the performance of the tower. Liu claims that the theoretical model has fast convergence relative to other dynamic models of the humidification tower. Liu et al. however compares his model for a spray tower to models developed for humidification towers containing structured packing.

4.2 Heat and Mass Transfer Theory

This section presents the derivation of a heat and mass transfer model aimed at solving the thermodynamics of the humidification tower. **Paper I** and **paper VI** presents the full derivation of the equations. The problem is

that the tower is adiabatic and not isothermal. This means that the temperature of the fluids engaged in heat and mass transfer are changing their temperature throughout the column. The temperature of the liquid of the high-pressure humidification process is also very close to the boiling point at the operating pressure, which means that the model must therefore account for the simultaneous heat and mass transfer process occurring when liquid is vaporized into the air. To solve the heat and mass transfer equations, the humidification tower is divided into several increments (see figure 4.1). The model then solves the heat and mass transfer equations for each increment from the bottom and upwards. Since the temperature changes through the tower, the model calculates the properties of liquid and moist air at the different segments. The model determines the heat and mass transport at the interface of each segment. The input data to the humidification model is at the bottom of the tower streams of the humidification tower. A boundary value has to be known at the top of the tower in order to stop the calculation which depends on the current use of the model. In determining the height of a tower, the inlet temperature of the water is used because this temperature is often limited by the heat recovery system and the pinch-point against boiling. When the height of the humidification tower has been determined it is possible to evaluate the performance of the humidification tower at different conditions. In order to calculate the off-design behavior of the humidification tower, the boundary values of the calculation method are changed to take into consideration that the geometry of the humidification tower is constant and the thermodynamic properties change.

4.2.1 Control Volume Analysis

The model developed here is based on a differential control volume around an incremental piece of the tower. The control volume is any selected region in space and the space outside the control volume is called the surroundings. The control volume is a selected tool that enables an analysis of the humidification system. In the control volume analysis, both mass and energy can cross the boundary of a control volume. Figure 4.1 shows a system with a control volume drawn around it.

To perform a control volume analysis of the tower, it is important to understand the physical behavior of the system being analyzed. The process of humidification within the humid air turbine starts when the compressor discharge air comes into direct contact with the humidification liquid. These two phases are not at equilibrium with each other and concentration and temperature gradients occur across the interface. These temperature and
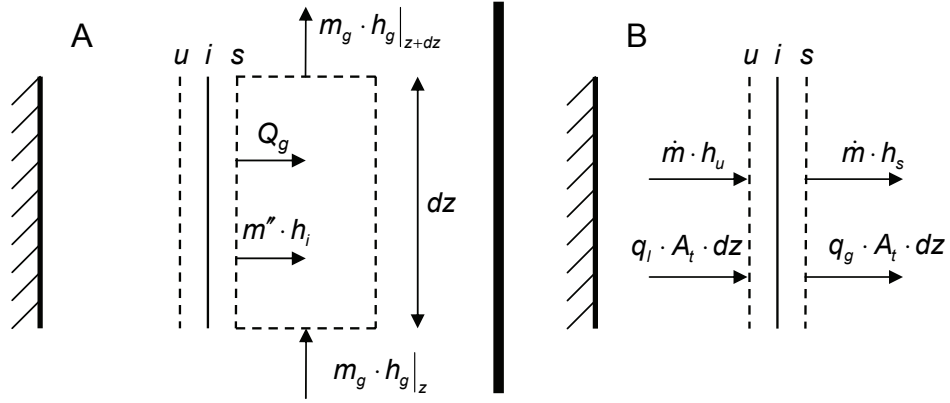
Figure 4.1: Infinitesimal control volume of the humidification tower

concentration gradients gives rise to two physical processes within the tower, heat and mass transfer. Energy and mass balances are set up across the control volume to account for the transfer processes.

Mass Balance on Gas Side

Figure 4.1 shows the control volume of a small element in the humidification tower. The subscript l denotes the liquid stream, g denotes the gas stream and i denote the interface between liquid and gas phase. The letters u and s denote the control surface on the liquid and gas side respectively. A mass balance for the control volume around the gas phase yields.

$$\frac{dm_g}{dz} = m'' \cdot A_t \tag{4.1}$$

in equation 4.1 m_g is the gas mass flow rate and m'' is the mass flux. Equation 4.1 shows that the increase in mass flow between the inlet and the outlet of the control volume is equal to the evaporation that occurs within that control volume.

Energy Balance on Gas Side

Similar to equation 4.1 an energy balance can be performed for the control volume around the gas phase. Figure 4.1 shows the different energy interactions between the gas and liquid phase. Depending on the conditions of the humidification process different energy transfers occur in the tower. At

the bottom of the tower it is not unusual that the temperature of the air is higher than the temperature of the liquid. This means that the air also supplies energy to the evaporation process. As the air moves up the tower the way the energy interactions takes place also changes and the energy required for the evaporation process is instead taken as sensible heat from the liquid. This means that the temperature of the liquid will decrease from the top of the humidification tower to the bottom. Taking into account all of the processes described above makes it possible to state the energy equation for the control volume on a differential basis as equation 4.2.

$$\frac{d(m_g \cdot h_g)}{dz} = q_g \cdot A_t + m'' \cdot A_t \cdot h_i \tag{4.2}$$

The heat transfer is taken care of by the parameter in q_g in equation 4.2. The parameter m'' is the mass flux through the interface. Equation 4.2 shows that the increase in energy through the control volume is dependant of the heat transfer between the phases and the evaporation of the liquid to the gas phase.

Interface Temperature

Equation 4.2 shows that the energy transfer depends on the enthalpy at the interface. This enthalpy has to be evaluated at the interface temperature. The interface temperature is an important variable in the calculation of the heat transfer from the surface to the bulk gas. Most models assume that the interface temperature is at the same temperature as the bulk liquid flow [14, 213]. This simplification is sufficiently accurate at low temperatures and at slow mass transfer rates [157]. Both Merkel and Enick use this simplification in their models and experiments show that this is a valid assumption when calculating the performance of atmospheric cooling towers and humidification towers [157]. However, experiments in the pilot plant show that the simplification of slow mass transfer rates restricts the use of the Merkel model in pressurized humidification towers. Part B in figure 4.1 shows a control volume drawn around the interface between the liquid phase and the gas phase, which makes it possible to apply an energy balance at the interface. The energy balance enables the calculation of the interface temperature.

$$\alpha_l(T_l - T_u) = \alpha_g(\Xi_H + \Phi_H)(T_s - T_g) + (m'' \cdot h_{fg})_1 + (m'' \cdot h_{fg})_2 \tag{4.3}$$

The mass transfer affects and distorts the temperature, velocity and concentration profiles of the boundary layers. Correction factors are introduced

to account for the high mass transfer rate [27, 157, 209, 221]. In equation 4.3, Ξ_H is the Ackerman factor and Φ_H is the heat transfer rate factor defined by equations 4.4 and equation 4.5.

$$\Xi_H = \frac{\Phi_H}{\exp(\Phi_H - 1)} \tag{4.4}$$

$$\Phi_H = \frac{N_1 C_{p1} + N_2 C_{p2}}{\lambda/l} \tag{4.5}$$

Paper I shows that it is possible to derive an expression for the interface temperature. The interface temperature can thus be calculated according to equation 4.6 [136].

$$T_i = \frac{1}{\alpha_l + \alpha_g}\left(\alpha_l \cdot T_l + \alpha_g \cdot T_g - \rho \cdot h_d \cdot \frac{\omega_i - \omega_g}{1 - \omega_i} \cdot h_{fg}\right) \tag{4.6}$$

The last term in equation 4.6 is the evaporated mass flow in the control volume. The parameter, h_d, is the mass transfer coefficient determined by equation 4.16. In equation 4.6 the Ackermann factor and the heat transfer rate factor has been set to one which is fairly close to the reality [138]. From equation 4.6 it can be realized that the liquid heat transfer coefficient, α_l, is needed to complete the calculation. The assumption in this model is that the fluid in the packing behaves as a fluid flowing down a flat plate. One further assumption is that the flow is laminar.

$$\alpha_l = \frac{\lambda_l}{\delta_l} \tag{4.7}$$

With these assumptions, the heat transfer coefficient can be calculated with equation 4.7 [151]. In equation 4.7 the parameter, λ_l, is the heat conductivity and the liquid film thickness δ_l is obtained from Perry [175].

4.2.2   Interface Equilibrium

To be able to predict the mass transfer, the concentrations of the different species are required at the bulk gases and liquids as well as for the interface. This means that there has to be some relation between the concentrations. The relationship between the concentrations of different species in the liquid and vapor phase can be represented as:

$$x_1 + x_2 = 1 \tag{4.8}$$

$$y_1 + y_2 + y_3 = 1 \tag{4.9}$$

Equation 4.8 and equation 4.9 shows that the sum of the species in each phase cannot be greater than one.

To determine the concentrations at the interfaces, a relation between the concentrations of the species in the liquid phase and the gas phase needs to exist. To find such an expression, consider the case of a mixture of ethanol and water. When this binary liquid is evaporating the mixing process is beneficial to the evaporation process. This is due to the higher partial pressure of the ethanol and also to favorable mixing effects. The mixing effect allows the ethanol to achieve a higher concentration in the air, which results in more ethanol transferring to the air. To determine the composition at the interface, the total pressure of the system is the sum of the partial pressures and must in some way be associated with the properties of the liquid.

It can be shown that the partial pressures of the different vapors are proportional to the saturation pressures of the different fluids according to equation 4.10 [70, 178].

$$y_i \cdot P = \gamma_i \cdot x_i \cdot p_i \tag{4.10}$$

In equation 4.10, γ is the activity coefficient of the species in the fluid. The activity coefficient can be considered as the parameter that determines how much the mixture deviates from the ideal solution. In the case of pure water the activity coefficient is equal to one and the solution obeys Raoult's law [70, 178].

4.2.3 The Mass Transfer

When the composition of the gas at the interface is known, the mass transfer between each phases can be calculated. As stated before the driving force for the mass transfer is the concentration gradient between the interface and the bulk gas. The film model has been used in **paper I** and **paper VI** to describe the mass transfer process. According to the film model all resistance to the mass transfer process is located inside a thin film [27, 157, 209, 221]. All the mass transfer occurs within this film. Outside this film, all concentration differences disappears due to turbulence.

The molar fluxes in the vapor phase can be stated as [24, 27, 58–60, 151, 155, 157, 200, 209, 213, 221]:

$$N_1 = J_1 + y_1^g \cdot \left(N_1 + N_2 \right) \tag{4.11}$$

$$N_2 = J_2 + y_2^g \cdot \left(N_1 + N_2 \right) \tag{4.12}$$

In equation 4.11 and equation 4.12 the parameters, J_1 and J_2, are the diffusive flux. The diffusive flux of a specie is the relative motion of the specie with respect the entire mixture. The diffusive flux, J_1 and J_2, of the different species is given by:

$$J_1 = c_t^g \cdot k_{11} \cdot \left(y_1^s - y_1^g\right) + c_t^g \cdot k_{12} \cdot \left(y_2^s - y_2^g\right) \tag{4.13}$$

$$J_2 = c_t^g \cdot k_{21} \cdot \left(y_1^s - y_1^g\right) + c_t^g \cdot k_{22} \cdot \left(y_2^s - y_2^g\right) \tag{4.14}$$

In equation 4.13 and equation 4.14, c_t^g is the molar density of the solution and the parameters $k_{i,j}$ is the mass transfer coefficients for the mass transfer. In the above equation air is considered to be an inert gas that does not dissolve in water. This only partly true because all gases are solvable in water. It is here assumed that the contribution of the air transfer into the water does not alter the equilibrium relations or the mass transfer rates in the mixture. This is also considered in references as [27, 209].

The mass transport of water and ethanol to the control surface also needs to be considered in the calculations. It is however sufficient to account for one mass transport since the other is taken care of by the requirement that the interface compositions must equal one according to equations(4.8– 4.9). The mass transport is thus given as:

$$N_1 = c_t^l \cdot k_l \cdot \left(x_1^l - x_1^u\right) + x_1^l \cdot \left(N_1 + N_2\right) \tag{4.15}$$

In equation 4.15, c_t^g is the molar density of the solution and the parameters $k_{i,j}$ is the mass transfer coefficients for the mass transfer. In equation 4.15 the diffusive flux has been written directly to simplify the equations.

The heat and mass transfer at any given location in the tower can be found by simultaneously solving the mass transfer equations with the equilibrium equations and an energy balance across the interface.

Mass Transfer Coefficient

The mass transfer coefficient, h_d, is determined by the Sherwood number, Sh. The Sh has experimentally been determined for counter current distillation and absorption columns with arranged packing and triangular flow channels by Bravo et al. [33–36, 81, 83, 190]. This model is used in **paper I** and **paper VI** to calculate the mass transfer coefficient.

$$Sh = \frac{h_d \cdot d_{eq}}{D_{ab}} = 0.0338 \cdot Re^{0.8} \cdot Sc^{0.333} \tag{4.16}$$

where h_d is the gas side mass transfer coefficient, d_{eq} is the equivalent diameter, D_{ab} is the diffusion coefficient, Re is the Reynolds number and Sc is the Schmidt number. The mass transfer coefficient, h_d, is corrected for high mass transfer fluxes to obtain the mass transfer coefficients, k_{ij}, of equation 4.13 and equation 4.14. The Reynolds number is defined as

$$Re = \frac{\rho_g \cdot d_{eg}\left(u_{g,eff} + u_{l,eff}\right)}{\mu_g} \tag{4.17}$$

where $u_{g,eff}$ is the effective velocity of the gas, $u_{l,eff}$ is the effective velocity of the liquid and μ is the viscosity. The equivalent diameter is defined as

$$d_{eq} = B \cdot H\left(\frac{1}{B + 2S} + \frac{1}{2S}\right) \tag{4.18}$$

where B=25 mm, H=7.9 mm and S=14.8 mm are geometric dimensions of the specific packing. The effective velocity of the air is determined by

$$u_{g,eff} = \frac{\dot{m}_g}{\rho_g \cdot A \cdot \varepsilon \cdot \sin\theta} \tag{4.19}$$

where ε is the void fraction and θ is the angle of inclination of the triangular flow channels in the packing. The effective velocity of the water is determined by

$$u_{l,eff} = \frac{3 \cdot \Gamma}{2 \cdot \rho_l}\left(\frac{\rho_l^2 \cdot g}{3 \cdot \mu_l \cdot \Gamma}\right)^{0.333} \tag{4.20}$$

where Γ is the flow rate per length and g is the gravitational acceleration. The flow rate per length is given by

$$\Gamma = \frac{\dot{m}_l}{A \cdot Per} \tag{4.21}$$

where Per the perimeter defined as

$$Per = \frac{4 \cdot S}{B \cdot H} \tag{4.22}$$

The Schmidt number is defined as

$$Sc = \frac{\mu_g}{\rho \cdot D_{ab}} \tag{4.23}$$

where the diffusion coefficient D_{ab}.

To determine the mass transfer coefficients, $k_{i,j}$ for the multi component mass transfer in equation 4.13 and equation 4.14 the binary mass transfer

coefficient, h_d, has to be converted. Different methods of calculating these coefficients can be found in the literature [3–6]. In this thesis the method by Taylor and Krishna was utilized to calculate the mass transfer coefficients [209]. A matrix R is created that contains the following elements:

$$R_{i,i} = \frac{y_i}{h_{i,n}} + \sum_{\substack{k=1 \\ k \neq i}}^{n} \frac{y_k}{h_{i,k}} \tag{4.24}$$

$$R_{i,j} = -y_i \left(\frac{1}{h_{i,j}} - \frac{1}{h_{i,n}} \right) \tag{4.25}$$

The matrix of the mass transfer equations is given according to the relationship:

$$\left[k^* \right] = \left[R \right]^{-1} \tag{4.26}$$

The parameter, k^* is referring to the coefficient of mass transfer for low mass transfer rates. Since the boundary layers are distorted due to the heat and mass transfer, correction factors have to be inserted. These correction factors are similar to the heat transfer process correction factors in equation 4.4 and equation 4.5. The elements of the mass transfer rate matrix, Φ_m is calculated according to

$$\Phi_{i,i} = \frac{N_i}{c_t h_{i,n}} + \sum_{\substack{k=1 \\ k \neq i}}^{n} \frac{N_k}{c_t h_{i,k}} \tag{4.27}$$

$$\Phi_{i,j} = -N_i \left(\frac{1}{c_t h_{i,j}} - \frac{1}{c_t h_{i,n}} \right) \tag{4.28}$$

Based on the mass transfer rate factor, the entire correction factor matrix, Ξ_m can now be calculated as

$$\Xi_m = \frac{\Phi_m}{\exp\left(\Phi_m - 1 \right)} \tag{4.29}$$

The corrected mass transfer coefficients, $k_{i,j}$ can now be calculated according to the following equation.

$$\left[k \right] = \left[k^* \right] \left[\Xi_m \right] \tag{4.30}$$

4.3   Experimental Work

There is no available experimental data in the literature on high pressure humidification in process equipment, i.e. for humidification towers in gas turbines. The pilot plant is used to study the evaporation process at elevated pressures and temperatures. The pilot plant is used in two ways to produce the required experimental data, the existing humidification tower in the pilot plant and a new separated humidification column. The existing humidification tower was used for the evaluation of the pilot plant in **paper I**. The ethanol humidification tower was used for the evaluation of **paper VI** and for further evaluation of the model developed in **paper I**.

4.3.1   The Existing Humidification Tower

Chapter 3 shows and describes the EvGT pilot plant at The Faculty of Engineering at Lund University in Lund. In that chapter, the humidification tower is well described. The pilot plant is equipped with a sophisticated measuring system that makes it possible to study the evaporation process directly in the gas turbine process. Measurements around the humidification tower can easily be extracted and made available for evaluation. As described in section 3.3 the pilot plant operates at a pressure of eight bar and the temperatures of the incoming water and the compressor discharge air can be altered to a certain degree. The highest temperature of the incoming water is determined by the saturation temperature of the water at the operating pressure of the gas turbine, which means around 170°C.

Section 3.3 also presents the pre-cooler. The pre-cooler is a plate heat exchanger that is installed prior to the aftercooler. The purpose of the pre-cooler is to cool down the water in the humidification circuit. This cooling results in cold water supplied to the aftercooler which makes it possible to lower the temperature of the compressor discharge air. The cooling water to the humidification circuit is taken from a separate water circuit within the building facilities of the EvGT pilot plant. This cooling is not taken care of by the internal heat recovery system of the gas turbine and is therefore creates a loss in thermal efficiency. The installation of the pre-cooler is however not meant to be a thermodynamic achievement. Instead, the installation of the pre-cooler adds another dimension to the pilot plant. It makes the pilot plant more flexible because more parameters can be changed during the experiments. This flexibility therefore makes it possible to test more operating conditions than could be performed without the pre-cooler.

4.3.2   The Ethanol Humidification Circuit

(1) Compressor
(2) Hydraulic brake
(3) Aftercooler
(4) Humidification tower
(5) Recuperator
(6) Combustor
(7) Expander
(8) Economizer
(9) Flue gas condenser
(10) Flue gas fan
(11) Water cleaner
(12) Water tank
(13) Pressure relief vessel
(14) Mixing tank
(15) Ethanol humidification tower
(16) Electrical heater
(17) Heat exchanger (1)
(18) Heat exchanger (2)
(19) Ethanol tank (1)
(20) Ethanol tank (2)
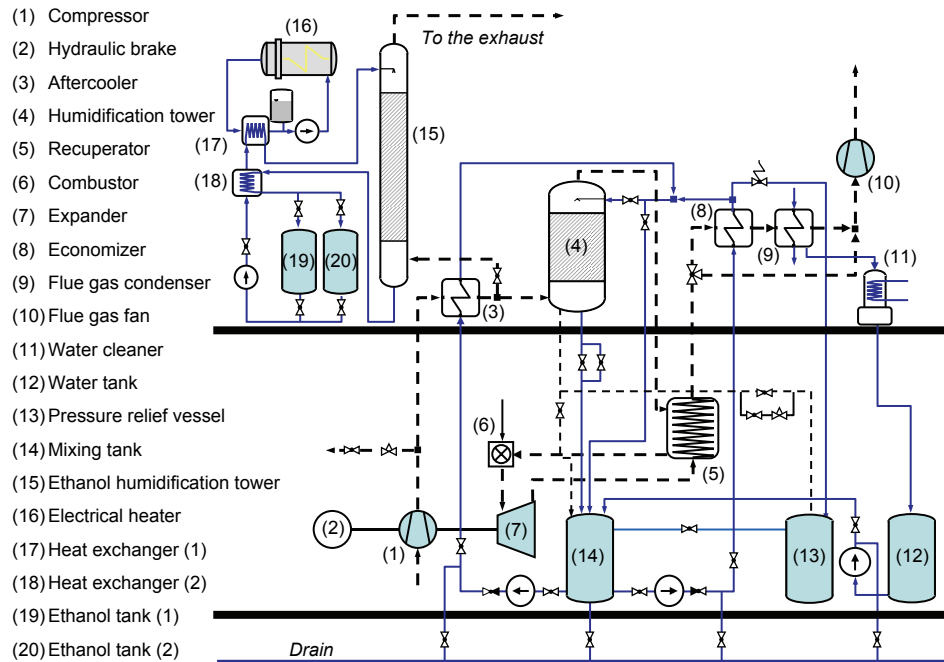
Figure 4.2: Bio-EvGT pilot plant

The ethanol humidification circuit was constructed by the author of this thesis in order to be able to investigate the humidification process. With the ethanol humidification circuit a number of humidification liquids can be tested without interfering with the gas turbine process itself. One of the ideas that was to be tested first was the humidification of a mixture of ethanol and water. This humidification circuit has therefore been titled the "ethanol humidification circuit" and will be referred to from hereon.

Using this external humidification process allows a degree of freedom which makes it possible to investigate the humidification process during more operating conditions. It is also valuable to be able to verify the humidification model developed in **paper I**, with the help of a second utility with another geometric construction under somewhat different conditions.

Gas Side of the Experiment Facility

Figure 4.2 shows the pilot plant with the modification of the ethanol humidification circuit. As can be seen from the figure a part of the compressor discharge air is extracted after the aftercooler (3). The amount of air that is extracted is regulated by a control valve located after the ethanol humidification tower (15). A mass flow meter is located just prior to the humidification tower and just after the aftercooler (3). This mass flow meter measures the amount of air that is bypassed through the gas turbine system. It is possible to extract the air from the gas turbine due to the evaporative mode that the gas turbine is working in. In this mode, water is evaporated which creates a mismatch between the compressor and the expander. To accommodate this increase in mass flow, air is bled off through the compressor bleed-off valve located after the compressor. When the ethanol humidification circuit is used, less air is extracted through the bleed-off valve and instead relocated to the ethanol humidification circuit.

The air enters the humidification tower at the bottom of the ethanol humidification tower (15). Inside the tower the compressor discharge air encounters the humidification liquid in a structured packing. The heat and mass transfer of interest occurs within this tower due to the fact that the compressor discharge air and the humidification liquid is not at equilibrium. The compressed air then leaves the tower saturated by the ethanol/water mixture at the top. The gas mixture is then passed to the chimney where it is vented into the atmosphere through the exhaust fan (10).

Liquid Side of the Experiment Facility

The supply of the evaporating liquid is stored in two 2 m^3 storage containers. In these containers, the required humidification liquid can be mixed to whatever concentration that is required for the experiment. The humidification liquid is pressurized and delivered to the ethanol humidification tower through a pump. The pressure in the ethanol humidification column is approximately the same as the operating pressure of the gas turbine.

The liquid is then heated to the desired temperature in two steps. It first recovers the remaining energy from the rest product from the ethanol humidification process. Then it enters a heat exchanger (17) where the mash is heated through a separate heating system. This heating system uses an electrical heater (16) to heat water that is pumped through the system.

The liquid enters the ethanol humidification tower at the top through a spray nozzle, which distributes the liquid evenly over the structured packing.

Good mass transfer needs large areas on which the mass transport can take place. Using a structured packing ensures that the heat and mass transfer can occur on a large area. After the humidification process, the water leaves the tower at the bottom.

The remaining energy in the mash flow is then utilized in a heat exchanger (18) which preheats the fresh entering mash-flow from the ethanol storage tanks (19). The remaining mash from the humidification process is now passed to the ethanol storage tank (20).

Ethanol Humidification Tower

Figure 4.3: Ethanol humidification tower in the pilot plant

The ethanol humidification tower is a pressure vessel that is designed to operate at a pressure of 16 bar and a temperature of 350°C. The total height of the ethanol humidification tower is five meters and the diameter is 0.350 m. Inside the ethanol humidification tower are two meters of structured packing. The structured packing has a specific area of 240 m^2/m^3. The structured packing consists of 10 equally sized units, which makes it possible to remove the units from the tower and vary the height. This flexibility makes it possible to study the impact of the height of tower packing to the

humidification process. A liquid distributor is installed 0.350 meters above the packing. The liquid distributor is a nozzle that is a full cone spray nozzle with a spray angle of 90° the tower to allow for a good water distribution

The difference between the humidification tower and the ethanol humidification tower is the inclusion of the mixing tank in the latter. This means that the ethanol humidification tower has a large volume at the bottom of the tower to collect the rest product of the ethanol humidification process.

4.3.3 Experimental Planning

Experimental planning of the experiments conducted with the experiment facility were performed. This section provides the experimental planning of the experiments conducted in two separate humidification circuits; the existing humidification tower and the ethanol humidification.

The Existing Humidification Circuit

The first experiments were conducted in the existing humidification tower. These experiments were run at many different operating conditions when the entire EvGT pilot plant was in operation. During the tests, the EvGT pilot plant is started and operated in four different load cases; 40, 50, 60 and 70%. These four cases enable the investigation of different operating conditions, which occur during the different load cases. After each test, the pilot plant is reconstructed so that four new operating conditions are achieved, such as different geometry or different temperatures.

The humidification tower is constructed so that the height of the packing in the humidification tower can be changed in intervals of 225 mm up to 900 mm. The packing is placed on a stabilization ring at the bottom of the tower and the required packing height is determined by loading or unloading the packing. This will result in a difference between the spray nozzles and the packing, which will create a form of spray tower between the packing and the nozzles. To avoid this spray effect, extensions of the nozzles have been constructed. These extensions makes it possible to have the same distance between the nozzles and the packing no matter what packing height is investigated.

Beside the ability to adjust the packing height, the pre-cooler and the aftercooler make it possible to operate the humidification tower at even higher operating conditions. The pre-cooler can be adjusted in 5 different steps, which sets the mass flow of cooling water through the pre-cooler. This

makes it possible to lower the temperature of the compressor discharge air before it enters the humidification tower.

The aftercooler was operated in three modes to evaluate both the humidification tower and the aftercooler; countercurrent mode, co-counter mode and without any aftercooler.

Measurements of the humidification tower contain pressure, mass-flow and temperature measurements. At each location, the temperature and pressure is measured by three separate measuring devices. The standard deviation between these measurement devices is less than 0.5°C. The EvGT pilot plant is used in the evaluation and several heat balances are used to evaluate the output from the measurements. This means that different sets of measurement points are used to evaluate the humidification tower through a heat balance over the entire EvGT pilot plant. This redundance in measurement points is used to make sure that the measurements have been made correctly and that the energy balance is fulfilled for every set of measurement data.

The Ethanol Humidification Circuit

The ethanol humidification tower (15) has been operated with both water and a mixture of water and ethanol. In this circuit, it is possible to change the liquid and gas flow through the tower. The mass flow of gases can be changed between 0 and the maximum amount of water evaporated in the humidification tower in the EvGT pilot plant. The experiments have mostly been operated with an air flow of 0.3 kg/s which means that some air still has to be bled off by the bleed-off valve in the pilot plant. The airflow is often set to a constant value during the test, while the liquid flow is varied. The liquid flow through the tower can be varied between 0 and 1 kg/s.

The heat input to the ethanol humidification circuit is determined by a separate heating circuit, which uses an electrical heater (16). The electrical heater can be controlled in four steps. These steps makes it possible to determine which set of resistance is used to heat the water in the heating circuit.

The liquid that is used as humidification liquid, is mixed in two large containers (19) and (20). The inlet ethanol concentration was 5.32, 9.35 and 13.2 mass percent for three different cases.

Measurements of the humidification tower contains pressure, mass-flow and temperature measurements. At each location, the temperature and pressure is measured in by two separate measuring devices. The standard deviation between these measurement devices is less than 0.4°C. The mass

flow of liquid through the circuit is measured by two mass flow meters at the inlet and the outlet. A separate heat balance around the heating circuit also makes it possible to determine the mass flow of liquid in the circuit. The mass flow of air into the ethanol humidification tower is determined in two ways; a mass flow meters measures the flow directly, and a heat balance across the EvGT pilot plant makes it possible to determine the mass flow indirectly. These ways of measuring the mass flow does not differ greatly.

The ethanol concentration was measured before and after the humidification tower. This was done by waiting for the system to become stable and then collecting a sample of the mixture of ethanol and water that exited the humidification tower.

The concentrations of ethanol were quantified by using gas chromatography. The gas chromatograph was a Varian 3700, equipped with an SGE split injector, a capillary column (length=25 m, inner diameter=0.25 mm, film thickness 0.25 μm) with DB–5 as the stationary phase (J&W) and a flame ionization detector. Nitrogen was used as carrier gas (2 ml/min) and n-propanol (2%) was used as an internal standard. The injector, column and detector temperatures were 240°C, 50°C, and 270°C, respectively. The samples were diluted with a propanol solution using a Sartorius L420S balance. All concentrations are given as relative mass (%). Each sample was injected at least three times.

4.4   Results

The calculations of the performance have been performed in two different ways. The height of the tower has been predicted by the model but the off-design performance of the tower is also validated based on the given geometry of the tower. This means that different boundary values were used for the two cases. For the design of the tower, a boundary value at the top of the tower is needed to complete the calculations. In the ethanol humidification tower the temperature of the liquid at the top of the tower is chosen as a boundary value. High temperatures of the humidification liquid enhances the evaporation process and it is therefore vital to achieve as high a temperature as possible. This means that the liquid temperature at the top of the tower is a dimensioning criteria of the humidification tower, and, thus is an obvious boundary value. The upper right diagram of figure 4.4 show the enthalpy of the air, saturation and operating lines. These are plotted against the temperature with an ethanol-water mixture as the evaporating fluid. Earlier experiments suggest that the model for the dif-
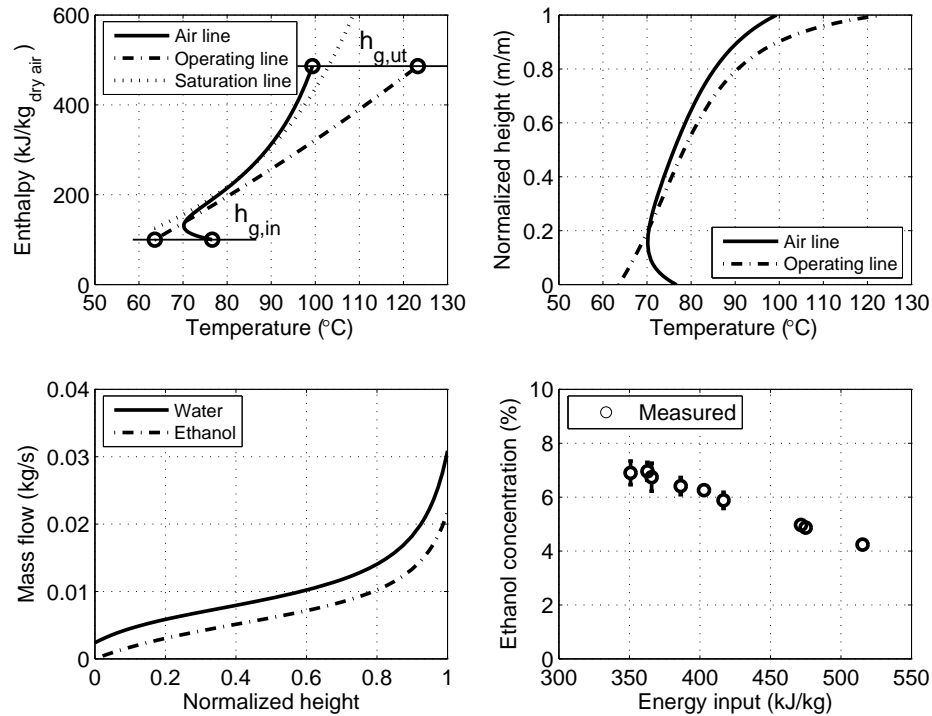
Figure 4.4: Results from ethanol experiments

fusion coefficients plays an important role for the airline [138]. This trend can also be seen for the evaporation of an ethanol-water mixture. This diagram also reveals that the air is seen to be somewhat supersaturated. This is a result also shown for the evaporation of water into an compressed air stream in humid air turbines. Research has focused on attempting to explain this behavior [115]. The answer to the supersaturated condition seems to be a consequence to that the model that uses the ideal gas law. This simplification leads to an error of around 3% for the case of water and air at an operating pressure of 8 bar [115]. In the case of the evaporation of a mixture of ethanol and water into the airstream, the difference is around 4%. Figure 4.5 shows the result of the calculations of the air and water operating lines for the humidification tower in the EvGT pilot plant. The humidification model calculates the exit conditions of the air stream. The Fuller–Schettler–Giddings model for predicting the diffusion coefficient was
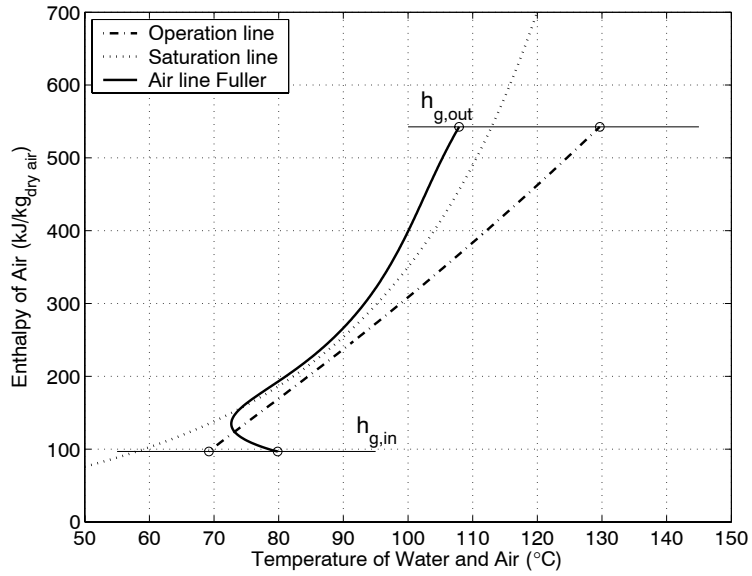
Figure 4.5: Results from water experiments

used. The inlet liquid temperature was 130°C and the outlet water temperature was 70°C. The inlet air temperature was 80°C.

Figure 4.5 shows that the pinch-point in the humidification tower is 2°C. This pinch-point is 1.5°C and therefore lower than the pinch-point in the existing humidification tower [136]. The super saturation is also clearly visible in figure 4.7. The slight curvature of the working line is also visible.

Chapter 5

The Bio-EvGT Process

This chapter presents the ethanol project. Section 5.1 presents a short background of the ethanol project. Section 5.2 details a description of the process scheme for the bio-EvGT. Section 5.3 provides a discussion of the model that is developed in **paper IV** and which predicts the behavior of the humidification process. This section also provides a discussion of the thermodynamic performance of the bio-EvGT cycle. Section 5.4 presents the economic model of the bio-EvGT process. The analysis is focuses on the optimum values retrieved from the thermodynamic optimization from section 5.3. This chapter contains some extensions to **paper IV, V, VII**.

5.1 Background

An increasing interest of using biomass as fuel to gas turbines has emerged during the last decades. This interest has developed due to environmental issues. Research in the environmental field has indicated that carbon dioxide may be responsible for global warming. It has therefore become very interesting to use biomass as fuel for power producing units. Biomass is considered to have zero net emissions of carbon dioxide which would therefore not contribute to global warming. Several new techniques for using biomass has been researched during the past years. The biomass fueled steam turbine power plant has been known for some time however a problem with this technique is poor efficiencies. In order to improve the efficiency of the biomass fueled power plant, different gas turbine configurations have been investigated. Externally fired gas turbines have also been investigated and it has been shown that the externally fired gas turbine can achieve electrical efficiencies of 38%, overall efficiencies of 86% at a low cost of electricity.

The environmental issue and the improved knowledge of the evaporative technology from the EvGT pilot plant soon led to an interest of using the evaporative technique to produce high efficiency gas turbines using biomass as fuel. In a doctoral thesis, Rosén introduced the concept of evaporating more than one fluid into the air [192]. The basic idea was to supply both water and fuel to the gas turbine.

A requirement for the evaporation process is that it must be possible to liquefy the biomass. One possible way in which to achieve a liquid fuel from biomass is to convert it into ethanol or methanol. Today, large-scale industrial plants produce ethanol by fermenting corn and seed. During the fermentation process, yeast or bacteria are added to start a reaction to create ethanol. The fermentation process produces a beer that has an ethanol concentration which ranges from 3–12 mass percent. This ethanol concentration depends among other things on the sugar content of the biomass. Different feedstock will therefore give different qualities to the beer.

Corn and seed are today the most common feedstock used to produce ethanol. Corn and seed typically give an ethanol concentration of 10–12 mass percent. The cost for producing ethanol today is high, which is due to the market price of the feedstock. Today, 40–70% of the cost for producing ethanol comes from the price of the feedstock [211]. To use corn or seed to produce fuel ethanol would make ethanol too expensive to compete with fossil fuels [211]. Current research today focuses on using different feedstock to produce ethanol. Cellulosic biomass today provides an ethanol concentration of 3 to 5 mass percent due to the difficulty of converting the cellulose and hemi-cellulose to sugar. In order to produce high concentrations of ethanol, the beer is distilled. The distillation stage produces a liquid with a concentration of 95 mass percent ethanol and 5 mass percent water.

In the bio-EvGT, the distillation process is replaced by a evaporation process. The evaporation process uses internal low-level heat in the EvGT cycle to extract the ethanol from the mash and transfer it into an airstream. Due to the high water content of the mash, water also evaporates into the airstream. Because the water enters the combustion chamber as a gas it is not harmful to the combustion process, however instead lowers the NO_x emissions from the combustion process. The evaporation process to supply the fuel to the gas turbine is not only limited to the EvGT cycles. The evaporation process can also function in combined-cycles and simple cycles as well. Even HAM engines may profit from this technique [192].

(1) Compressor
(2) Intercooler
(3) Aftercooler
(4) Humidifier
(5) Recuperator
(6) Combustor
(7) Turbine
(8) Generator
(9) Economizer
(10) Flue gas condenser
(11) Ethanol humidification tower
(12) District heating
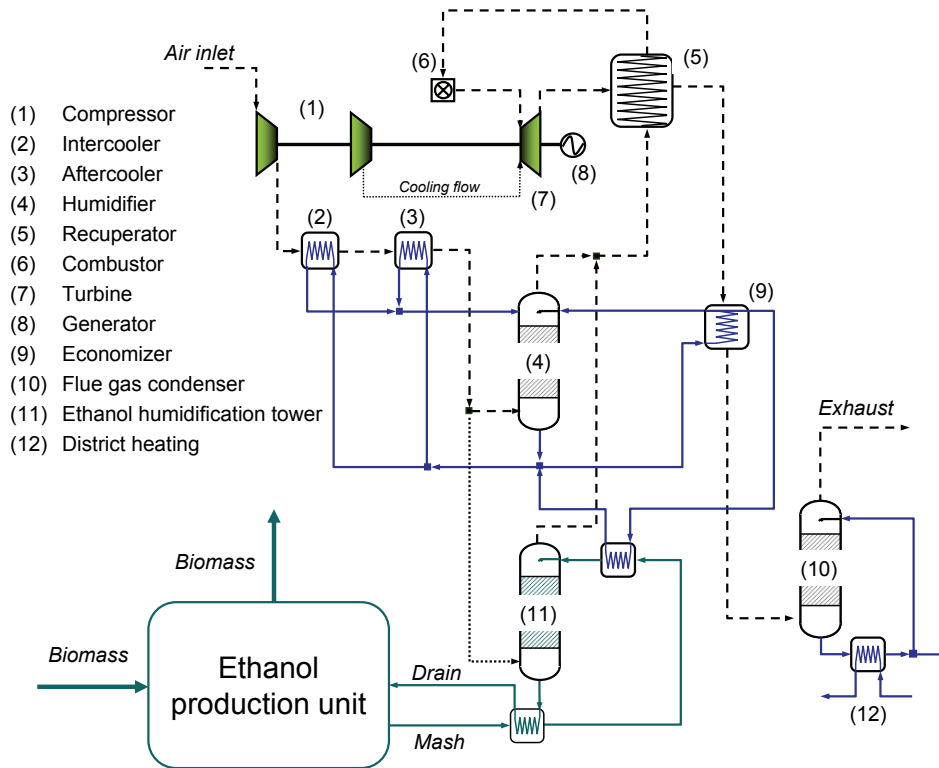
Figure 5.1: Flow sheet of an bio-EvGT

5.2   The Bio-EvGT Process

The process studied in this chapter is the bio-EvGT process. The bio-EvGT process utilizes low-grade energy to evaporate a mixture of ethanol and water. The evaporated gas mixture is then passed to the combustor where it is combusted to the desired combustor outlet temperature. Figure 5.1 shows the flow sheet of the gas turbine processes which are compared in this thesis; the natural gas fired gas turbine and the bio-EvGT. The working principle of both cycles are similar and they will therefore be described together. The bio-EvGT presented here is using a recuperator to heat both the fuel stream and the airstream. This process is used in **paper VII**.

In figure 5.1, the air led into the gas turbine compressor (1) where the air pressure is increased to the system pressure. The compression process is divided into two steps with an intercooler heat exchanger (2) placed between

the two sections. The intercooler decreases the temperature of the air which lowers the compression work. After the compressor the air then passes an aftercooler (3) which decreases the temperature of the air once again before it enters the humidification tower (4).

The air then passes the humidification tower where it encounters warm water which has been heated in the heat recovery processes in the intercooler (2), aftercooler (3) and economizer (9). Heat and mass transfer occurs causing the water to cool down and evaporate while the mass flow of air increases due to the evaporation.

The air leaves the humidification tower saturated with air at a low temperature. The air then passes the recuperator (5) which preheats the air with the help of the exhaust gases from the gas turbine expander (7). The air is then burned in the combustor together with natural gas in order to reach the combustor outlet temperature. After the expansion in the expander (7), exhaust gases pass the recuperator (5) where it is cooled down by the humidified air. The flue gases then pass the economizer (9) where it heats a part of the humidification liquid. The EvGT cycle in figure 5.1 has been equipped with a flue gas condenser (10) which extracts the remaining energy from the flue gases by condensing some of the water in the flue gases. This condensation makes it possible for the EvGT cycle to be self-sufficient of water. The heat extracted in the flue gas condenser (10) is delivered to a district heating network through the heat exchanger (12).

In the bio-EvGT cycle, a part of the compressor discharge air is bypassed the humidification circuit and led to the ethanol humidification circuit. This bypassed flow passes an ethanol humidification tower (11) where it encounters a mash-flow with an ethanol concentration between 3–12 mass percent ethanol [211]. Simultaneous heat and mass transfer occurs within the ethanol humidification tower (11) which leads to the transfer of water and ethanol to the compressor discharge air. The air then leaves the ethanol humidification tower (11) and enters the recuperator (5) where it is preheated. The mixture is then passed to the combustion chamber (6) where it is combusted as a fuel. The temperature of the binary liquid is reduced when it passes the ethanol humidification tower (11). The remaining energy in the mash flow preheats the entering mash-flow. The mash-flow is then preheated with humidification water from the economizer (9).

Figure 5.1 shows that the airstream and the ethanol fuel stream is connected before the recuperator. This is only a simplified version of the process scheme. In reality the fuel stream and the airstream would have been separated and lead through two separate recuperators. The mixture of air, water
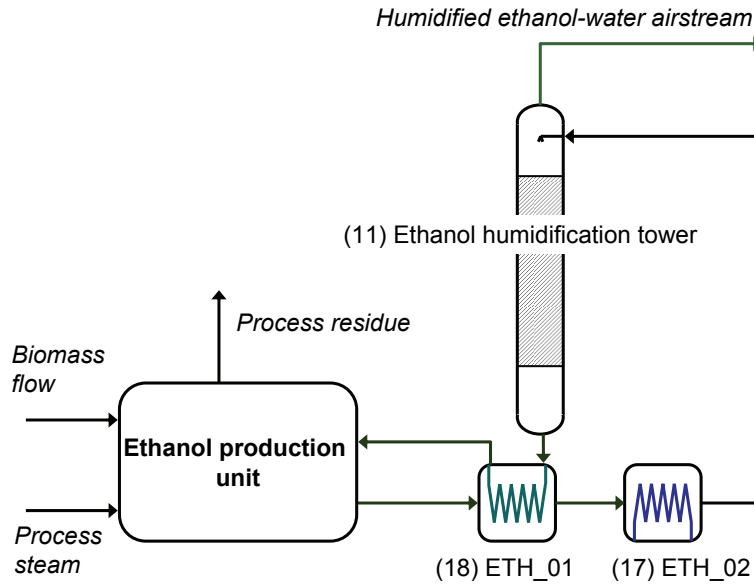
Figure 5.2: Ethanol production facility

and ethanol will therefore be treated as a fuel when it enters the combustion chamber.

5.2.1 Ethanol Production Facility

Figure 5.1 shows that the recuperated bio-EvGT receives fuel from an external circuit, the ethanol production unit. The ethanol production unit converts biomass to a liquid mixture of ethanol and water. In this process, not all of the original biomass can be converted into ethanol. Instead, a residue of biomass is formed as a bi-product to the ethanol production process. The theoretical amount of ethanol that can be converted from the biomass in this study is 319.6 kg ethanol per 1000 kg of dry biomass delivered to the process. Due to irreversibility within the process the actual yield is assumed to be 294.34 kg ethanol per 1000 kg biomass to the process.

The residue that has formed contain large quantities of lignin and cellulose. It is estimated that the remaining solid has a lower heating value of 9722 kJ/kg [1, 222]. This residue has some energy left, which can be utilized when the water has been extracted. The water is extracted by a filter press and is then used to generate steam that is needed internally within

the ethanol production unit. The steam required for the pre-treatment of the biomass is used so that the hydrolysis process can proceed.

Due to its complexity, the ethanol production facility has not been modeled in detail in **paper V** or **paper VII**. Instead, the ethanol production facility in this thesis is based on the work performed by the National Renewable Energy Laboratory, (NREL). The NREL has studied the production of ethanol from lignocellulosic biomass in several articles [1, 8, 13, 150, 199, 222]. The work performed by NREL is very detailed as it treats the economical and thermodynamic process parameters of ethanol production. The NREL process design includes feedstock handling and storage, product purification, waste water treatment, lignin combustion, product storage and all other required utilities used to produce ethanol.

The ethanol production facility, presented by NREL, is a complete facility that produces 95% pure ethanol. To achieve this level of purity several distillation steps have to be performed [1]. These additional steps are not necessary in the recuperated bio-EvGT. The idea behind the bio-EvGT is to utilize the low concentrated mash instead of the pure ethanol. This means that energy can be saved since the distillation units are not required. To adapt the work performed by NREL to the calculations in this article, the process equipment that is not needed for the mash production is stripped from the ethanol production unit. The remaining plant, proposed by NREL, is then assumed to be linearly scalable to the amount of ethanol that the plant is producing.

Figure 5.1 shows that the drain flow of liquid from the ethanol humidification tower (11) is redirected back into the ethanol production unit. It is here that an assumptions is made that all of the ethanol which has not transferred into the air can be reused in the ethanol production facility. It is known that a high concentration of ethanol reduces the efficiency of the conversion processes and currently the focus on research is on how to be able to redirect liquid currents of ethanol back into the ethanol production process [211].

5.3   Thermodynamic Modeling of the Bio-EvGT

This section provides a discussion on the model developed in **paper IV** which describes the thermodynamic performance of the ethanol humidification process. This model is then used to predict the performance of the bio-EvGT process.

5.3.1   Basic Modeling of the Humidification Process

In **paper IV**, a model was developed to be able to predict the humidification process in a simple way. This is necessary if parameter variations of the bio-EvGT should be performed in an efficient manner. Experimental data from the pilot plant, described in section 4.3, was used to calibrate the developed model. The model developed in **paper IV** is similar to the model of the humidification tower. The model of the humidification tower has been described by Jordal [123].

The mass and energy balances are solved for the ethanol humidification tower. The boundary values for these equations is that the pressure is the same at the inlet air side and the outlet air side. The pressure of the entering liquid is set to the operating pressure of the gas turbine. The temperatures and mass flows at the inlets are also known from the energy balance across the entire cycle and is therefore used as additional boundary values. Another boundary value is required to be able to predict the temperature and composition of the gas that leaves the tower. An expression is developed in **paper IV** that relates the amount of evaporated mass to the amount of dry air entering the humidification tower.

As for the humidification tower, the working line can not cross the saturation line [95]. A pinch-point is therefore introduced in the ethanol humidification model to make sure that the working line does not intersect the saturation line. This is carried out by assuming that the working line can be considered a straight line. Figure 4.4 show that the working line in the ethanol humidification tower actually is fairly straight. Similarly, examining figure 4.4 also reveals that the derivative of the working line is the same as the derivative of the saturation line at the pinch-point. This makes it possible to relate the derivative of the saturation line to the derivative of the working line in the ethanol humidification tower. A small vertical distance, ΔT, then determines the pinch-point in the tower. The pinch-point can be calculated by the use of the straight line approximation described by [122]. The development of the model is described in **paper IV**.

5.3.2   Thermodynamic Evaluation

The model used in **paper IV** is used to predict the performance of the bio-EvGT process. The results from the thermodynamic studies of the bio-EvGT is discussed in this section.

Figure 5.3 shows the thermodynamic performance of the recuperated bio-EvGT cycle. The left diagram in figure 5.3 shows the thermodynamic
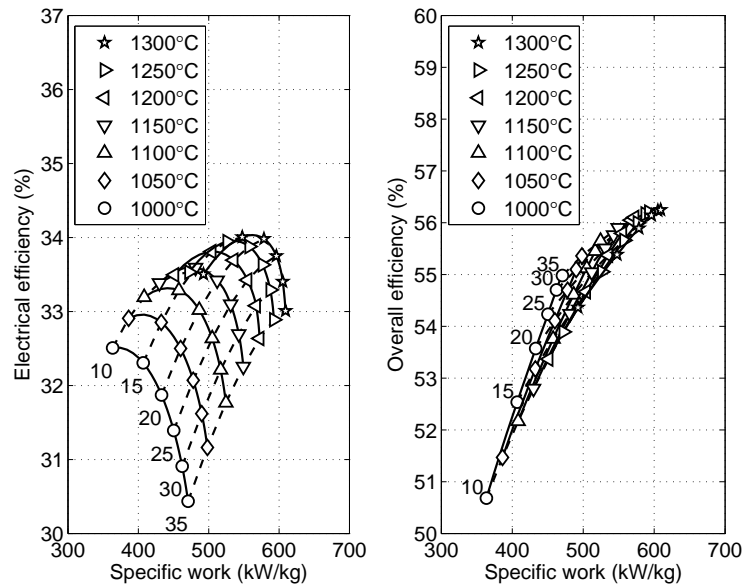
Figure 5.3: Thermodynamic performance of the bio-EvGT process

performance of the bio-EvGT as a function of the specific work. The calculations have been performed for pressure ratios ranging from 10 to 35 and for combustor outlet temperatures, (COT), between 1000°C and 1300°C. The air is limited to 1300°C due to the inability of the air to carry unlimited amounts of ethanol. The COT is therefore determined by the amount of air that passes the ethanol humidification tower (11), seen in figure 5.1.

Figure 5.3 shows that the efficiency increases as the combustor outlet temperature increases. The optimum pressure ratio for the bio-EvGT cycle increases from 10 to 17.5 as the combustor outlet temperature of the cycle increases. Figure 5.3 shows that the specific work output from the bio-EvGT varies between 350 kW/kg to 620 kW/kg and the thermal efficiency of the cycle varies between 30.4% to 34%. Figure 5.3 shows that the maximum electrical efficiency of the bio-EvGT is 34% for the EvGT system. This efficiency is achieved at a pressure ratio of 17.5 and a combustor outlet temperature of 1300°C.

The recuperated bio-EvGT gas turbine behaves as a natural gas fired EvGT. This is due to the fact that the humidification process is almost the same whether it passes the humidification tower or the ethanol humidification tower. The humidified airstreams are then mixed together before it

enters the recuperator. The recuperator increases the temperature of the gas mixture in the same way it would have in a natural gas fired EvGT. The maximum efficiency of the bio-EvGT should be compared to the maximum efficiency of the natural gas fired EvGT The efficiency of the natural gas fired EvGT is 50%. This means that approximately 32% of the thermal efficiency has been used to produce the ethanol in the ethanol production unit.

The right diagram in figure 5.3 shows the overall efficiency of the bio-EvGT. The overall efficiency is important for the behavior of the gas turbine in a district heating network. The overall efficiency is defined as the amount of utilized energy produced from the amount of energy supplied to the gas turbine. The overall efficiency is defined as the work output and the heat output to the district heating divided by the energy supplied, thus:

$$Overall \ efficiency = \frac{W_{net} + Q_{district \ heating}}{Supplied \ energy} \qquad (5.1)$$

The required input is however based on the amount of fuel added to the process.

Figure 5.3 shows that the overall efficiency increase as the pressure ratio increases. The overall efficiency does not increase as much when the combustor outlet temperature increase. However, the specific work of the bio-EvGT increases slightly as the combustor outlet temperature increases. The overall efficiency of the cycle varies between 50.8% to 56.2% as the specific work varies between 350 kW/kg to 620 kW/kg. The maximum overall efficiency achieved in this system is 56.2% at a pressure ratio of 35 and a combustor outlet temperature of 1300°C. This is fairly low compared to the steam turbine which achieves an overall efficiency of 88%. The quality of the heat produced by the gas turbine is also low and the temperature delivered to the district heating network is around 55–65°C. This is because the recuperated bio-EvGT utilizes the low-level energy efficiently which means that there less energy available for the district heating network.

5.4 Economical Modeling

Decisions in the engineering society is based on the combination of energy balances and economical calculations. In the deregulated electricity market, power utilities have to be profitable in order to withstand the market competition. A way of performing economic calculations is to calculate the cost of electricity based on the total capital investment (TCI), fuel cost (FC) and

operation and maintenance cost, (U_{fix} and U_{var}) [15].

$$Y_{el} = \frac{TCI \cdot \psi + \dot{m}_f \cdot c_f}{T_{eq} \cdot P} + U \qquad (5.2)$$

In equation 5.2, ψ, is the annuity factor. In order to calculate the cost of electricity, it is therefore important to calculate the total capital investment, which is the sum of the direct, indirect and working cost of the construction phase. When constructing a power plant, previous knowledge of these cost are often already well known to the company. However, when constructing a new process, estimations of the cost is not known and needs to be estimated in some way. There are different ways of estimating the factors required for the construction phase and they are often taken as a percentage of the total capital investment of the plant. Average factors for the calculations of the TCI in **paper V** and **paper VII** is taken from references [23, 176, 215].

Cost of Equipment

Performing economic calculations of power plants requires knowledge of the price of the equipment. The price of ordinary power plant equipment is usually already known by the manufacturer. Calculating the price of novel cycles is not that easy since the equipment cannot be found anywhere else in the literature. To estimate cost of equipments there are many estimation methods available in the literature [23, 176, 215]. The cost of an item can often be considered a function of different properties that the equipment has. The calculations of the different kinds of equipment can be performed according to equation 5.3.

$$Product\ equipment\ cost = f\big(size,\ material,\ type\ of\ equipment\big) \qquad (5.3)$$

Equation 5.3 shows that the production equipment cost is a function of several different properties associated with the product. Large databases of cost information have been established and is available in the literature. These databases often comes in the form of an estimation chart, which is an easy way to get the approximate value of an equipment. Estimation charts are constructed from a large number of correlations of cost and design data. These chart are somewhat inaccurate and they should not be used as an exact value, but rather as an average cost in preliminary cost estimations. In these estimation charts, the cost of an item of equipment is plotted as a straight line in a log–log diagram. The slope of this straight line is the coefficient, α, and it represents an important cost-estimating parameter as

shown by equation 5.4.

$$C_{PE,Y} = C_{PE,W} \left(\frac{X_Y}{X_W} \right)^{\alpha} \tag{5.4}$$

Equation 5.4 enables the purchase cost of an equipment item ($C_{PE,Y}$) at a given capacity or size (X_Y) to be calculated when the purchase cost of the same equipment item ($C_{PE,W}$) at a different capacity of size (X_W) is known [23,176,215]. When the scaling exponent, α is unknown the *six-tenths rule* is used, which means that the scaling exponent is considered to be 0.6 [23]. In **paper V** and **paper VII** the equipment cost of process machinery, extraction vessels and vessels has been taken from the reference [176]. The cost data for the gas turbine has been taken from the gas turbine world handbook [9]. However, an evaporative gas turbine does not exist and this needs to be taken into account for the economical studies. In **paper V** and **paper VII** it has been assumed that the gas turbine has the same cost as a simple cycle gas turbine rated at the same power output. Most estima-

Table 5.1: Economic assumptions for **paper V** and **VII**

Assumption for the cost of electricity	
Steam turbine investment cost ($/kW$_e$)	2532
Interest rate (%)	6
Economic life (years)	20
Fuel price (USD/MWh)	15.25
Load (h)	6000
Labor charges and other fixed charges (% of TPC)	8
Maintenance (% of TCI)	4

tion charts and cost estimation data are based on a reference year when the prices where collected. Equipment costs can however vary considerably over the years and must therefore updated to costs that are representative of the date considered for the calculation. This is achieved by using cost indices, which is an inflation indicator. In **paper V** and **paper VII** this was used to transfer the data to 2002.

$$Present\ cost = Original\ cost \left(\frac{index\ value\ at\ present}{original\ index\ value} \right) \tag{5.5}$$

Equation 5.2 also contains the fuel price for the process. The ethanol production facility requires more material than just the biomass. From the

reports by NREL it can be found that the fuel price makes up about 65% of the cost of raw material to the ethanol production unit. The cost of the raw material must be included in the analysis. The cost of biomass that can be used in the ethanol production facility is estimated to be around 4–10 \$/MWh. Taking into consideration the other raw material for the process results in a price of approximately 15 \$/MWh.

It was stated earlier that the ethanol production facility produced a residue of a combustible solid, the lignin cake. This additional fuel, which is not used in the process, can be sold and considered an income for the power plant. The value of this additional income is difficult to decide. The produced residue is here considered to have the same market value as the feedstock used in the process. This residue has been refined in the ethanol production facility and is easier to handle than the original biomass. It is therefore argued that the value of this residue should amount to the same value or more than the original biomass. In **paper V** and **paper VII**, it has been assumed that the value of the residue is the same as the biomass feedstock price.

5.4.1 Economic Performance

It is seen in equation 5.5 and from the discussion in previous sections, that the cost of energy and electricity depends on the parameters such as the fuel cost, discount rate and the utilization time. A power plant is a large investment that have book lives of at least 20 years and during this time the variables in equation 5.5 vary significantly. It is therefore very difficult to forecast the cost of energy and electricity of this power plant over a long period of operating time. A sensitivity analysis have therefore been performed in **paper V** and **paper VII** to take into considerations all the variations of the conditions.

The economic analysis performed in this section is performed on 5 different cycles, which are all fueled with biomass except for cycle 4. These cycles are tested and evaluated in **paper V** and **paper VII**. The cycles have been recalculated from the papers so that they will be compared on the same principles The cycles studied in this section are:

- Cycle 1: bio-EvGT with an aftercooler and economizer;

- Cycle 2: bio-EvGT with an aftercooler, intercooler and economizer;

- Cycle 3: bio-EvGT with recuperated fuel stream and with an aftercooler, intercooler and an economizer;
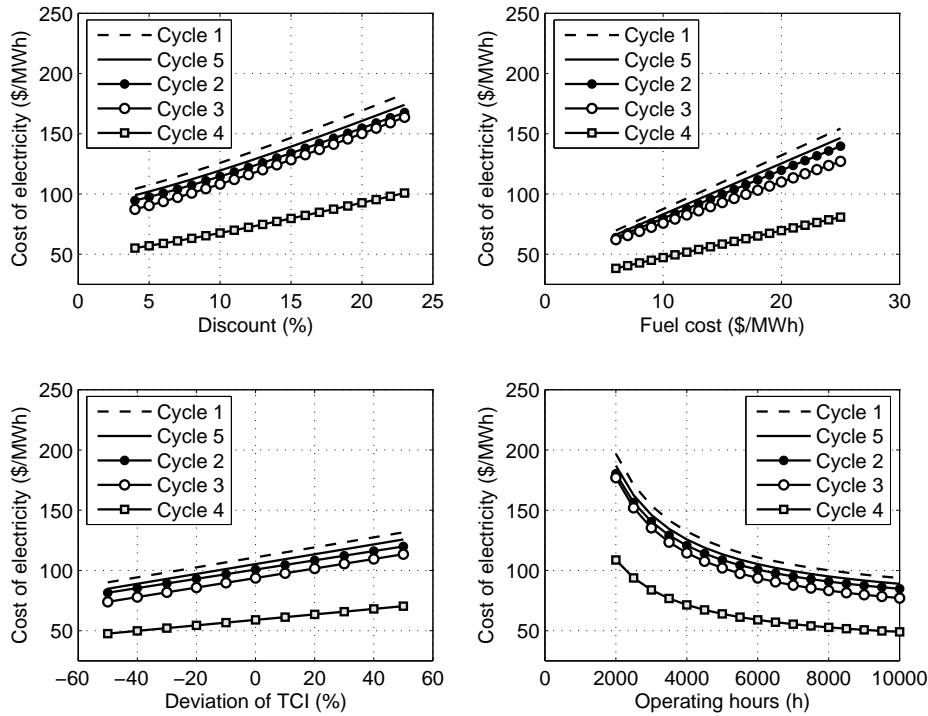
Figure 5.4: Sensitivity analysis of the cost of electricity

- Cycle 4: EvGT cycle with an aftercooler, intercooler, economizer and a recuperator; and

- Cycle 5: bio-mass fired steam turbine.

Cycle number 4 and cycle 5 are used as a reference cases, and the others are compared to them.

The upper left diagram shows the influence of different discount rates on the cost of electricity. The cost of electricity of the recuperated EvGT cycle is the lowest of the bio-EvGT cycles. This is because the recuperated cycle behaves exactly as an EvGT system, which means that it has a high efficiency compared to the other systems. The main loss in the recuperated bio-EvGT is the production of ethanol from the biomass. The cost of electricity for the base case is 80.68 $/MWh. The cost of electricity for the intercooled and aftercooled gas turbine is 95.61 $/MWh and 106.35 $/MWh for the aftercooled engine. The steam turbine, which is optimized for highest electrical efficiency, has a cost of electricity of 105.3 $/MWh.
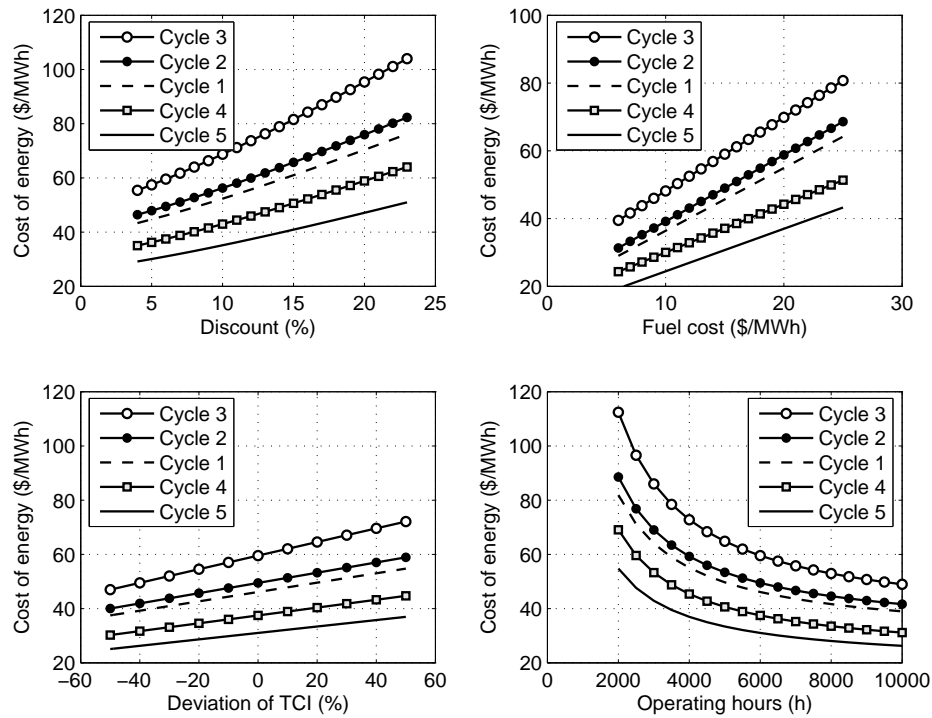
Figure 5.5: Sensitivity analysis of the cost of energy

The natural gas fired EvGT cycle has the lowest cost of electricity of all the cycles. This is because the losses associated with the ethanol production are not a factor here. The cost of electricity for the base case of the EvGT is around 50.99 $/MWh. This high cost differs from the numbers calculated by Jonsson [118] and it is inline with the cost estimated by Fredriksson-Möller [158].

The impact of the fuel cost on the cost of electricity can be seen in the upper right diagram of figure 5.4. The cost of electricity for the natural gas fired EvGT decreases to 39.76 $/MWh for a fuel price of 10 $/MWh. For the bio-EvGT cycles a fuel cost of 5 $/MWh would result in a cost of electricity of 54 $/MWh.

The total capital investment is a parameter that is estimated which means that it can be off by a factor 3. The lower diagram of figure 5.4 shows the influence of the error in the estimation TCI on the cost of electricity. An error of 50% decreases the COE by approximately 10%.

The lower right diagram in figure 5.4 shows the impact of operating time on the cost of electricity for each different cycles.

The cost of energy of the different cycles have also been calculated. The natural gas fired EvGT has the lowest cost of energy of 29.06 $/MWh. The quality of the heat delivered to the district heating network is however higher for the steam turbine. The cost of energy for the recuperated bio-EvGT is 49.36 $/MWh which is the most expensive cycle. This is due to the fact that the internal heating system within the cycle is very good and not much energy is left to the flue gas condenser. This means that less energy can be delivered to the district heating network.

Table 5.2 shows the performance calculations of the bio-EvGT cycles. The assumptions for the economic calculations can be found in table 5.1. The operating and maintenance cost of the plants are considered to be 10% of the cost of electricity. Table 5.2 presents the thermodynamic performance of the different cycles in two sizes; 4 MW and 20 MW. The table also shows the total capital investment of the cycles. The middle part of the table shows the contribution of each part of the power plant to the total capital investment cost. The cost of installation etc. is included in this figures.

Table 5.2 shows that the cost of electricity is lowest for the reference cycle 4. This is not surprising since it has the highest thermal efficiency and a low total capital investment cost. The recuperated bio-EvGT also shows a low cost of electricity compared to the other cycles in the comparison.

Table 5.2 also be shows that the ethanol production unit corresponds to 50–60% of the total capital investment of the bio-EvGT.

Table 5.2: Economic result of the analysis

Cycle		1	2	3	4	1	2	3	4	5	5
Power	MW	4	4	4	4	20	20	20	20	4	20
Heat	MW	5.9	4.1	2.3	2.3	26.6	24.4	12.7	12.7	26.3	27.3
η_{el}	-	25.0	27.8	32.5	49.6	24.6	27.7	34.0	52.0	26.3	27.3
η_{tot}	-	60.0	56.6	51.2	78.1	57.5	57.1	55.6	85.0	88.5	88.5
GT	%	28.10	30.32	27.39	58.73	21.25	23.20	25.98	59.19	-	-
HE	%	4.63	5.75	4.42	9.49	2.22	2.80	5.80	12.54	-	-
HT	%	2.08	1.16	2.13	4.58	1.88	1.34	2.41	5.22	-	-
Pump	%	1.75	1.15	1.63	3.50	0.88	0.78	0.66	1.43	-	-
Mash	%	52.52	50.97	53.37	-	60.74	59.03	53.77	-	-	-
Fluegas	%	10.83	10.25	11.06	23.71	13.03	12.85	11.38	24.62	-	-
TCI	kUSD	10,277	9,523	11,847	5,524	45,063	41,271	36,868	17,043	10,127	50,635
TCI	$/MWh	2,569	2,381	2,962	1,381	2,253	2,064	1,843	852	2,532	2,532
COE	$/MWh	110.89	100.74	93.74	59.00	106.35	95.61	80.68	47.50	105.30	105.30
COEn	$/MWh	46.13	49.48	59.56	37.48	45.62	46.34	49.36	29.06	31.03	31.77

Chapter 6

Summary & Concluding Remarks

This thesis has focused on the humidification strategies in gas turbine engines and in particular, the evaporative gas turbine. An experimental facility has been built to study the evaporation processes associated with evaporative cycles. The experimental test facility has also been used to study a thermodynamic cycle which utilizes the evaporation technique to evaporate a mixture of ethanol and water into a fuel. This cycle, which is called the bio-EvGT, was first presented by Rosén [192]. The bio-EvGT introduces another dimension to the zero-emission society and represents an interesting alternative for the future. The conclusions that can be drawn from this thesis are listed below.

- The author has introduced an aftercooler into the evaporative gas turbine pilot plant. Knowledge and experience of the aftercooler has been gained through experimental work. The measurements from the pilot plant have been used to validate the thermodynamic models for EvGT cycles. The measurements of the performance of the aftercooler have been compared to the simple cycle, recuperative cycle and the EvGT cycle without an aftercooler. The knowledge of the use of an aftercooler has been improved. It has been shown that the thermal efficiency of the EvGT pilot plant has increased from 21% to an estimated 35% due to the introduction of the aftercooler.

- It has been shown through experiments that the plate heat exchanger aftercooler improves the performance of the EvGT cycle. The aftercooler has a pinch-point of $0.1°C$ and a pressure drop on the air side

of 1.6%. It has also been shown that the pinch-point in the humidification tower has increased from 3.5°C to 5.4°C due to the installation of the aftercooler. The installation of the aftercooler has increased the enthalpy exchange within the humidification tower. It has also been shown that the temperature of the humid air after the humidification tower is approximately 2.5–3% lower than the temperature predicted by the heat balance software. This difference can be explained by the fact that the heat balance model approximates humid air as an ideal gas.

- Thermodynamic calculations of the performance of gas turbines equipped with an aftercooler have been performed. Experience from the experimental work on the EvGT pilot plant has been transferred into the thermodynamic calculations. This has made it possible to more accurately determine the performance of EvGT power plants. The thermodynamic analysis showed that the use of an aftercooler increases the efficiency of an evaporative gas turbine.

- Modifications of the pilot plant have been performed in order to investigate the behavior of the humidification tower. A theoretical model based on heat and mass transfer equations have been presented in this thesis. The developed theoretical model in this thesis makes fewer assumptions than prior theoretical models for humidification processes. The developed model is very sensitive to the thermodynamic properties used in the calculations. It has been shown that the developed theoretical model can predict the height of the humidification tower with an accuracy of 10%.

- A second humidification process has been designed and built at the Department of Energy Sciences at Lund University. This new experimental facility has made it possible to operate a humidification tower at several new operating conditions. This experimental facility has further increased the knowledge of evaporation processes at elevated temperatures and pressures. This second humidification tower has made it possible to further test the theoretical model developed for the humidification tower. It is also used to test the working principle of the ethanol humidification process by making it possible to evaporate a liquid mixture of ethanol and water

- A theoretical model for the study of the humidification process in the ethanol humidification tower has been developed. The theoretical

model predicts the on and off design behavior of the ethanol humidification tower and the humidification tower. It has been shown that the model can predict the performance of the ethanol humidification tower with an accuracy of 15%. It has also been shown that the height of the ethanol humidification tower can be estimated within 15%.

- Tests have been performed with a droplet separator in the humidification tower. It has been experimentally shown that there are no droplets entrained in the air flow after the humidification tower when the droplet separator is in operation.

- It has been shown that it is possible to evaporate a mixture of ethanol and water into an air stream at elevated temperatures and pressures. It has also been shown that it is possible to obtain a combustible gas with a lower heating value between 1.5 and 3.8 MJ/kg.

- First law thermodynamic calculations and optimizations have been performed with the bio-EvGT cycle. Three configurations of the bio-EvGT have been studied; the aftercooled cycle, the aftercooled and intercooled cycle and the aftercooled, intercooled and recuperated cycle. It has been shown that the bio-EvGT can achieve efficiencies of 34% which can be compared to the biomass fueled steam turbine cycle that have a thermal efficiency of 27.3%. It has also been shown that the bio-EvGT has a favorable cost of electricity compared to the biomass fueled steam turbine cycle. It has also been shown that the cost of the ethanol production facility amounts to 50–60% of the total capital investment of the bio-EvGT.

The main scientific contributions by the author to this field of research have been both experimental and theoretical. The main experimental contributions by the author have been:

- to erect the first evaporative gas turbine with an aftercooler and to put this pilot plant into operation;

- to gain operating experience from the evaporative gas turbine;

- to show that it is possible to operate the evaporative gas turbine pilot plant with an aftercooler;

- to modify the evaporative gas turbine pilot plant in order to investigate the humidification process within the EvGT cycle; and

- to erect a pressurized humidification circuit in order to study evaporation processes within EvGT cycles.

The main theoretical contributions by the author to this field of research have been:

- to evaluate unique data from the operation of the aftercooled evaporative gas turbine pilot plant;

- to establish models for the humidification process in evaporative gas turbines;

- to carry out a comparative study of the bio-EvGT cycle; and

- to establish theoretical models for the binary evaporation process in the bio-EvGT cycle.

Chapter 7

Summary of Papers

Paper I *Experimental and Theoretical Results of a Humidification Tower in an Evaporative Gas Turbine Cycle Pilot Plant*, Lindquist, T., Thern, M., Torisson, T., presented at ASME TURBO EXPO, June 2002, Amsterdam, The Netherlands.

In this paper, a theoretical mode has been developed for the simultaneous heat and mass transfer occurring in the humidification tower. The model has been validated with measured data from the pilot plant. It has been shown that the air and water can be calculated throughout the column in a satisfactory manner. The height of the packing can be predicted within an uncertainty range of 10%. The result of the calculation is most sensitive to the properties of the diffusion coefficient, viscosity and thermal conductivity due to the complexity of the polar gas mixture of water and air. The contribution to this paper by the author was in establishing and implementing the model, providing data, evaluating the results and in the preparation of the paper.

Paper II *Experimental and Theoretical Evaluation of a Plate Heat Exchanger aftercooler in an evaporative gas turbine cycle Pilot Plant*, Thern, M., Lindquist, T., Torisson, T., presented at ASME TURBO EXPO, June 2003, Atlanta, Georgia, USA.

In this paper, the results of the tests with an evaporative gas turbine cycle with an aftercooler are presented. The measured data is compared to the results from the heat balance calculations. It has been shown that the aftercooler in an evaporative gas turbine cycle increases the enthalpy change,

hence humidification ration in the air. This leads to higher power density and higher electrical efficiencies of the cycle. The pressure-drop of the air side of the aftercooler was measured to be 1.6%. The pinch-point in the aftercooler on the cold side was measured to be 0.1°C. The pinch-point in the humidification tower increased from 3.5°C to 5.4°C due to material constraints. The water exiting the humidification tower has been reduced by 26°C from 105°C to 79°C, which facilitates more heat recovery from the flue gases in the economizer. If the cycle was to have an intercooler, the intermediate temperature would be lower, hence less compression work. The contribution to this paper by the author was in carrying out the performance tests, evaluating the data, verifying the data with the heat balance calculation and the preparation of the paper.

Paper III *Trigeneration: Thermodynamic performance and cold expander aerodynamic design in humid air turbines*, Genrup, M., Thern, M., Assadi, Mohsen., presented at ASME TURBO EXPO, June 2003, Atlanta, Georgia, USA.

This paper presents the trigeneration process based on humid air turbines. The basic principle of trigeneration is to interrupt the expansion at an elevated pressure level and extract heat from the working medium. The final expansion then takes place at low-temperature admission levels resulting in very cold temperatures at the turbine exhaust. This paper presents thermodynamic calculations of the humid air turbine concept in conjunction with the tri-generation. Further on, the paper presents the expander design criterion for the cold expander. The author of this thesis developed the models for the trigeneration process and performed the cycle analysis. Magnus Genrup performed the through-flow analysis of the cold expander with the commercial code SC-90T.

Paper IV *The ethanol-water humidification process in EvGT cycles*, Thern, M., Lindquist, T., Torisson, T., presented at ASME TURBO EXPO, June 2004, Vienna, Austria.

This paper presents the results from the first humidification process that evaporates a mixture of ethanol and water into an airstream at elevated temperatures and pressures. The experimental facility has been operated in several different operating modes. It has been shown that the humidification process is feasible and produces a combustible gas. It has also been

shown that this technology extracts about 60-80% of the ethanol from the mash. The composition of the resulting gas depends on the temperatures, flow rates and composition of the incoming streams. The tests have shown that the produced gas has a lower heating value between of 1.8 to 3.8 MJ/kg. The produced gas with heating values in the upper range is possible to use as fuel in the gas turbine without any pilot flame. Initial models of the ethanol humidification process have been established and the initial test results have been used for validating developed models. The contribution to this paper by the author was carrying out the performance tests, evaluating the data, verifying the data with the heat balance calculation and the preparation of the paper.

Paper V *Thermo-economic evaluation of bio-ethanol humidification EvGT cycle*, Thern, M., Lindquist, T., Torisson, T., presented at ASME TURBO EXPO, June 2005, Reno-Tahoe, Nevada, USA.

This article presents the latest development in the evaporative technology, the evaporation of bio-ethanol in a gas turbine power plant as a means to reduce the emission of greenhouse gases. This concept is evaluated and compared to a direct-fired Rankine cycle in the size range of 3-5 MWe and 15-30 MWe concerning plant efficiency and investment cost. All power cycles studied have been modeled in IPSEpro™, a heat and mass balance software, using advanced component models developed by the authors. It has been shown that the evaporation technology can be used with different types of cycle configurations attaining electrical efficiencies of 29% for a simple version of a humid air turbine. The humid air turbine can sustain a combustor outlet temperature of 1100°C without supplementary firing. The contribution to this paper by the author was developing the thermodynamic model of the ethanol humidification tower. The author also carried out the economic and thermodynamic calculations and prepared the paper.

Paper VI *Experimental and theoretical investigation of a evaporative fuel system for heat engines*, Thern, M., Lindquist, T., Torisson, T., Submitted to Journal of Energy Conversion and Management.

In this paper, a theoretical model has been established for the simultaneous heat and mass transfer occurring in the ethanol humidification tower which has been validated with experiments. Experimental and theoretical work has been performed for the humidification of both mono and binary liquids

into an airstream at elevated temperatures and pressures. It has been shown that the air, water and ethanol can be calculated throughout the column in a satisfactory way. The height of the column can be estimated with an error of 15% compared with measurements. It has been shown that the results from the theoretical model are most sensitive of the properties of the diffusion coefficient, viscosity, thermal conductivity and activity coefficient, due to the complexity of the polar gas mixture of water and air. It has also been shown that the developed model is able to predict the off-design performance of the ethanol humidification process within 15% accuracy. The contribution to this paper by the author was carrying out the performance tests, evaluating the data and verifying the data with the heat balance calculation. The author has also used the experimental data to verify and test the developed theoretical model and prepared the paper.

Paper VII *The bio-ethanol fired EvGT cycle*, Thern, M., Lindquist, T., Torisson, T., Submitted to Journal of Energy Conversion and Management.

This article presents the thermodynamic and economic performance of the recuperated bio-EvGT cycle, biomass fueled steam turbine, intercooled and aftercooled EvGT cycle, the aftercooled EvGT cycle and the natural gas fired EvGT cycle. A parametric study of the effect of combustor outlet temperature (COT), pressure ratio and different fuel strategies on the thermodynamic and economic performance of the cycle is investigated. All thermodynamic calculations are performed with the heat balance software IPSEpro$^{\mathrm{TM}}$. The result shows that the thermal efficiency increases by 7%, compared to the intercooled and aftercooled bio-EvGT. The result is that the recuperated bio-EvGT cycle achieves an electrical efficiency of 34% at a pressure ratio of 17.5 bar and a combustor outlet temperature of 1300°C. The cost of electricity decreases with the introduction of the recuperator by 20%, compared to the other bio-EvGT configurations. The cost of electricity is half the cost as for the steam turbine. The contribution of the author was in the calculations and preparation of the paper.

Bibliography

[1] A. Aden, M. Ruth, K. Ibsen, J. Jechura, K. Neeves, J. Sheehan, and B. Wallace. Lignocellulosic Biomass to Ethanol Process Design and Economics Utilizing Co-current Dilute Acid Prehydrolysis and Enzymatic Hydrolysis for Corn Stover. Technical report NREL/TP–510–32438, National Renewable Energy Laboratory, Golden, Colorado, USA, jun 2002.

[2] I. S. Akmandor, Ö. Öksuz, S. Gokaltun, and M. H. Bilgin. Genetic Optimization of Steam Injected Gas Turbine Power Plants. In *ASME TURBO EXPO'02*, Amsterdam, The Netherlands, 2002.

[3] V. Alopaeus. Calculation of Multicomponent Mass Transfer Between Dispersed and Continuous Phases. *Acta Polytechnica Scandinavica, Chemical Technology Series*, –(283):1–35, 2001.

[4] Ville Alopaeus. On Approximate Calculation of Multicomponent Mass Transfer Fluxes. *Computers and Chemical Engineering*, 26(3):461–466, 2002.

[5] Ville Alopaeus, Juhani Aittamaa, and Harry V. Norden. Approximate High Flux Corrections for Multicomponent Mass Transfer Models and Some Explicit Methods. *Chemical Engineering Science*, 54(19):4267–4271, 1999.

[6] Ville Alopaeus and Harry V. Norden. Calculation Method for Multicomponent Mass Transfer Coefficient Correlations. *Computers and Chemical Engineering*, 23(9):1177–1182, 1999.

[7] K. Annerwall and G. Svedberg. A Study on Modified Gas Turbine Systems with Steam Injection or Evaporative Regeneration. *ASME COGEN-TURBO, IGTI*, 6:1–8, 1991.

[8] Anon. Technical and Economic Evaluation Wood to Ethanol Process. Technical report Draft, CHEM systems, Tarrytown, New York, USA, aug 1990.

[9] Anon. Gas Turbine World Handbook, 2003. Pequot Publishing, Inc., ISSN 0883–458X.

[10] N. Aronis and R. Leithner. Combined Cycle with Low Quality Heat Integration and Water Injection into the Compressed Air. *Proceedings of ECOS*, 6:1–8, 2002. Berlin, Germany.

[11] N. Aronis and R. Leithner. Combined Cycle with Low Quality Heat Integration and Water Injection into the Compressed Air. *Energy*, 29:1929–1943, oct-dec 2004.

[12] L.V. Arsen'ev and A.L. Berkovich. Parameters of Gas-turbine Units with Water Injected into the Compressor. *Thermal Engineering (English translation of Teploenergetika)*, 43(6):461–, 1996.

[13] J. E. Atchison and J. R. Hettenhaus. Innovative Methods for Corn Stover Collection, Handling, Storing and Transportation. Technical report NREL/TP–510–33893, National Renewable Energy Laboratory, Golden, Colorado, USA, apr 2004.

[14] Halasz B. A general mathematical model of evaporative cooling devices. *Revue Generale de Thermique*, 37(4):245–255, 1998.

[15] Rolf Bachmann, Henrik Nielsen, Judy Warner, and Rolf Kehlhofer. *Combined-Cycle Gas & Steam Turbine Power Plants*. Pennwell Books, 2nd edition, aug 1999.

[16] J. A. M. Baken and B. van den Haspel. Optimized Operation of Steam-Injected Gas Turbine Cogeneration Units. *ASME COGEN-TURBO, IGTI*, 3:259–265, 1988.

[17] M. A. Bartlett and M. O. Westermark. Experimental Evaluations of Air Filters and Metal Ion Migration in Evaporative Gas Turbine Cycles. In *Proceeding of IJPG 2001*, New Orleans, USA, jun 2001.

[18] M. A. Bartlett and M. O. Westermark. Modelling of Alkali Contaminant Flows in Evaporative Gas Turbines. In *Proceeding of ASME TURBO EXPO'01*, New Orleans, USA, jun 2001.

[19] Michael Bartlett. *Developing Humidified Gas Turbine Cycles.* Doctoral thesis, Royal Institute of Technology, Department of Chemical Engineering and Technology, Division of Energy Processes, SE–10044 Stockholm, 2002. ISSN 1104–3466,ISBN 91–7283–443–9.

[20] A. M. Bassily. Effects of Evaporative Inlet and Aftercooling on the Recuperated Gas Turbine Cycle. *Journal of Applied Thermal Engineering*, 21:1875–1890, nov 2001.

[21] A. M. Bassily. Performance Improvements of the Intercooled Reheat Regenerative Gas Turbine Cycles Using Indirect Evaporative Cooling of the Inlet Air and Evaporative Cooling of the Compressor Discharge. In *Proc. Instn. Mech. Engrs.*, volume 215, Part A, pages 545–557, 2001.

[22] A. M. Bassily. Performance Improvements of the Intercooled Reheat Recuperated Gas-Turbine Cycle Using Absorption Inlet-Cooling and Evaporative After-Cooling. *Applied Energy*, 77:249—272, 2004.

[23] Adrian Bejan, George Tsatsaronis, and Michael Moran. *Thermal Design & Optimization.* John Wiley & Sons, 1st edition, 1996.

[24] Jaime Benitez. *Principles and Modern Applications of Mass Transfer Operations.* John Wilew & Sons, 2002.

[25] S. Benson, William U. Chandler, James A. Edmonds, M. Levine, H. Chum, James J. Dooley, and Jeff S. Logan. Carbon Management: Assessment of Fundamental Research Needs. *IEA Greenhouse Gas R&D Programme workshop on Carbon Capture and Sequestration*, 1998.

[26] D. J. Benton and W. R. Waldrop. Computer Simulation of Transport Phenomena in Evaporative Cooling Towers. *Journal of Engineering for Gas Turbines and Power*, 110:190–196, apr 1988.

[27] R. Byron Bird, E. Stewart Warren, and N. Lightfoot, Edwin. *Transport Phenomena.* John Wiley & Sons, 2nd edition, 2002.

[28] G. Blanco and L. L. Ambs. Cost Optimization of Water Recovery Systems for Steam Injected Gas Turbines. In *Proceeding of ASME TURBO EXPO'02*, Amsterdam, The Netherlands, jun 2002.

[29] G. Blanco and L. L. Ambs. Water Recovery Systems for Steam Injected Gas Turbines: An Economic Analysis. In *Proceeding of the 15th International Conference on Efficiency, Costs, Optimization, Simulation and Environmental Impact of Energy System*, volume 2, pages 711–718, jun 2002.

[30] O. Bolland and J. F. Stadaas. Comparative Evaluation of Combined Cycles and Gas Turbine Systems with Water Injection, Steam Injection, and Recuperation. *Journal of Engineering for Gas Turbine and Power*, 117:138–145, jan 1995.

[31] M. P. Boyce, Y. K. Byas, and W. L. Trevillion. The External Combustion Steam Injected Gas Turbine for Cogeneration. In *Proceedings of the 13th Intersociety Energy Conversion Engineering Conference*, volume 1, pages 860–865, San Diego, California, aug 1978. Society of Automotive Engineers.

[32] S. Bram and J. de Ruyck. Exergy Analysis Tools for ASPEN Applied to Evaporative Cycle Design. In *Proceeding of the 9th International Conference on Efficiency, Costs, Optimization, Simulation and Environmental Aspects of Energy System*, volume 1, pages 217–224, jun 1996.

[33] J. L. Bravo, J. A. Rocha, and J. R. Fair. Pressure Drop in Structural Packings. *Hydrocarbon Processing*, 65(3):45–49, 1986.

[34] Jose L. Bravo and James R. Fair. Generalized Correlation for Mass Transfer in Packed Distillation Columns. *Industrial & Engineering Chemistry, Process Design and Development*, 21(1):162–170, 1982.

[35] Jose L. Bravo, J. A. Rocha, and J. R. Fair. Mass Transfer in Gauze Packings. *Hydrocarbon Processing*, 64(1):91–95, 1985.

[36] Jose L. Bravo, J. Antonio Rocha, and James R. Fair. Comprehensive Model for the Performance of Columns Containing Structured Packings. *Institution of Chemical Engineers Symposium Series*, 1(128):489–507, 1992.

[37] D. H. Brown and A. Cohn. An Evaluation of Steam Injected Combustion Turbine Systems. *Journal of Engineering for Gas Turbine and Power*, 103:13–19, jan 1981.

[38] J. B. Burnham, M. H. Giuliani, and D. J. Moeller. Development, Installation and Operating Results of a Steam Injection System (STIG$^{\text{TM}}$) in a General Electric LM5000 Gas Generator. *Journal of Engineering for Gas Turbine and Power*, 109:257–263, jul 1987.

[39] S. M. Camporeale and B. Fortunato. Design and Off-Design Performance of Advanced Mixed Gas-Steam Cycle Power Plants. In *Proceedings of the Intersociety Energy Conversion Engineering Conference*, volume 2, pages 695–701, Washington, USA, aug 1996.

[40] S. M. Camporeale and B. Fortunato. Performance of a Mixed Gas-Steam Cycle Power Plant Obtained Upgrading an Aero-Derivative Gas Turbine. *Journal of Energy Conversion and Management*, 39:1683–1692, nov–dec 1998.

[41] S. M. Camporeale and B. Fortunato. Aero-Thermodynamic Simulation of a Double-Shaft Industrial Evaporative Gas Turbine. In *Proceeding of ASME TURBO EXPO'00*, Münich, Germany, jun 2000.

[42] S. M. Camporeale and B. Fortunato. Performance of Evaporative Cycle Gas Turbines Derived from Aeroengines. *Journal of Propulsion and Power*, 16(6):1011–1021, nov 2000.

[43] C. Carcasci, L. Cosi, D. Fiaschi, and G. Manfrida. SEMI-Closed HAT (SC-HAT) Power Cycle. In *Proceeding of ASME TURBO EXPO'00*, Münich, Germany, may 2000.

[44] Donald S. L. Cardwell. *From Watts to Clausius - The Rise of Thermodynamics in the Early Industrial Age*. Heinemann Educational Books Ltd., 48 Charles Street, London, W1X 8AH, 1971.

[45] Yunus A. Çengel and Michael A. Boles. *Thermodynamics: An Engineering Approach*. McGraw–Hill, New York, 4$^{\text{th}}$ edition, 2002.

[46] G. Cerri and G. Arsuffi. Calculation Procedure for Steam Injected Gas Turbine Cycles with Autonomous Distilled Water Production. In *Proceeding of ASME TURBO EXPO'86*, Düsseldorf, West Germany, jun 1986.

[47] G. Cerri and G. Arsuffi. Steam Injected Gas Generators in Power Plants. In *1987 ASME COGEN-TURBO: International Symposium on Turbomachinery, Combined-Cycle Technologies and Cogeneration.*, volume 1 of *ASME Int Gas Turbine Inst Publ IGTI*, pages 45–54, Montreaux, France, 1987.

[48] G. Cerri and G. Arsuffi. Steam-Injected Gas Turbine Integrated with a Self-Production Demineralized Water Thermal Plant. *Journal of Engineering for Gas Turbine and Power*, 110:8–16, jan 1988.

[49] R. Cevasco, J. Parente, A. Traverso, and A. F. Massardo. Off-design and Transient Analysis of Saturators for Humid Air Turbine Cycles. In *Proceedings of ASME TURBO EXPO 2004*, Vienna, Austria, jun 2004.

[50] D. Y. Cheng. Regenerative parallel compound dual-fluid heat engine. US Patent No. 3,978,661, 1978.

[51] D. Y. Cheng and A. L. C. Nelson. Experimental Results of Hot Section Metal Temperature Measurements of Rolls-Royce Allison 501KH under Massive Steam Injection. In *Proceeding of ASME TURBO EXPO'02*, Amsterdam, The Netherlands, jun 2002.

[52] D. Y. Cheng and A. L. C. Nelson. The Chronological Development of the CHENG Cycle Steam Injected Gas Turbine During the Past 25 years. In *Proceeding of ASME TURBO EXPO'02*, Amsterdam, The Netherlands, jun 2002.

[53] P. Chiesa, G. Lozza, E. Macchi, and S. Consonni. An Assessment of the Thermodynamic Performance of Mixed Gas–Steam Cycles: Part B—Water-Injected and HAT Cycles. *Journal of Engineering for Gas Turbine and Power*, 117:499–508, jul 1995.

[54] L. C. Chow and J. N. Chung. Evaporation of Water into a Laminar Stream of Air and Superheated Steam. *American Society of Mechanical Engineers (Paper)*, pages 8 –, 1982.

[55] L. C. Chow and J. N. Chung. Evaporation of Water into a Laminar Stream of Air and Superheated Steam. *International Journal of Heat and Mass Transfer*, 26(3):373–380, 1983.

[56] A. Cohn. Steam-Injected Gas Turbines versus Combined Cycles. EPRI *Journal*, pages 40–43, oct–nov 1988.

[57] Dexter T. Cook, John E. McDaniel, and A. D. Rao. HAT cycle Simplifies Coal Gasification Power. *MPS Review*, pages 20–25, may 1991.

[58] J. M. Coulson, J. F Richardson, J. R. Blackhurst, and J. H. Harker. *Chemical Engineering: Fluid Flow, Heat Transfer and Mass Transfer*,

volume 1. Butterworth-Heinemann, Linacre House, Jordan Hill, Oxford OX2 8DP, 225 Wildwood Avenue, Woburn, MA 01801-2041, 6th edition, 1999.

[59] E. L. Cussler. *Multicomponent Diffusion*. Elsevier, first edition, 1976.

[60] E. L. Cussler. *Diffusion, Mass Transfer in Fluid Systems*. Cambridge University Press, second edition, 1997.

[61] F. Dalili, M. Andrén, J. Yan, and M. Westermark. The Impact of Thermodynamic Properties of Air-Water Vapor Mixtures on Design of Evaporative Gas Turbine Cycles. In *Proceedings of ASME TURBO EXPO 2001*, New Orleans, USA, jun 2001.

[62] Farnosh Dalili. *Humidification in Evaporative Power Cycles*. Doctoral thesis, Royal Institute of Technology, Department of Chemical Engineering and Technology, Division of Energy Processes, SE–10044 Stockholm, 2003. ISSN 1104–3466.

[63] William H. Day and Ashok D. Rao. FT4000 HAT: a 250 MW Class Aero-Derivative Gas Turbine. In 10th *Annual* EPRI *Conference on Gasification Power Plants*, Houston, TX, USA, oct 1991. EPRI, USA.

[64] William H. Day and Ashok D. Rao. FT4000 HAT with natural gas fuel. In ASME COGEN-TURBO—6th *International Conference on Gas Turbines in Cogeneration and Utility Industrial and Independent Power Generation*, volume 7 of *ASME Int Gas Turbine Inst Publ IGTI*, pages 239–245, Houston, TX, USA, sep 1992. Publ by ASME, New York, NY, USA.

[65] V. de Biasi. 12-MW Demo Plant Proposed to Prove out CHAT Technology. *Gas Turbine World*, pages 22–25, may–jun 1999.

[66] V. de Biasi. Aquarius Design Recovers Water from Exhaust for Steam Injection. *Gas Turbine World*, pages 14–18, mar–apr 2000.

[67] V. de Biasi. LM6000 Sprint Design Enhanced to Increase Power and Efficiency. *Gas Turbine World*, pages 16–19, jul–aug 2000.

[68] V. de Biasi. DOE Evaluating CHAT for Next Generation Gas Turbine Program. *Gas Turbine World*, pages 12–17, may–jun 2001.

[69] V. de Biasi. Air Injected Power Augmentation Validated by Fr7FA Peaker Tests. *Gas Turbine World*, pages 12–15, mar–apr 2002.

[70] Noel de Nevers. *Physical and Chemical Equilibrium for Chemical Engineers*. John Wilew & Sons, first edition, 2001.

[71] M. De Paepe and E. Dick. Cycle Improvements to Steam Injected Gas Turbines. *International Journal of Energy Research*, 24(12):1081–1107, oct 2000. ISSN: 0363–907X.

[72] M. De Paepe and E. Dick. Technological and economical analysis of water recovery in steam injected gas turbines. *Applied Thermal Engineering*, 21(2):135–156, jan 2001. ISSN: 1359–4311.

[73] J. de Ruyck, S. Bram, and G. Allard. REVAP® Cycle: A New Evaporative Cycle without Saturation Tower. *Journal of Engineering for Gas Turbine and Power*, 119(3):893–897, oct 1997.

[74] J. de Ruyck, K. Maniatis, G. Baron, and K. Pottie. A Biomass Fuelled Cogeneration Plant Based on an Evaporative Gas Turbine Cycle at the University of Brussels. In *1991 ASME COGEN-TURBO: International Symposium on Turbomachinery, Combined-Cycle Technologies and Cogeneration.*, volume 6 of *ASME Int Gas Turbine Inst Publ IGTI*, pages 443–452, Budapest, Hungary, 1991.

[75] J. de Ruyck, F. Peeters, S. Bram, and G. Allard. An Externally Fired Evaporative Gas Turbine Cycle for Small Scale Biomass CHP Production. In *1994 ASME COGEN-TURBO: International Symposium on Turbomachinery, Combined-Cycle Technologies and Cogeneration.*, volume 9 of *ASME Int Gas Turbine Inst Publ IGTI*, pages 631–640, Portland, OR, USA, 1994.

[76] F. Di Maria and V. Mastroianni. Humid Air Turbine Cycle Blade Cooling Exergetic Analysis. *International Journal of Energy Research*, 23(10):841–852, aug 1999. ISSN: 0363–907X.

[77] N.R Dibelius, M. B. Hilt, and R. H. Johnson. Reduction of Nitrogen Oxides from Gas Turbines by Steam Injection. ASME Paper, mar–apr 1971. 4 pages.

[78] R. Digumarthi and C. Chang. Cheng-cycle Implementation on a Small Gas Turbine Engine. *Journal of Engineering for Gas Turbine and Power*, 106:699–702, jul 1984.

[79] S. Dodo, S. Nakano, T. Inoue, M. Ichinose, M. Yagi, K. Tsubouchi, K. Yamaguchi, and Y. Hayasaka. Development of an Advanced Microturbine System using Humid Air Turbine Cycle. In *Proceedings of the*

ASME Turbo Expo 2004, volume 6, pages 167–174, Vienna, Austria, jun 2004.

[80] D. Eckardt and P. Rufli. Advanced Gas Turbine Technology: ABB/BCC Historical Firsts. *Journal of Engineering for Gas Turbines and Power*, 124(3):542–549, jul 2002.

[81] James R. Fair, A. Frank Seibert, M. Behrens, P.P. Saraber, and Z. Olujic. Structured Packing Performance — Experimental Evaluation of Two Predictive Models. *Industrial and Engineering Chemistry Research*, 39(6):1788–1796, 2000.

[82] A. C. Fischer, H. U. Frutschi, and H. Haselbacher. Augmentation of Gas Turbine Power Output by Steam-Injection. In *Proceedings of ASME TURBO EXPO 2001*, New Orleans, USA, jun 2001.

[83] Carl W. Jr. Fitz, John G. Kunesh, and Ahmad Shariat. Performance of Structured Packing in a Commercial-scale Column at Pressures of 0.02-27.6 bar. *Industrial & Engineering Chemistry Research*, 38(2):512–518, 1999.

[84] W. R. Foote and B. Lake. Gas Turbine Power Plant Cycle with Water Evaporation. U.S. Pat. 2,869,324, jan 1959.

[85] W. E. Fraize and C. Kinney. Effects of Steam Injection on the Performance of Gas Turbine Power Cycles. *Journal of Engineering for Power, Transactions ASME*, 101(2):217–227, 1979.

[86] H.U. Frutschi and A. Plancherel. Comparison of Combined Cycles with Steam Injection and Evaporisation Cycles. *American Society of Mechanical Engineers, International Gas Turbine Institute (Publication) IGTI*, 3:137–145, 1988.

[87] Edward N. Fuller, Paul D. Schettler, and J. Calvin Giddings. A New Method for Prediction of Binary Gas-Phase Diffusion Coefficients. *Journal of Industrial and Engineering Chemistry*, 58(5):19–27, may 1966.

[88] W. L. R. Gallo. Comparison Between the HAT Cycle and other Gas-Turbine Based Cycles: Efficiency, Specific Power and Water Consumption. *Energy Conversion and Management*, 38(15–17):1595–1604, 1997.

[89] W. L. R. Gallo, G. Bidini, N. Bettagli, and B. Facchini. Effect of Turbine Blade Cooling on the HAT (Humid Air Turbine) Cycle. *Energy*, 22(4):375–380, 1997.

[90] Waldyr L.R. Gallo, Gianni Bidini, Niccola Bettagli, and Bruno Facchini. Evaporator Process Simulation and the HAT Cycle (humid air turbine) Performance. *American Society of Mechanical Engineers (Paper)*, page 7, 1995.

[91] Jürgen Gmehling and Ulfert Onken. *Vapor-Liquid Equilibrium Data Collection: Aqueous-Organic Systems*, volume 1 of *Chemistry Data Series*. DESCHEMA, 1$^{\text{st}}$ edition, mar 1977.

[92] N. D. Ågren and M. O. J. Westermark. Design Study of Part-flow Evaporative Gas Turbine Cycles: Performance and Equipment sizing — Part II: Industrial Core. *Journal of Engineering for Gas Turbines and Power*, 125(1):216–227, 2003.

[93] N.D. Ågren and M.O.J. Westermark. Design Study of Part-flow Evaporative Gas Turbine Cycles: Performance and Equipment sizing — Part I: Aeroderivative Core. *Journal of Engineering for Gas Turbines and Power*, 125(1):201–215, 2003.

[94] Niklas Ågren. *Simulation and Design of Advanced Gas Turbine Cycles*. Licentiate thesis, Royal Institute of Technology, Department of Chemical Engineering, Division of Energy Processes, SE–100 44, Stockholm, 1997. ISSN 1104–3466.

[95] Niklas Ågren. *Advanced Gas Turbine Cycles with Water-Air mixtures as Working Fluids*. Doctoral thesis, Royal Institute of Technology, Department of Chemical Engineering and Technology, Division of Energy Processes, SE-10044 Stockholm, 2000. ISSN 1104–3466,ISRN KTH/KET/R–120–SE.

[96] N. Găsparović and J. G. Hellemans. Gas Turbines with Heat Exchanger and Water Injection in the Compressed Air. In *Proceedings of Instn. Mech. Engrs. 1970–1971*, volume 185, pages 953–961, Delft, The Netherlands, jul 1971.

[97] N. Găsparović and J. G. Hellemans. Gas Turbines with Heat Exchanger and Water Injection in the Compressed Air. *Combustion*, 44(6):32–40, 1972.

[98] N. Găsparović and D. Stapersma. Gas Turbines with Heat Exchangers and Water Injection in the Compressed Air. *Combustion*, 45(6):6–16, 1973.

[99] Alan Hale, Milt Davis, and Jim Sirbaugh. A Numerical Simulation Capability for Analysis of Aircraft Inlet - Engine Compatibility. *Proceedings of the ASME Turbo Expo 2004*, 2:127–137, 2004.

[100] Shigeo Hatamiya, Hidefumi Araki, and Shin'ichi Higuchi. An Evaluation of Advanced Humid Air Turbine System with Water Recovery. *Proceedings of the ASME Turbo Expo 2004*, 7:585–591, 2004.

[101] W. R. Hawthorne and G. de V. Davis. Calculating Gas-Turbine Performance — Rapid Method for Finding Conditions of Optimum Efficiency. *Journal of Engineering*, pages 361–365, mar 1956.

[102] Richard Wilson Haywood. *Analysis of Engineering Cycles: Power, Refrigerating and Gas Liquefaction Plant*. Pergamon Press, 4th edition, 1991.

[103] V. Hensley, Reece. Theoretical Performance of an Axial-flow Compressor in a Gas-turbine Engine Operating with Inlet Water Injection. Technical Report Technical note 2673, National Advisory Committee for Aeronautics, Lewis Flight Propulsion Laboratory, Cleveland, Ohio, mar 1952.

[104] S. Higuchi, S. Hatamiya, N. Seiki, and S. Marushima. A Study of Performance on Advanced Humid Air Turbine Systems. In *Proceedings of the International Gas Turbine Congress 2003 Tokyo*, nov 2003.

[105] P. G. Hill. Aerodynamic and Thermodynamic Effects of Coolant Injection on Axial Compressors. *Aeronautical Quarterly*, pages 331–349, nov 1963.

[106] J. H. Horlock. Compressor Performance with Water Injection. In *Proceedings of ASME TURBO EXPO 2001*, New Orleans, USA, jun 2001.

[107] J.H. Horlock. Heat Exchanger Performance with Water Injection (with Relevance to Eaporative Gas Turbine (EGT) Cycles). *Energy Conversion and Management*, 39(16–18):1621–1630, 1998.

[108] Carlos Härtel and Peter Pfeiffer. Model Analysis of High-fogging Effects on the Work of Compression. *American Society of Mechanical Engineers, International Gas Turbine Institute, Turbo Expo (Publication) IGTI*, 2:689–698, 2003.

[109] G. L. Hubbard, V. E. Denny, and A. F. Mills. Droplet Evaporation: Effects of Transients and Variable Properties. *International Journal of Heat and Mass Transfer*, 18(9):1003–1008, sep 1975.

[110] Steve Ingistov. Interstage Injection System for Heavy Duty Industrial Gas Turbine Model 7EA. *American Society of Mechanical Engineers, International Gas Turbine Institute, Turbo Expo (Publication) IGTI*, 2001.

[111] Masaru Ishida and Jun Ji. Proposal of Humid Air Turbine Cycle Incorporated with Absorption Heat Transformer. *International Journal of Energy Research*, 24(11):977–987, 2000.

[112] Koichi Ito, Ryohei Yokoyama, and Y. Matsumoto. Optimal Operation of Cogeneration Plants with Steam Injected Gas Turbines. *American Society of Mechanical Engineers, International Gas Turbine Institute (Publication) IGTI*, 5:93–100, 1990. Operations;.

[113] Koichi Ito, Ryohei Yokoyama, and Yoshikazu Matsumoto. Effect of Steam Injected Gas Turbines on the Unit Sizing of a Cogeneration Plant. *American Society of Mechanical Engineers (Paper)*, pages 1–8, 1994.

[114] Xiaoyan Ji, Xiaohua Lu, and Jinyue Yan. Phase Equilibria for the Oxygen-water System up to Elevated Temperatures and Pressures. *Fluid Phase Equilibria*, 222–223:39–47, 2004. Thermodynamic models;Fugacity coefficients;.

[115] Xiaoyan Ji and Jinyue Yan. Saturated Thermodynamic Properties for the Air-water System at Elevated Temperatures and Pressures. *Chemical Engineering Science*, 58(22):5069–5077, 2003. Air-water systems;.

[116] Hongguang Jin, Hongbin Zhao, Zelong Liu, Shimin Deng, and Ruixian Cai. Novel EFHAT System with Enhancement of Humidification by Recovery of GT Exhaust Latent Heat. *American Society of Mechanical Engineers, International Gas Turbine Institute, Turbo Expo (Publication) IGTI*, 2 A:485–492, 2002.

[117] Dag Johnson. Ægidius Elling. *Tekniskt Ukeblad*, 108(47):1165–1175, dec 1961.

[118] Maria Jonsson. *Advanced Power Cycles with Mixtures as the Working Fluid*. Doctoral thesis, Royal Institute of Technology, Department of Chemical Engineering and Technology, Division of Energy Processes, SE–10044 Stockholm, 2003. ISSN 1104–3466, ISBN 91–7283–443–9.

[119] Maria Jonsson and Jinyue Yan. Exergy Analysis of Part Flow Evaporative Gas Turbine Cycles—Part 1: Introduction and Method. *American Society of Mechanical Engineers, International Gas Turbine Institute, Turbo Expo (Publication) IGTI*, 2 A:457–464, 2002.

[120] Maria Jonsson and Jinyue Yan. Exergy Analysis of Part Flow Evaporative Gas Turbine Cycles—Part 2: Results and Discussion. *American Society of Mechanical Engineers, International Gas Turbine Institute, Turbo Expo (Publication) IGTI*, 2 A:465–473, 2002.

[121] Maria Jonsson and Jinyue Yan. Economic Assessment of Evaporative Gas Turbine Cycles with Optimized Part Flow Humidification Systems. *American Society of Mechanical Engineers, International Gas Turbine Institute, Turbo Expo (Publication) IGTI*, 3:1–10, 2003.

[122] K. Jordal and T. Torisson. Comparison of Gas Turbine Cooling with Dry Air, Humidified Air and Steam. In *Proceedings of ASME TURBO EXPO 2000*, Munich, Germany, may 2000.

[123] Kristin Jordal. *Modeling and Performance of Gas Turbine Cycles with Various Means of Blade Cooling*. Doctoral thesis, Lund Institute of Technology, Lund University, P.O. Box 118, SE-221 00 Lund, may 2001.

[124] Saul Allan Kane. Axial Flow Compressor Cooling System. US Patent 2,549,819, dec 1948.

[125] T.S. Kim, C.H. Song, S.T. Ro, and S.K. Kauh. Influence of Ambient Condition on Thermodynamic Performance of the Humid Air Turbine Cycle. *Energy (Oxford)*, 25(4):313–324, 2000.

[126] D.A. Kolp and D.J. Moeller. World's First Full STIG LM5000 Installed at Simpson Paper Company. *Journal of Engineering for Gas Turbines and Power, Transactions of the ASME*, 111(2):200–210, 1989.

[127] Paul H. Kydd and William H. Day. Steam Injection in Gas Turbines having fixed Geometry Components. US Patent 3,693,347, sep 1972.

[128] E. D. Larson and R. H. Williams. Steam-injected gas turbine. *Journal of Engineering for Gas Turbines and Power, Transactions of the ASME*, 109(1):55–63, 1987.

[129] E.D. Larson and R.H. Williams. Biomass-fired Steam-injected Gas Turbine Cogeneration. *American Society of Mechanical Engineers, International Gas Turbine Institute (Publication) IGTI*, 3:57–66, 1988.

[130] Andrea Lazzaretto and Fabio Segato. Thermodynamic Optimization of the HAT Cycle Plant Structure—Part 1: Optimization of the Basic Plant Configuration. *Journal of Engineering for Gas Turbines and Power*, 123(1):1–7, 2001.

[131] Andrea Lazzaretto and Fabio Segato. Thermodynamic Optimization of the HAT Cycle Plant Structure—Part II: Structure of the Heat Exchanger Network. *Journal of Engineering for Gas Turbines and Power*, 123(1):8–16, 2001.

[132] Andrea Lazzaretto and Fabio Segato. A Thermodynamic Approach to the Definition of the HAT Cycle Plant Structure. *Energy Conversion and Management*, 43(9–12):1377–1391, 2002.

[133] E.W. Lemmon and R.T. Jacobsen. Viscosity and Thermal Conductivity Equations for Nitrogen, Oxygen, Argon, and Air. *International Journal of Thermophysics*, 25(1):21–69, 2004.

[134] Minghong Li and Qun Zheng. Wet Compression System Stability Analysis. In *Proceedings of ASME TURBO EXPO'04*, Vienna, Austria, jun 2004.

[135] Torbjörn Lindquist. *Theoretical and Experimental Evaluation of the EvGT-process*. Thesis for degree of licentiate in engineering, Lund Institute of Technology, Lund University, P.O. Box 118, SE–221 00 Lund, dec 1999.

[136] Torbjörn Lindquist. *Evaluation, Experience and Potential of Gas Turbine Based Cycles with Humidification*. Doctoral thesis, Lund Institute of Technology, Lund University, P.O. Box 118, SE–221 00 Lund, sep 2002.

[137] Torbjörn Lindquist, Per Rosén, and Lars-Ola Olsson. Humid Cycles—A Novel Way to Increase Performance of Marine Propulsion Systems. *Proc. of the 23rd World Congress on Combustion Engine Technology for Ship Propulsion, Power Generation, Rail Traction*, 2, may 2001.

[138] Torbjörn Lindquist, Marcus Thern, and Tord Torisson. Experimental and Theoretical Results of a Humidification Tower in an Evaporative Gas Turbine Cycle Pilot Plant. *American Society of Mechanical Engineers, International Gas Turbine Institute, Turbo Expo (Publication) IGTI*, 2 A:475–484, 2002.

[139] Torbjörn O. Lindquist, Per M. Rosén, and Tord Torisson. Evaporative Gas Turbine Cycle—A Description of a Pilot Plant and Operating Experience. *American Society of Mechanical Engineers, Advanced Energy Systems Division (Publication) AES*, 40:511–520, 2000.

[140] Torbjörn O. Lindquist, Per M. Rosén, and Tord Torisson. Theoretical and Experimental Evaluation of the EvGT-process. *American Society of Mechanical Engineers, Advanced Energy Systems Division (Publication) AES*, 40:457–469, 2000.

[141] M. Lorgere and J. M. Carrasse. Gas-steam Cycle with Water Injection. In *Conference on peak-load coverage*, 1969.

[142] Mattias Lundberg. Latent heat utilization in steam-injected gas turbine applications. *American Society of Mechanical Engineers, International Gas Turbine Institute (Publication) IGTI*, 6:9–18, 1991.

[143] Vladimir V. Lupandin, Viktor I. Romanov, Villy A. Krivutsa, and Villy V. Lupandin. Design, Development and Testing of a Gas Turbine Steam Injection and Water Recovery System. In *Proceedings of ASME TURBO EXPO 2001*, New Orleans, Lousiana, USA, jun 2001.

[144] Alf Lysholm. Gas Turbine System. US Patent 2,115,112, apr 1938.

[145] Alf Lysholm. Gas Turbine System. US Patent 2,115,338, apr 1938.

[146] Enick R. M., Klara S. M., and Marano J. J. A Robust Algorithm for High-pressure Gas Humidification. *Computers and Chemical Engineering*, 19(10):1051, 1995.

[147] Jonsson M. and Yan J. Humidified Gas Turbines—A Review of Proposed and Implemented Cycles. *Energy*, 30(7):1013–1078, 2005.

[148] E. Macchi, S. Consonni, G. Lozza, and P. Chiesa. An Assessment of the Thermodynamic Performance of Mixed Gas–steam Cycles: Part A—Intercooled and Steam-injected Cycles. *Journal of Engineering for Gas Turbine and Power*, 117:489–498, jul 1995.

[149] K. Mathioudakis. Analysis of the Effects of Water Injection on the Performance of a Gas Turbine. *Journal of Engineering for Gas Turbines and Power*, 124(3):489–495, 2002.

[150] Andrew McAloon, Frank Taylor, and Winnie Yee. Determining the Cost of Producing Ethanol from Corn Starch and Lignocellulosic Feedstocks. Technical report NREL/TP–580–28893, National Renewable Energy Laboratory, Golden, Colorado, USA, oct 2000.

[151] Warren McCabe, Julian Smith, and Peter Harriott. *Unit Operations of Chemical Engineering*. McGraw–Hill, 6th edition, 2000.

[152] A. J. Meacock and A. J. White. The Effect of Water Injection on Multi-spool Gas Turbine Behavior. In *Proceedings of ASME TURBO EXPO'04*, Vienna, Austria, jun 2004.

[153] Ehsan Mesbahi, Mohsen Assadi, Tord Torrison, and Torbjörn Lindquist. A Unique Correction Technique for Evaporative Gas Turbines (EvGT) Parameters. In *Proceedings of ASME TURBO EXPO'01*, New Orleans, USA, jun 2001.

[154] Robert L. Messerlie and Adelbert O. Tischler. Test Results of a Steam Injected Gas Turbine to Increase Power and Thermal Efficiency. *Proceedings of the Intersociety Energy Conversion Engineering Conference*, pages 615–625, 1983.

[155] Stanley Middleman. *An Introduction to Mass & Heat Transfer: Principles and Analysis and Design*. John Wilew & Sons, 1997.

[156] Benjamin Miller. Gas Turbine Process Using Two Heat Sources. US Patent 2.678,532, may 1954.

[157] Anthony F. Mills. *Mass Transfer*. Prentice–Hall, Upper Saddle River, New Jersey 07458, first edition, 2001.

[158] Björn Fredriksson Möller, Mohsen Assadi, Mitsuru Obana, and Athanasios Mitakakis. Optimisation of HAT-Cycles - with and without CO_2 Capture. *Proceedings of the ASME Turbo Expo 2004*, 7:461–468, 2004.

[159] G. Negri di Montenegro, R. Bettocchi, G. Cantore, and P.E. Laudi. Comparative Analysis of STIG Cycles and Post Combustion Influence. *American Society of Mechanical Engineers, International Gas Turbine Institute (Publication) IGTI*, 5:101–106, 1990.

[160] Y. Mori, H. Nakamura, T. Takahashi, and K. Yamamoto. A highly efficient regenerative gas turbine system by new method of heat recovery with water injection. In *Proceedings of the 1983 Tokyo International Gas Turbine Congress*, pages 297–303, Tokyo, Japan, 1983. Paper No. 83–Tokyo–IGTC–38.

[161] Thomas R. Morton and Ashok D. Rao. Perspective for Advanced High Efficiency Cycles Using Gas Turbines. Technical report, Flour Daniel, –.

[162] M. Nakahamkin and M. I. Patel. Transient Characteristics of Small (CHAT) Plant. Technical report, EPRI, nov 1997.

[163] M. Nakahamkin, E. Swensen, M. Patel, H. Potashnik, and H. Paprotna. Evaluation of Cascaded Humidified Advanced Turbine (CHAT) Power Plant Options for TVA. Technical report, EPRI, nov 1996. Project 3816–01.

[164] M. Nakahamkin, E. Swensen, M. Patel, H. Potashnik, and H. Paprotna. (CHAT) Plant Design. Technical report, EPRI, dec 1996. Project 2620–14.

[165] M. Nakahamkin and E. Swenson. Small (CHAT) Plant. Technical report, EPRI, nov 1997.

[166] M. Nakhamkin, E. Swensen, H. Paprotna, P. Yankowich, N. Marchionna, and A. Cohn. Combustion Studies of Natural Gas and Syn-Gas with Humid air. Technical report, EPRI, Palo Alto CA, USA, 1994.

[167] M. Nakhamkin, Ronald Wolk, B. Potashnik, T. Butler, and Ronald Hall. Injecting Humidified and Heated Air to Meet Peak Power Demands. In *Proceedings of ASME TURBO EXPO'00*, Munich, Germany, may 2000. 2000–GT–596.

[168] Michael Nakhamkin and Seyfettin C. Gulen. Transient Analysis of the Cascaded Humidified Advanced Turbine (CHAT). *American Society of Mechanical Engineers (Paper)*, page 8 pp, 1995.

[169] Michael Nakhamkin, Eric C. Swensen, John M. Wilson, Gavin Gaul, and Michael Polsky. Cascaded Humidified Advanced Turbine (CHAT). *American Society of Mechanical Engineers (Paper)*, page 8 pp, 1995.

[170] A. L. C. Nelson and D. Y. Cheng. A Fifty Percent Plus Efficiency Mid Range Advanced Cheng Cycle. In *Proceedings of ASME TURBO EXPO'02*, Vienna, Austria, jun 2002. GT–2002–30123.

[171] Parente J. O., Traverso A., and Massardo A. F. Saturator Analysis for an Evaporative Gas Turbine Cycle. *Applied Thermal Engineering*, 23(10):1275–1293, 2003.

[172] Oscar Patric Ostergren. Method of and Means for Utilizing the Latent Heat of the Steam in Steam Power Apparatus. Patent no. GB190112415, aug 1901.

[173] J. Parente, A. Traverso, and A. F. Massardo. Micro Humid Air Cycle Part A: Thermodynamic and Technical Aspects. In *Proceedings of ASME TURBO EXPO'03*, Atlanta, Georgia, USA, jun 2003.

[174] J. Parente, A. Traverso, and A. F. Massardo. Micro Humid Air Cycle Part A: Thermoeconomic Analysis. In *Proceedings of ASME TURBO EXPO'03*, Atlanta, Georgia, USA, jun 2003.

[175] Robert H. Perry, Don W. Green, and James O. Maloney. *Perry's Chemical Engineers' Handbook*. McGraw–Hill, seventh edition, 1997.

[176] Max S. Peters, Klaus D. Timmerhaus, and Ronald E. West. *Plant Design and Economics for Chemical Engineers*. McGraw-Hill, 5th edition, 2003.

[177] Bruce E. Poling, John M. Prausnitz, and John P. O'Connel. *The Properties of Gases and Liquids*. McGraw–Hill, 5th edition, 2001.

[178] John M. Prausnitz, Rüdiger N. Lichtenthaler, and Edmundo Gomes de Azevedo. *Molecular Thermodynamics of Fluid-Phase Equilibria*. Prentice Hall International Series in the Physical and Chemical Engineering Sciences. Prentice–Hall, Upper Saddle River, New Jersey 07458, 3rd edition, 1999.

[179] V. A. Rabinovich and V. G. Beketov. *Moist Gases: Thermodynamic Properties*. Begell House, New York, 1995.

[180] A. D. Rao, Paul J. Bautista, and Valerie J. Francuz. An Evaluation of Advanced Gas Turbine Cycles. *6th International Conference and Exhibition for the Power Generation Industries*, nov 1993.

[181] A. D. Rao, V. J. Francuz, F. J. Mulato, B. Sng, and E. W. West. A Feasibility and Assessment Study for FT 4000 Humid Air Turbine (HAT). Technical report, EPRI, sept 1993. Project 3251–05.

[182] Ashiyoku Domarupari Rao. Process for Producing Power. European Patent 0,150,990, aug 1985.

[183] Ashiyoku Domarupari Rao. Process for Producing Power. US Patent 4,829,763, may 1989.

[184] Ashok Domalpalli Rao and J. R. Joiner. A Technical and Economic Evaluation of the Humid Air Turbine Cycle. In *Seventh Annual International Pittsburgh Coal Conference*, pages 437–446, sep 1990. CONF–900958.

[185] Ashok Domalpalli Rao, Alvin L. Tanner, and Tam H. Vu. Closed Cycle Gas Turbine with Humidification of the Working Fluid. *Proceedings of the Intersociety Energy Conversion Engineering Conference*, 5:493–498, 1991.

[186] I.G. Rice. Steam-injected gas turbine analysis: Steam rates. *Journal of Engineering for Gas Turbines and Power, Transactions of the* ASME, 117(2):347–353, 1995.

[187] Ivan G. Rice. Steam-injected Gas Turbine Analysis — Part I — Steam Rates. *American Society of Mechanical Engineers (Paper)*, page 8 pp, 1993.

[188] Ivan G. Rice. Steam-injected Gas Turbine Analysis — Part II — Steam Cycle Efficiency. *American Society of Mechanical Engineers (Paper)*, page 8 pp, 1993.

[189] Ivan G. Rice. Steam-injected Gas Turbine Analysis — Part III — Steam Regenerated Heat. *American Society of Mechanical Engineers (Paper)*, page 8 pp, 1993.

[190] J. Antonio Rocha, Jose L. Bravo, and James R. Fair. Distillation Columns Containing Structured Packings: A comprehensive Model for Their Performance. Part 2 — Mass-transfer Model. *Industrial & Engineering Chemistry Research*, 35(5):1660–1667, 1996.

[191] Luke H. Rogers and David H. Archer. Performance Calculations and Research Direction for a Water Enhanced Regenerative Gas Turbine Cycle. *Proceedings of the Intersociety Energy Conversion Engineering Conference*, 1:949–954, 1993.

[192] Per M. Rosén. *Evaporative Cycles — in Theory and in Practise*. Ph d. thesis, Lund Institute of Technology, Lund University, P.O. Box 118, SE–22100 Lund, Sweden, aug 2000.

[193] Per M. Rosén and Lars-Ola Olsson. Sätt att tillföra ånga till insugsluften till en förbränningsmotor och en anordning därtill. Swedish patent no. 502452, 1995.

[194] Per M. Rosén and Lars-Ola Olsson. A Novel Technique for Reducing the NO_X Emissions and Increasing the Efficiency of a Turbo-charged Diesel Engine, Using Humidification of the Compressed Air. *Proceedings of* ECOS *'96, Efficiency, Costs, Optimization, Simulation and Environmental Aspects of Energy Systems*, 1:641–646, jun 1996. ISBN 91–7170–664–X, ISSN 1104–3466.

[195] I. Roumeliotis and K. Mathioudakis. Evaluation of Interstage Water Injection Effect on Compressor and Engine Performance. In *Proceedings of ASME TURBO EXPO'05*, Reno-Tahoe, Nevada, USA, jun 2005. GT2005–68698.

[196] I. Roumeliotis, K. Mathioudakis, and N. Aretakis. Performance Analysis of Twin-spool Water Injected Gas Turbines Using Adaptive Modeling. In *Proceedings of ASME TURBO EXPO'03*, Atlanta, Georgia, USA, jun 2003. GT2003–38516.

[197] Magnus C. Rydstrand, Mats O. Westermark, and Michael A. Bartlett. An Analysis of the Efficiency and Economy of Humidified Gas Turbines in District Heating Applications. *Proceedings of the 15th International Conference on Efficiency, Costs, Optimization, Simulation and Environmental Aspects of Energy Systems*, 2:695–703, jul 2002.

[198] Norio Sayama and Hiromi Nakamura. Regenerative Gas Turbine with Water Addition and Method of Operation Thereof. European Patent EP 0,053,045, jun 1982.

[199] Daniel Schell, Cynthia Riley, Paul Bergeron, and Pamela Walter. Technical and Economic Analysis of an Enzymatic Hydrolysis Based

Ethanol Plant. Technical report Draft, Solar Energy Research Institute, Golden, Colorado, USA, jun 1991.

[200] D. B. Spalding. *Convective Mass Transfer*. Arnold, 1$^{\text{st}}$ edition, 1963.

[201] Roland Span. *Multiparameter equations of state-An accurate source of thermodynamic property data*. Springer Verlag, Berlin, 1$^{\text{th}}$ edition, 2000.

[202] Irwin Stambler. Spray Cooling Inlet and Compressor Flow Increases Hot Day Plant Rating. *Gas Turbine World*, pages 37–42, may–jun 1997.

[203] S.S. Stecco, U. Desideri, and N. Bettagli. Humid Air Gas Turbine Cycle: A Possible Optimization. *American Society of Mechanical Engineers (Paper)*, page 7 pp, 1993.

[204] S.S. Stecco, U. Desideri, B. Facchini, and N. Bettagli. Humid Air Cycle: Some Thermodynamic Considerations. *American Society of Mechanical Engineers (Paper)*, page 8 pp, 1993.

[205] Alfred Strasser. Cheng Cycle Cogeneration System: Technology and Typical Applications. *American Society of Mechanical Engineers, International Gas Turbine Institute (Publication) IGTI*, 6:419–428, 1991.

[206] J. Szargut. Cogeneration of Network Heat in the Set of a Humid Air Turbine. *Energy (UK)*, 27(1):1–15, 2002/01/.

[207] Jan Szargut. Cogeneration of Network Heat in the Set of a Humid Air Turbine. *ECOS 2000*, 1:423–434, 2000.

[208] Ireneusz Szczygiel. Thermodynamic Analysis of Different Humid Air Turbine Schemes. *Proceedings of ECOS*, 2:719–725, 2002. Berlin, Germany.

[209] Ross Taylor and R. Krishna. *Multicomponent Mass Transfer*. Wiley Series in Chemical Engineering. John Wiley & Sons, 605 Third Avenue, New York, NY 10158-0012, 1$^{\text{st}}$ edition, 1993.

[210] A. S. Teja and P. Rice. Generalized corresponding states method for the viscosities of liquid mixtures. *Industrial & Engineering Chemistry, Fundamentals*, 20(1):77–81, 1981.

[211] Charlotte Tengborg. *Bioethanol Production: Pretreatment and Enzymatic Hydrolysis of Softwood*. Doctoral thesis, Lund University, Department of Chemical Engineering 1, Lund University, Sweden, may 2000. ISSN 1100–2778, ISRN LUTKDH/(TKKA-1004/1–82/(2000)), ISBN 91–7874–069–X.

[212] A. Traverso and A. F. Massardo. Thermoeconomic Analysis of Mixed Gas-steam Cycles. *Applied Thermal Engineering*, 22(1):1–21, 2002.

[213] Robert Ewald Treybal. *Mass Transfer Operations*. McGraw-Hill Classic Textbook Reissue. McGraw–Hill, 3$^{\text{rd}}$ edition, 1980.

[214] K. Tsubouchi, N. Yasugahira, S. Yoshida, R. Kaneko, and T. Sato. Evaluation of Water Droplet Erosion for Advanced Large Steam Turbine. *American Society of Mechanical Engineers, Power Division (Publication) PWR*, 10:245–251, 1990.

[215] Gael D. Ulrich. *A Guide to Chemical Engineering Process Design and Economics*. John Wiley & Sons, 1984.

[216] M. Utamura, I. Takehara, and H. Karasawa. MAT, A Novel, Open Cycle Gas Turbine for Power Augmentation. *Energy Conversion and Management*, 39(16–18):1631–42, 1998/11/.

[217] Motoaki Utamura, Takaaki Kuwahara, Hidetaro Murata, and Nobuyuki Horii. Effects of Intensive Evaporative Cooling on Performance Characteristics of Land-based Gas Turbine. *American Society of Mechanical Engineers, Power Division (Publication) PWR*, 34–2:321–328, 1999.

[218] J. van Liere and G. H. M Laagland. The TOPHAT Project: Swirl Flash Technology to Reduce Maintenence Cost. In *Proceedings of ASME TURBO EXPO'00*, München, Germany, may 2001.

[219] Paul von Heiroth, Jan-Olof Gustafsson, and Torbjörn Lindquist. Model of an Evaporative Cycle for Heat and Power Production. *Energy Conversion and Management*, 40(15):1701–1711, 1999.

[220] W. Wagner, J.R. Cooper, A. Dittmann, J. Kijima, H.J. Kretzschmar, A. Kruse, R. Mares, K. Oguchi, H. Sato, I. Stocker, O. Sifner, Y. Takaishi, I. Tanishita, J. Trubenbach, and T. Willkommen. The IAPWS Industrial Formulation 1997 for the Thermodynamic Properties of Water and Steam. *Journal of Engineering for Gas Turbines and Power*, 122(1):150–180, 2000.

[221] J. A. Wesselingh and R. Krishna. *Mass Transfer in Multicomponent Mixtures.* Delft University Press, P.O. Box 98 2600 MG, Delft, The Netherlands, 1$^{\text{st}}$ edition, 2000.

[222] Robert Wooley, Mark Ruth, John Sheehan, Kelly Ibsen, Henri Majdeski, and Adrian Galvez. Lignocellulosic Biomass to Ethanol Process Design and Economics Utilizing Co-current Dilute Acid Prehydrolysis and Enzymatic Hydrolysis Current and Futuristic Scenarios. Technical report NREL/TP–580–26157, National Renewable Energy Laboratory, Golden, Colorado, USA, jul 1999.

[223] Carl L. Yaws. *Chemical Properties Handbook: Physical, Thermodynamic, environmental, transport, safety and health related properties for organic and inorganic chemicals.* McGraw–Hill, 1999.

Appendix A

Thermal Properties

The calculation of the performance of the humidification tower cannot be performed if no property data exists. There have been many studies of the thermal properties of system throughout history. The simplest relationship between gases is the ideal gas law:

$$PV = m\frac{R_u}{M_g}T \qquad (A.1)$$

This equation is used to model the gas phase in this thesis. There are more complex equation that more accurately describes the behavior of a real gas [114, 115, 179]. It is however shown by experiments that this ideal gas law can be used with satisfactorily results.

A.1   Evaluation Conditions

To use the equations for mass transfer, all properties must be evaluated at a suitable reference temperature. Different approaches have been suggested in the literature and Chow and Hubbard [54, 55, 109] proposed that these properties for mass transfer should be evaluated at a mean film temperature and a mean water mass fraction. Chow later suggested that the mean values of the properties should be calculated at a mean value of one third of the bulk value and two thirds of the interface value [54, 55]. This method has been referred to as the one-third rule. No evidence that this method presents more accurate results than ordinary mean value or interface values has been established in the literature [157]. To be sure calculations of both methods were used and it was found that there was no significant difference between the two models in the calculation of the tower height.

A.2   Thermodynamic Properties

Several studies have been performed to predict the thermodynamic properties of gases and liquids. These methods become more and more complex over the years. Multi-parameter equations of state are becoming more popular as the computer power increases. These equations are very complex but yields very good results compared to the experimental values [201]. One big limitation of the equations of state is the lack of experimental data that can verify and lay the foundation for the equations of states. A group of countries financed the production of a multi-parameter equation of state for water. The group is called the *International Association for the Properties of Water and Steam*, IAPWS. The group collected data points and equations were fitted to the data [220]. These equations have been published by the organization and are now considered standard within the industry. It has been easy to standardize the steam table due to the wide range of data points that are available for water. A similar standardized equation has not been developed for gases. Several equations exists but none of them has been considered a standard in the same way as the IAPWS steam tables. The IAPWS-IF97 a formulation for water has been used in this thesis to calculate the state of water substance in both the liquid and gaseous phase. The IAPWS have also produced equations for calculating thermal conductivity and viscosity and they have also been used throughout this thesis.

Lemmon et al. have also developed a multi-parameter equation of state for air [133]. This equation is used in the model in **paper I** and **paper VI**. Ordinary polynomials for the calorific properties of ethanol has been used and they were taken from reference [223].

A.3   The Activity Coefficient

The activity coefficient represents the departure from ideality due to mixing with the other species in the liquid. Many researchers have studied the activity coefficient which has resulted in a large database for the correlation of the activity coefficient for different mixtures [70,91,178]. A frequently used

model is the van Laar equation presented by equations A.2 and A.3.

$$\log \gamma_1 = \frac{A_{12} x_2^2}{\left(\dfrac{A_{12}}{A_{21}} x_1 + x_2 \right)^2} \tag{A.2}$$

$$\log \gamma_2 = \frac{A_{21} x_1^2}{\left(x_1 + \dfrac{A_{21}}{A_{12}} x_2 \right)^2} \tag{A.3}$$

The coefficients, A_{12} and A_{21}, are functions of temperature. These coefficients can be assumed to be constant within a small temperature range. For the evaluation of the experimental data, a constant value for the coefficients in equation A.2 and equation A.3 is used. The value used in the calculations are constant according to reference: [91].

A.4   The Diffusion Coefficient

The diffusion coefficient can be determined in several ways. In this thesis the model by Fuller–Schettler–Giddings for diffusion coefficient have been used. This model is developed according to the theory of Maxwell-Stefan, which models the gas molecules as hard spheres. The method of Fuller–Schettler–Giddings yields the diffusion coefficient with an error estimation of 5.4% [87, 178].

$$D_{ab} = \frac{1.0 \cdot 10^{-7} \cdot T_g^{1.75} \cdot \sqrt{\dfrac{M_g + M_l}{M_g \cdot M_l}}}{P \left(\sum v_g^{1/3} + \sum v_l^{1/3} \right)} \tag{A.4}$$

where M_g and M_l are the molecular weights of gas and liquid respectively, p is the absolute total pressure and v_g and v_l are the diffusion volumes for gas and liquid respectively.

A.5   Viscosity

The viscosity of the simple fluids needs to be known in order to calculate the viscosity of a mixture. The viscosities of the different fluids are taken from different sources in the literature. For the water substance the IAPWS

formulation is used to find out both the viscosity of the gas and the liquid phase [220]. For the other fluids in the gas and liquid, polynomials from Yaws have been used [223].

A.5.1 Gas Viscosity

Special mixture rules apply to calculating the viscosity of gases. Several mixture rules have been developed through history and their applicability varies. In this thesis the method developed by Reichenberg has been used. This method is a simplification of the massive kinetic theory of gases developed by Chapman and Enskog [177]. The method of Reichenberg is a simplification of this rigorous theory and is applicable to gas mixtures at low pressures. The method has been correlated to account for polar components such as water and it generally give results with only a few percent errors. The equation for gas viscosity is given by equation

$$\eta_m = \sum_{i=1}^{n} K_i \left(1 + 2 \sum_{j=1}^{i-1} H_{ij} K_j + \sum_{j=1\neq i}^{n} \sum_{k=1\neq i}^{n} H_{ij} H_{ik} K_j K_k \right) \qquad (A.5)$$

In equation A.5, η_m is the dynamic viscosity of the mixture and the parameter n denotes the number of components in the mixture. The other

parameters in equation A.5 is calculated according to:

$$K_i = \frac{y_i \eta_i}{y_i + \eta_i \sum\limits_{k=1 \neq i}^{n} y_k H_{ik} \left[3 + \left(2M_k/M_i\right)\right]}$$

$$H_{ij} = \sqrt{\frac{M_i M_j}{32\left(M_i + M_j\right)^3}} \cdot \left(C_i + C_j\right)^2 \cdot \frac{\left[1 + 0.36 \cdot T_{rij}\left(T_{rij} - 1\right)\right]^{1/6} F_{Rij}}{\sqrt{T_{rij}}}$$

$$U_i = \frac{\left[1 + 0.36 \cdot T_{ri}\left(T_{ri} - 1\right)\right]^{1/6} F_{Ri}}{\sqrt{T_{ri}}}$$

$$C_i = \frac{M_i^{1/4}}{\sqrt{\mu_i U_i}}$$

$$F_{Ri} = \frac{T_{ri}^{3.5} + \left(10\mu_{ri}\right)^7}{T_{ri}^{3.5}\left[1 + \left(10\mu_{ri}\right)^7\right]}$$

$$T_{rij} = \frac{T}{\sqrt{T_{ci}T_{cj}}}$$

$$T_{ri} = \frac{T}{\sqrt{T_{ci}}}$$

The parameter μ_{ri} is the dipole moment of the molecule of specie i. To employ the Reichenberg method of viscosity for gas mixtures, the viscosity, molecular weight, dipole moment, critical temperature and critical pressure must be known for the individual specie in the mixture. This information can easily be obtained from reference books such as Perry's and Poling [175,177].

A.5.2 Liquid Viscosity

The development of a theory that can predict the dynamic viscosity of a liquid is a more complex problem than the development of a model for gases. This is due to the complex behavior of molecules of liquids. The method of calculating the liquid mixture viscosity is the method by Teja and Rice. This model is based on a corresponding states method to predict the behavior of the liquid mixture. Equation A.6 shows the mixing rule by

Teja and Rice.

$$\ln\bigl(\eta_m\varepsilon_m\bigr) = \ln\bigl(\eta_m\varepsilon_m\bigr)^{R1} + \Bigl(\ln(\eta\varepsilon)^{R2} - \ln(\eta\varepsilon)^{R1}\Bigr)$$

$$\cdot\frac{\omega_m - \omega^{R1}}{\omega^{R2} - \omega^{R1}} \quad \text{(A.6)}$$

where the subscripts R1 is and R2 is water and ethanol respectively, η is the viscosity, ω is the acentric factor and ε is the inverse viscosity and is defined as:

$$\varepsilon = \frac{V_c^{2/3}}{\sqrt{T_c M}} \quad \text{(A.7)}$$

The mixing rules assumes that the parameters in the mixture, parameters with the subscript m, in equation A.7 is calculated according to:

$$V_{cm} = \sum_i \sum_j x_i x_j V_{cij}$$

$$T_{cm} = \frac{\sum_i \sum_j x_i x_j T_{cij} V_{cij}}{V_{cm}}$$

$$M_m = \sum_i x_i M_i$$

$$\omega_m = \sum_i x_i \omega_i$$

$$V_{cij} = \frac{(V_{ci}^{1/3} + V_{cj}^{1/3})^3}{8}$$

$$T_{cij} V_{cij} = \psi_{ij}\bigl(T_{ci} T_{cj} V_{ci} V_{cj}\bigr)^{1/2}$$

It should be noted that the individual viscosities, η_m^{R1} should not be evaluated at the system temperature but at a temperature T_{cm}. The term ψ_{ij} is an experimental parameter which has to be determined for the specific mixture under consideration. The value of this parameter for a mixture of ethanol and water is $\psi_{ij} = 1.36$ [210].

A.6   Conductivities

This section presents the way the thermal conductivities of the liquid and the gas is calculated. The conductivity of the different fluids are taken

from different sources in the literature. For the water substance the IAPWS formulation is used to find out both the conductivity of the gas and the liquid phase [220]. For the other species in the gas and liquid, polynomials from Yaws have been used [223].

A.6.1 Gas Conductivity

The method, developed by Mason and Saxena, has been used to calculated the gas conductivity of the gas [177]. This method can be stated as:

$$
\lambda_m = \sum_{i=1}^{n} \frac{y_i \lambda_i}{\sum\limits_{j=1}^{n} y_j A_{ij}}
\tag{A.8}
$$

In this equation, y_i, y_j is the mole fraction of the species in the mixture and the parameter, A_{ij} is calculated according to:

$$
A_{ij} = \frac{\varepsilon \left(1 + \sqrt{(\lambda_{\mathrm{tr}i}/\lambda_{\mathrm{tr}j})} \left(M_i/M_j\right)^{1/4}\right)^2}{\sqrt{8\left(1 + \left(M_i/M_j\right)\right)}}
\tag{A.9}
$$

where M is the molecular weight of the species and λ_{tr} is the monatomic value of the thermal conductivity and ϵ is a parameter equal to one in this calculation. The ratio between the thermal conductivities are here calculated as:

$$
\frac{\lambda_{\mathrm{tr}i}}{\lambda_{\mathrm{tr}j}} = \frac{\Gamma_j \left(\exp 0.0464 T_{ri} - \exp 0.2412 T_{ri}\right)}{\Gamma_j \left(\exp 0.0464 T_{rj} - \exp 0.2412 T_{rj}\right)}
\tag{A.10}
$$

where Γ is defined as:

$$
\Gamma = 210 \left(\frac{T_c M^3}{P_c^4}\right)^{1/6}
\tag{A.11}
$$

The Mason and Saxena method calculates the conductivity within about 3-8% accuracy.

A.6.2 Liquid Conductivity

To calculate the conductivity of the binary liquid mixture the method by Jamieson et al. is used [177]. Jamieson states that conductivity of a mixture can be written as:

$$
\lambda_m = w_1 \lambda_1 + w_2 \lambda_2 - \alpha\left(\lambda_2 - \lambda_1\right)\left(1 - \sqrt{w_2}\right) w_2
\tag{A.12}
$$

where w_1 and w_2 is the weight fractions of the different components in the liquid, and, λ_1 and λ_2 are the pure component thermal conductivities. The numbering of the components is numbered so that $\lambda_1 \leq \lambda_2$. α is an adjustable parameter, which is set to one due when their is a lack of experimental data. It is estimated that this method determines the liquid mixture conductivity within about 7% [177].